Multi-proxy reconstruction of Holocene environmental change from sediments of Lake Rzęśniki, Northeast Poland

Master's Thesis

Faculty of Science, University of Bern

presented by

Giulia Wienhues

2019

Supervisors:

Prof. Dr. Martin Grosjean

Institute of Geography and Oeschger Center for Climate Change Research

PD Dr. Hendrik Vogel

Institute of Geological Sciences

Advisor:

Stamatina Makri

Institute of Geography and Oeschger Center for Climate Change Research

Abstract

Climate change and anthropogenic activities are influencing aquatic ecosystems (IPCC, 2013). The physical and biochemical cycles in water bodies are tightly linked to environmental and climatic conditions, so they respond sensitively to changes in these boundary conditions. Emerging anoxia and meromictic conditions in lakes have substantial consequences on lake ecology (Jenny et al. 2016, Steffen et al. 2015) and it is important to understand their development and effects on ecosystems over long time-scales. Understanding of the paleoenvironmental history provides important insights into natural and environmental factors, which is important in light of future development of freshwater systems. To date, few studies aimed at a better understanding of factors contributing to and ecosystem consequences of meromixis have been conducted.

Lake Rzęśniki, a small dead ice lake in NE Poland, is an interesting site to study how productivity and meromixis operate in tandem in lake systems characterized by a dense forest catchment with limited runoff and input of soil substrates. Almost the entire sedimentary record of Lake Rzęśniki is varved, making it suitable for a high resolution paleoenvironmental study. The aim of this study was to reconstruct the environmental history of Lake Rzęśniki in course of the Holocene, specifically with the focus on the evolution of meromixis and paleoproductivity in the context of a low erosional input and catchment vegetation dynamics.

In this thesis, high-resolution hyperspectral imaging (HSI) proxies were applied: total chlorophyll for aquatic primary production and bacteriopheophytin *a* (Bphe-*a*) for meromixis. Additionally, sedimentary pigments were extracted and measured by HPLC to create a pigment stratigraphy and to calibrate the HSI data. The multi-proxy record was completed by scanning XRF data and measurements of total organic carbon, and biogenic silica determined by Fourier Transform Infrared Spectroscopy (FTIRS). The core chronology is based on radiocarbon dating of abundant terrestrial plant macrofossils.

The analyses revealed that strong seasonal anoxia occurs naturally in Lake Rzęśniki and lake mixing, catchment processes and phytoplankton dynamics are closely related. Anthropogenic deforestation and wind mixing were identified as main driving factors for the disappearance of bottom meromixis in the 16th century. Sedimentary redox-sensitive elements (Fe, Mn) and the pigment Bphe-*a* appear to be the most diagnostic indicators tracking those changes. The findings were supported by sedimentary pigments related to phytoplankton assemblage's changes.

Table of Contents

List of Figures

Appendix

List of Tables

Appendix

1. Introduction

Climate change and anthropogenic activities are influencing aquatic ecosystems. The physical and biochemical cycles in such systems are tightly linked to environmental and climatic conditions. Thus they respond sensitively to changes in these boundary conditions. Climate warming predicted by global climate models and the increase in temperatures that has occured, already today, will have substantial consequences on these ecosystems (IPCC 2013; Sahoo et al. 2011). Recent studies report a deterioration of freshwater systems which is mainly attributed to anthropogenic influences such as human-induced eutrophication (Jenny et al. 2016a; Steffen et al. 2015). The quantification and assessment of the natural and anthropogenic drivers of climate change is one of the major challenges in climate research (IPCC 2013). In order to be able to disentangle natural variability from anthropogenic disturbances, it is necessary to look into the past. The investigation of paleoenvironmental history can thus provide us with important insights into natural climate and environmental variability, which is needed to understand and evaluate the changes today and to improve future climate models and scenarios (Braconnot et al. 2012; Snyder 2010).

Thanks to their high temporal resolution, laminated lake sediments are useful archives in reconstructing climatic and environmental changes through time (Adrian et al. 2009). Small lakes, especially, are sensitive recorders of the slightest changes in the climate and catchment (Fedotov et al. 2015). A variety of chemical and environmental indicators is preserved in these lake sediments, which can be used as a basis for investigating specific processes and conditions that took place in the lake itself and in the lake catchment.

Eutrophic and meromictic conditions in lake systems can be naturally and anthropogenically driven. However, due to the lack of long-term data, it is difficult to identify specific causes. Are the conditions currently observed natural, anthropogenic, or a combination of both? Related questions are: when did the human influence start? How has this affected the lake systems? What were the natural preconditions? Postglacial lake sediments have great potential to help us answer these questions (Tylmann et al. 2013).

It has been shown that many lakes in northern Poland are annually laminated and thus suitable for high resolution studies (Tylmann et al. 2013). However, Lake Rzęśniki in northeast Poland is still unexplored, which is why we have no detailed paleoenvironmental analysis of this lake. Thus, the aim of this study for the Master's thesis is to reconstruct the climatic and environmental history of Lake Rzęśniki in northeastern Poland, specifically with the focus on meromixis and paleoproductivity.

2. State of research

2.1. Lake mixing and anoxia

Freshwater systems are very sensitive to climatic and environmental changes. For instance, fluctuations in temperature or nutrient input can have a great impact on the mixing regime of a lake. The frequency of mixing fundamentally determines the physical, chemical and biological properties of a lake.

Broadly, lake mixing is driven by the regional climate conditions. According to the thermal lake classification by Wetzel (2001) most lakes in temperate latitudes are dimictic, which means a lake undergoes two mixing events in spring and fall. During the summer and winter season the water column is stratified. This stratification forms due to thermal and the related density gradient of the water column. During the seasonal temperature change in spring and fall, these gradients dissolve (homothermal conditions), and the water circulates vertically (Håkanson and Jansson 2002). The mixing dynamics in a lake are important for the oxygen and nutrient concentrations in the water column and thus for living organisms. Under stratified conditions, the oxygen produced in the photic zone is separated from the bottom layer of a lake (hypolimnion) by the metalimnion. As a result, the bottom waters can become oxygen depleted (hypoxia) by benthic O_2 respiration. This natural mixing and stratification process can be amplified by human impact or climate change.

A compilation study by Jenny et al. (2016b) revealed that human activities and nutrient release are the main forcing factors of an apparent global spread of hypoxia in freshwater systems since AD 1850 (Fig. 1). Beside anthropogenic impact, recent studies also reported an amplification of bottom-water anoxia due to climate change (i.e temperature and precipitation anomalies) (Jenny et al. 2014). Lake model simulations by Woolway and Mechant (2019) indicate that lakes are predicted to undergo weaker mixing and change to more permanently stratified systems, causing a deterioration of oxygen conditions in many lakes. The combined effect of excessive nutrient input and global warming is predicted to increase the extent and severity of hypoxia (Posch et al. 2012; Diaz and Rosenberg 2008).

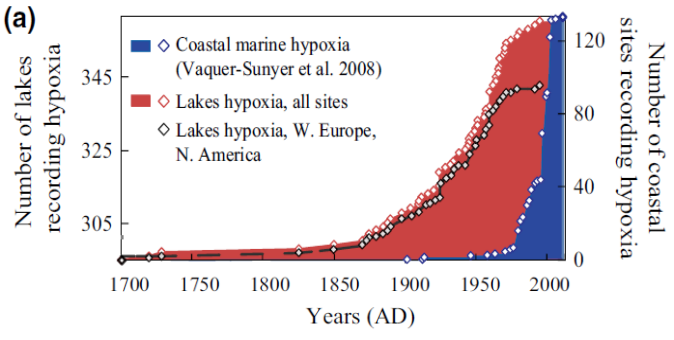

Figure 1: Emergence of hypoxia conditions during the Anthropocene and the distinct increase of hypoxia in the last 300 years (Jenny et al. 2016b)

The effects of oxygen depletion on faunal communities and biogeochemical cycles are considerable. It is reported, that oxygen-stressed ecosystem show changes in the food web structure, collapse of aquatic communities and decline in ecosystem functioning (Friedrich et al. 2014; Levin et al. 2009). Nevertheless, an accurate assessment of the emergence of oxygen depletion in water remains difficult since hypoxia can also be of natural origin.

2.2. Meromixis

Meromixis describes a type of lake stratification in which the water body remains partly unmixed for long periods of time (Hutchinson and Löffler 1956), such that the monimolimnion (the deepest layer of a meromictic lake), remains anoxic and enriched in dissolved chemical species (Fig. 2). Lakes can be permanently meromictic or can evolve into meromictic conditions through environmental and climatic changes. Based on the different processes that can lead to meromixis different classifications exist: ectogenic meromixis is caused by external flows of different salinity or turbidity, whereas endogenic or biogenic meromixis is formed by degradation of organic matter or salt exclusion through ice cover formation (Walker and Likens 1975). The deepest portion of the water body is isolated through density, chemical or temperature gradients. Due to the permanent reducing conditions in the bottom waters and sediment-water interface, previously complexed nutrients can be remobilized and redissolved into the water body. Organic matter decomposition is reduced and organic material accumulates on the lake bottom (Gulati 2017).

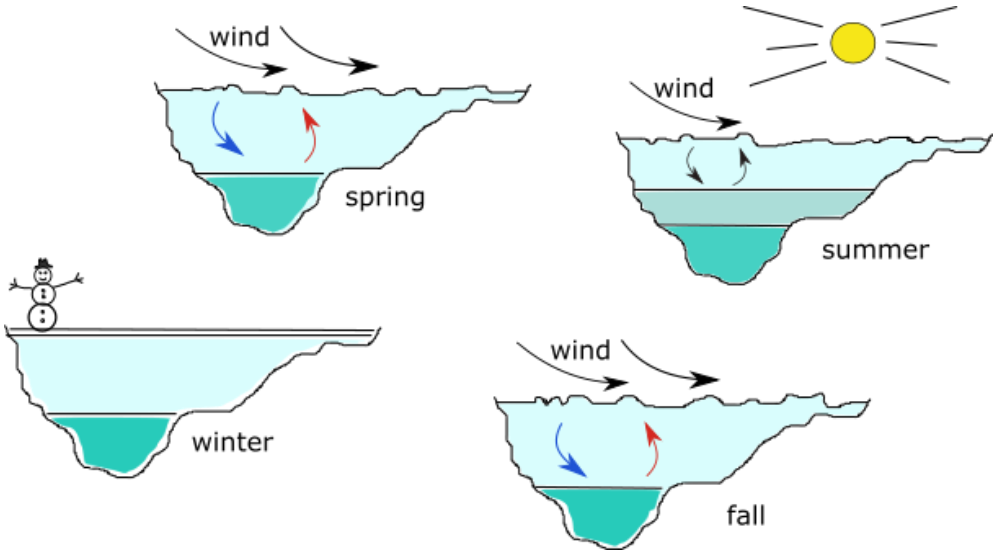

Figure 2: Typical annual stratification and mixing cycle in a meromictic lake. The monimolimnion remains throughout the whole year unaffected by the mixing in the mixolimnion (redrawn Gulati et al. 2017)

The ecology of permanently stratified lakes has been more thoroughly researched than the different driving factors of formation and disappearance of meromixis. Only a few studies exist where this phenomenon was observed and investigated in the last century (e.g Rogozin et al. 2017; Fast and Tyler 1981) and even less over longer time scales. One reason is the limited amount of monitoring data recorded in the last centuries that facilitates the detection of meromixis. Looking back in time, detailed limnological measurements are missing, and instead the use of paleo indicators is required. However, as was shown before, it is crucial to understand the effects on and development of meromixis and bottom water anoxia over long time-scales.

2.3. Eutrophication and productivity – Impact on lake mixing

It is widely known, that excessive anthropogenic nutrient input increases the eutrophication of freshwater bodies. Nowadays, eutrophication has been recognized worldwide as one of the most important threats for aquatic systems. The consequences of fertilization are persistent algal blooms that affect planktonic photosynthesis as well as microbial degradation of the produced organic matter (Ansari et al. 2011). This can have a major impact on bottom water anoxia, even without considering changes in the mixing regime

Stratification of lakes is closely linked to biological activity and nutrient availability in the water body. As the term biogenic meromixis already implies, permanent stratification can emerge by geochemical cycles and production and dissolution of organic products (Walker and Likens 1975). The higher the photosynthetic activity in the photic zone, the more organic matter reaches the bottom water. This organic matter has to be decomposed, which consumes oxygen and releases CO_2 (oxic respiration). The oxygen depletion and dissolution of decomposition end products enhances the density gradient in the water column. Consequently, "the more productive a lake is, the more important this process can be for stabilizing stratification" (Boehrer and Schultze 2008).

The oxygen depletion from bottom waters during stratified productive seasons can lead to dissolution of chemical species. Under anoxic conditions, calcite or iron can be remobilized into the hypolimnion, which effectively contributes to bottom water density. Under increasing photosynthetic activity and increasing pH, biogenic calcite precipitates and can become redissolved in the bottom water. Indeed, it is reported, that many biogenic meromictic lakes are stabilized by calcite dissolution or iron cycling (Rodrigo et al. 2001; Hongve 2002). Anthropogenic eutrophication of lakes can additionally enhance water column stability by increasing primary production through nutrient input. A reduction of nutrient inputs was even found to have a reversible effect on biogenic meromixis (Scharf and Björk 1992). Nevertheless,

case studies have shown that anoxic conditions can persist even when eutrophication symptoms have disappeared (Jacquet et al. 2005).

2.4. Reconstructing paleoproductivity and mixing regime

In order to overcome the lack of instrumental records, it is necessary to use paleolimnolgical approaches based on the principle that past changes of lake ecosystems are preserved in the sediment. Indeed, a simple indication for the oxygenation history of bottom waters is the sediment texture. Many lakes exhibit laminations that are used as indicators of hypoxia, because the formation of sediment laminations only appears when oxygen concentrations fell below a critical threshold and bioturbation is absent (Jenny et al. 2014; Tylmann et al. 2013; Zolitschka et al. 2015).

In addition, permanent or seasonal anoxic conditions in lakes are also suitable for preserving chemical and biological compounds that carry signatures from the water column. In particular, the analysis of highly resolved geochemical proxies from bottom sediments has been widely used as a method for paleo environmental reconstructions (Meyers 1994; Wick et al. 2003). The interpretation of many of these proxies does not differ between meromictic and non-meromictic lakes. However, there are specific chemical properties that can affect the bottom sediments of meromictic lakes and, thus, need to be taken into account in their analysis (Gulati 2017).

2.4.1. Biogeochemical composition of the sediment

The geochemical composition of lake sediment provides an important insight into chemical cycling and oxygenation of the water column. The abundance of specific elements can be important indications for eutrophic or anoxic conditions in the past. In particular, the abundance of redox-sensitive elements is highly dependent on the oxygenation within bottom waters and sediments and, therefore, also on the mixing of the lake.

A good example is Mn and its oxides, which undergoes rapid reductive dissolution under anoxic conditions and, conversely, oxidic precipitation when the seasonal mixing of the water column reaches the hypolimnion and oxygenates it (Hamilton-Taylor and Davison 1995). Fe undergoes redox-dependent transformations similar to Mn, but because of its higher absorption capacity to humic substances and more chalcophile character, its abundance in the sediment is driven to a smaller degree by the oxygenation of the hypolimnion (Hamilton-Taylor and Davison 1995). Because of this general redox-sensitive behaviour of Mn and Fe and the fact that Fe oxidizes faster than Mn, the Fe/Mn ratio is often used as a proxy for bottom water anoxia (e.g.

Davies et al. 2015). However, sedimentological factors and sediment focusing limit the applicability of this ratio (Naeher et al. 2013; Friedrich et al. 2014). Other elements like Ca, Br or the ratios Si/Ti or S/Al are associated, in general, with high lake productivity (Davies et al. 2015). The above-mentioned biogeochemical processes are important in holomictic as well as in meromictic lakes. But, in contrast, biogeochemical products can accumulate in much higher concentrations and are easier to obtain in meromictic lakes (Hongve 2002).

Changes in primary production are often linked to variations in the organic compounds within the sediment. Phases of enhanced biological productivity are often expressed in increased values of organic matter content in the sediment. General paleoproductivity indicators such as total organic carbon (TOC) or biogenic silica (BSi) contents are commonly and conveniently used to detect long-term temporal changes (Meyers and Teranes 2001). BSi is formed by siliceous phytoplankton such as diatoms and is buried in the sediment. However, it is mentioned in literature that the use of BSi as a paleoproductivity proxy might be only applicable to oligotrophic lakes with long-residence times, because it, may be confounded by biogeochemical depletion of dissolved silicate (Conley and Schelske 2001).

Furthermore, type and amount of organic matter can also reveal past environmental conditions. Organic matter can be terrestrial originating from soil erosion and litter input, or autochthonous. To identify the source of the organic matter, the atomic ratio between total carbon and total nitrogen (TC/TN) is commonly used (Meyers 1997). Whereas aquatic organic matter has low TC/TN values of 4 to 10, terrestrial organic matter shows TC/TN values of 20 and higher (Meyers 1994; Meyers and Teranes 2001). However, since there are numerous processes other than aquatic primary production and import of terrestrial OM which can influence the amount of sedimentary organic carbon such as decomposition in the water column and sediment , the TC/TN ratio should be always combined with additional proxies indicating productivity (Gulati 2017).

2.4.2. Fossil pigments

A powerful method for reconstructing paleoproductivity changes in lake systems is sedimentary pigments, also called fossil pigments. They are produced by algae and other photosynthesizing organisms and can be linked to specific groups of organisms, which have different physiological requirements and show varying responses to chemical and physical parameters (Leavitt and Hodgson 2001; Wetzel 2001). Chloropigments (chlorophylls *a*, *b*, *c* and derivatives) and carotenoids (carotenes and xanthophylls) can be found in all photosynthetic aquatic organisms.

Pigments are degraded in the water column and upper sediments (biofilm) by chemical and biological processes. Therefore, pigment stability is highly variable between groups. Major processes affecting pigment degradation and preservation are photo/chemical-oxidation (light irradiance and redox conditions) and biodegradation (zooplankton grazing and microbial degradation) (Guilizzoni and Lami 2003). However, rapid burial of pigments in sediments under anoxic, dark and cold conditions favors pigment preservation (Leavitt 1993a; Reuss et al. 2005) . In general, carotenoids degrade more rapidly in the water column, whereas they are much more stable than chlorophylls after incorporation into the sediment (Guilizzoni et al. 2002). Because of this reason, carotenoids hold the highest potential as paleoecological biomarkers (Reuss et al. 2005).

It has been shown that changes in pigment concentration correlate with total algal biomass and specific algal groups, which reflect changes in the bio-productivity and lake conditions like anoxia, grazing, stratification and light availability (Leavitt and Hodgson 2001). The presence of chlorophyll α and β indicate oxygenic primary producers (Reuss et al. 2005; Squier et al. 2002). Bacteriochlorophyll and cyanopigments indicate anoxic events (Squier et al. 2002), whereas the chlorophyll degradation product (e.g. pheophorbide *a*) are diagnostic for grazing activity (Bianchi et al. 1988; Cartaxana et al. 2003). The variety of carotenoids in general is important for taxonomy studies and assessing changes in phytoplankton assemblages (Leavitt and Hodgson 2001).

Algae and bacterial pigments in the sediment and sediment traps have also been used to study the history of meromictic lakes (e.g. Brown, McIntosh, and Smol 1984; Hodgson et al. 1998; Rybak and Dickman 1988). A unique feature of meromictic lakes is the presence of anoxygenic phototrophic purple and green sulfur bacteria that are located in or immediately below the chemocline. These bacteria use available light and reduced compounds such as sulfur, H_2S or ferrous iron as electron donor for photosynthesis (Gulati 2017). Carotenoids from sulfur photosynthetic anaerobic bacteria such as okenone and isorenieratene (Guilizzoni et al. 2002) or the bacteriochlorophyll derivative bacteriopheophytin a (Butz et al. 2016) are used as proxies for permanent stratification and related chemical conditions in the lake. However, it is also reported that these pigments can be produced, but in much lower biomass, during a summer stratification with an anoxic hypolimnion (Rogozin et al. 2012; Overmann and Manske 2006). A compiled summary of all principle pigments, their origin, stability and proxy interpretation is given in Table 1.

Pigment ratios have often been applied as additional proxies in aquatic research to assess pigment preservation, zooplankton grazing and lake trophy. The Chl-α/pheopigments-α (Chl-α index) and the chlorin preservation index (CPI) {Chla-α/ Chl-α + pheopigments-α} are used as

biomarkers for pigment preservation and, indirectly, to assess zooplankton grazing intensity. High Chl-α indices and CPI values constant and around 0.2 indicate good sedimentary pigment preservation (Deshpande et al. 2014; Buchaca and Catalan 2008). Furthermore, the CP index is an indication of the degree of pigment degradation in the lake system (Buchaca and Catalan 2008). The CD/TC ratio {chlorophyll derivatives /total carotenoids} is an index for lake trophic state changes. Blue-green algae are rich in carotenoids and dominate in eutrophic conditions. Therefore, low CD/TC values are associated with eutrophic conditions, when carotenoids produced by blue-green algae are dominating the ratio (Guilizzoni and Lami 2003). In addition, total carotenoids can be also used to infer past total phosphorus concentrations in the water column, which is associated to the general lake trophy. Guilizzoni et al. (2011) developed a transfer function to infer past total phosphorus concentrations by using photospectrometer measures of total carotenoids (TC).

Table 1: Summary of principal pigments and their affinity, source, stability and proxy use (modified from Jeffrey, Mantoura, and Wright 1997; Leavitt and Hodgson 2001; Guilizzoni and Lami 2003 and in text references). Stability is shown from 4= low to 1= high

Pigment	Affinity (major group)	Stability	Source	Proxy description and significance
Chlorophylls				
Chlorophyll *a*	plantae, algae	3	planktonic, littoral	marker for total algal biomass; excluding prochlorophyte biomass
Chlorophyll *b*	plantae, Chlorophyta, Eugelnophyta	2	planktonic, littoral	distinguishes green algae from all other algal types
Chlorophyll derivatives				
Pheophytin *a*	Chl a derivative (general)	1	planktonic, littoral, terrestrial , sedimentary	
Pheophytin *b*	Chl b derivative (general)	2	planktonic, littoral, terrestrial , sedimentary	marker for phototrophic green algae
Pheophorbide *a*	Chl a derivatives (grazing, senescent diatoms)	3	planktonic, littoral, sedimentary	zooplankton grazing (food web intensity) and oxidation
Pyropheo(pigments): - Pyropheophorbide *a* - Pyropheophytin *a*	Dinoyphyta, Bacillariophyta, Chrysophyta	2	littoral, sedimentary	
Bacteriochlorophylls				
Bacteriopheophytin-*a*	Phyotosynthetic bacteria (Rodospirillaceae and Chromatiaceae) (Buchaca & Catalan 2008)	-	-	marker for anoxogenic phototrophic bacteria at the chemocline in meromictic lakes (Butz et al. 2016)
Carotenoids				
a) Carotenes				
β-carotene [ββ-carotene]	plantae, algae, some phototrophic bacteria	1	planktonic, littoral, terrestrial	marker for primary production and total phototroph abundance (Leavitt et al 1993)
α-carotene [βε-carotene]	Cryptophyta, Crysophyta, Dinophyta, some Chlorophyta	2	planktonic, littoral	
b) Xanthophylls				
Fucoxantin	Dinophyta, Bacillariophyta, Chrysophyta, Cryprophyta	2	planktonic, littoral	marker for diatoms
Diadinoxanthin	Dinophyta, Bacillariophyta, Chrysophyta, Cryptophyta	3	planktonic,littoral, sedimentary (may interconvert together in lake sediments - phototransformation).	
Diatoxanthin	Bacillariophyta, Dinophyta, Chrysophyta	2		
Dinoxanthin	Dinophyta (minor pigment)	-	-	Dinoflagellate occurrence
Peridinin	Dinophyta	4	planktonic	
Alloxanthin	Cryptophyta, Dinophyta	1	planktonic	water level (?)
Zeaxanthin	Chlorophyta, Cyanobacteria, Chrysophyta, Dinophyta	1	planktonic, littoral	useful marker for cyanobacteria when they are major component of the population
Canthaxanthin	colonial Cyanobacteria, Herbivores	1	planktonic, littoral	
Echinenone	Cyanobacteria	1	planktonic, littoral	phosphate eutrophication
Lutein	Chlorophyta, Euglenophyta, Plantae	1	planktonic, littoral, terrestrial	marker for green algal abundance
Neoxanthin	Chlorophyta, Euglenophyta, Plantae	4	littoral	
Violaxanthin	Chlorophyta, Euglenophyta, Plantae	4	littoral	
Antheraxanthin	Chlorophyta, Prasinophyta, Crysophyta, Eustigmatophyta	-	-	

2.5. Research questions and design

This Master's thesis project investigates the Holocene environmental history of Lake Rzęśniki with a special focus on productivity changes and meromixis. In order to achieve this goal, the following research questions will be investigated:

- Does the sediment of Lake Rzęśniki show changes in productivity throughout Holocene times?
- Does the sedimentary record show meromictic events? If yes, when did these meromictic conditions occur?
- Can specific driving factors of these changes be detected? Are these changes climatic or human induced, in-lake processes or influenced by changes in the catchment?
- When has the anthropogenic influence started and to what extent is it displayed in the sedimentary record? And how has human impact influenced lake mixing regime?

To answer these questions, we use several different methods in order to obtain a multi-proxy data set (Fig. 3). The whole analysis was based on lake sediment cores taken from Lake Rzęśniki in September 2017. Firstly, non-destructive scanning methods (Multi-Sensor Core Logger (MSCL), Micro-X-ray Fluorescence (µXRF) and Hyperspectral Imaging (HSI)) were applied. In addition, a core-to-core correlation was made based on a visual inspection of the core halves and on the magnetic susceptibility coherence. The µXRF and HSI scans were performed on one core half, and these provide information about the sediments´ geochemical composition, lake productivity, and oxygen conditions at high resolution.

Following these steps, a discrete subsampling for the radiocarbon analysis was made on one quarter of the split core, with a sampling resolution of 30 cm in order to have one ^{14}C sample per 500 years (Blaauw et al. 2018). The subsampling for loss on ignition (LOI), CNS and FTIRS was done on the other core quarter with 5 cm resolution, and a pigment analysis was performed in 10 cm steps. Sediment cubes of 3 cm^3 in volume were taken in order to have enough material for all four analyses. The resulting multi-proxy data set was analyzed statistically in order to answer our research questions.

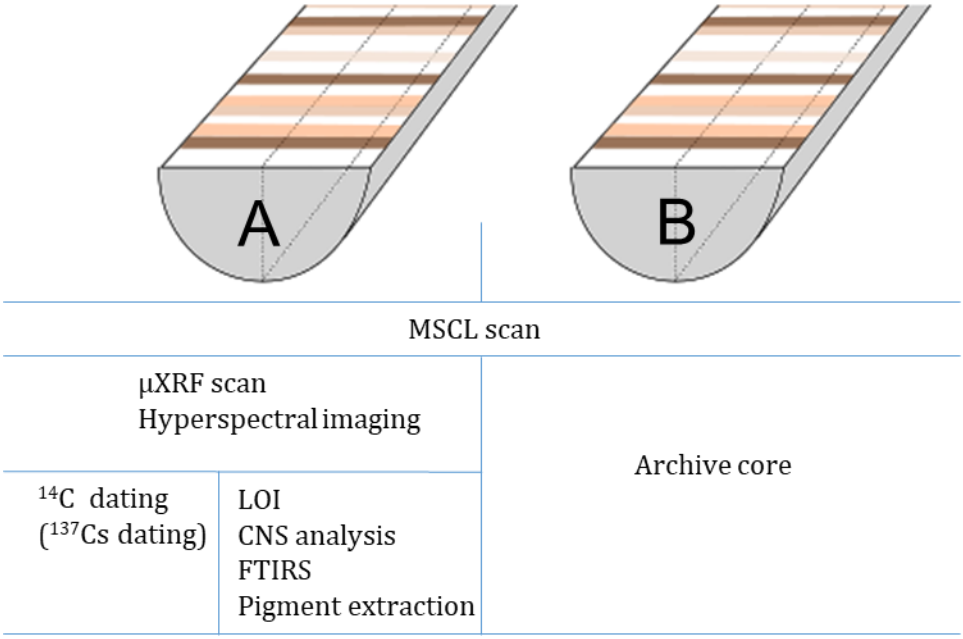

Figure 3: Overview on the procedures undertaken on core halves of Lake Rzęśniki

3. Site description

3.1. Masurian Lake District

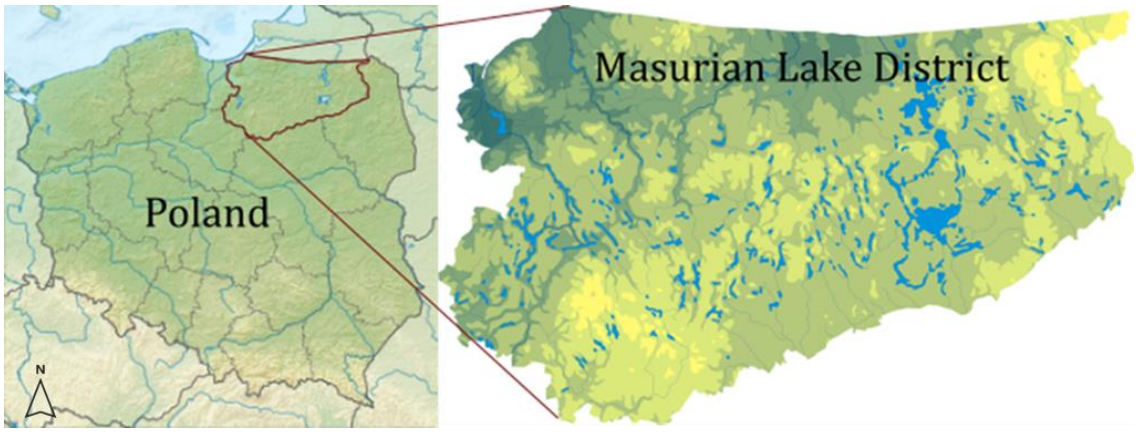

Figure 4: Location of the Masurian Lake District in Poland

The Masurian Lake District or Masurian Lakeland is a postglacially formed lowland landscape in north-eastern Poland (Fig. 4) with the highest areal density of lakes in the country (Choinski 2007 in Tylmann et al. 2017). It extends from the low Vistula River to the borders of Russia and Lithuania, and covers overall an area of 5,200 km^2. The dominant glaciation period was the Pomerian phase of the Vistulian glaciation (16-15 ka BP), which formed today's surface geology with moraine tills, sands and gravels. Holocene sediments are present as fluvial and organic deposits (Tylmann et al. 2017). The regional climate is continental and characterized by strong seasonality with a mean annual temperature of 6.5°C (mean T_{Jan} = 4.5°C and mean T_{Jul} = 17.5°C). The mean annual precipitation is around 570 mm with predominantly summer precipitation. It belongs to the coldest lowland climates in Poland (Wacnik et al. 2012; Tylmann et al. 2017). Podzols and cambisols are the dominant soil types in that region. The potential natural vegetation of the Great Masurian Lake District is composed of subboreal types of oak-hornbeam forest, whereas the present vegetation is dominated by pine and mixes pine-forests. As a result of anthropogenic impact since the Late-Holocene, there is a great disparity between the current and potential vegetation in that area (Wacnik et al. 2012).

3.2. Climate reconstruction of the Holocene

The southeastern Baltic region is still lacking of paleoclimatological studies that support understanding of regional climate change. Nevertheless, there is evidence that the regional climate of north-east Europe corresponds with large-scale climate characteristics captured in study sites in Central and Northern Europe (Seppä et al. 2009).

After deglaciation of the area (<15 ka BP), the onset of the Holocene is indicated by a decrease of Lateglacial shrub vegetation in palynological datasets at 11 600 cal yr BP (e.g. Lauterbach et al. 2011; Goslar et al. 1999). It is suggested that the early Holocene warming in northeastern Europe was delayed, and cool and continental climate persisted in the south-eastern Baltic until 10 000 cal yr BP (Lauterbach et al. 2011). The temperature increased in the early Holocene and reached a plateau-like level, known as the Holocene Thermal Maximum (HTM). The climate of the mid-Holocene (~9000 - 5800 cal yr BP) can be generally described as relatively warm, humid and stable, providing optimal climate conditions for vegetation development. The most pronounced abrupt cooling in European Holocene climate records is the 8.2 ka event, a freshwater-forced North-Atlantic cold event (Klitgaard-Kristensen et al. 1998; von Grafenstein et al. 1998). A cooling of about 1.0°C followed by an abrupt climate warming of about 2.0°C was recorded in several high-resolution records (Seppä et al. 2009; Veski et al. 2004). Related environmental changes to this abrupt cooling could also be observed in study sites in Poland (Fiłoc et al. 2017) and Denmark (Bjerring et al. 2013). Another large-scale cooling has been recorded at 5800-5100 cal yr BP from the North Atlantic and central Europe and is related to reduced westerly circulation strength in northern Europe (e.g. Moros et al. 2004).

The Late Holocene (last 4000 years) is generally characterized by a linear cooling trend (Seppä et al. 2009). This general cooling trend was interrupted by three positive temperature deviations and low humidity observed in many different records in Northern Europe. The first warm period is dated to the end of the HTM from 5000 to 4000 cal yr BP and the second was a 2000-year long warm period recorded from 3000 to 1000 cal yr BP, including the Roman Warm Period (2000 cal yr BP) and the Medieval Warm Period (1000 cal yr BP). The latter period favored expansion of agriculture and related deforestation in northeastern Poland (Wacnik et al. 2012). The third positive climate anomaly is the large-scale observed warming of the last 150 years in Northern Europe (e.g. Tarand and Nordli 2001).

According to Seppä et al. (2009) two cold anomalies with lower temperatures and increased humidity are recorded between 3800 and 3000 cal yr BP and from 500 to 100 cal yr BP. The timing and length of the first cold anomaly differs in European records (Rosen et al. 2002, Jessen et al 2005). Nevertheless, there is evidence of enhanced humid conditions and higher water levels during that period in Poland between 3850-2700 cal yr BP (1900-1750 BC) in the

Woryty region (e.g. Berglund et al. 1996). This is consistent with Välirante et al. (2007) and Rundgren (2008) who observed wetter conditions in peat bogs. The second cold period corresponds with the Little Ice Age (LIA), peaking in the late 1500s to the early 1800s (Moberg et al. 2005).

3.3. Lake Rzęśniki

3.3.1. Catchment and morphology of Lake Rzęśniki

Lake Rzęśniki (53°51.6' N, 21°57.2'E; 125.3 m a.s.l) located in the Masurian Lake District in northeastern Poland (Fig. 5). The lake was formed by the melting of dead ice in a deep channel or within a glacial outwash plain, which is situated southeast of the Pomerian moraines (Tylmann et al. 2014). The morphology of the basin is relatively simple with a maximum depth of 26 m in the central part of the basin and average depth of 7.8 m. Lake Rzęśniki has a northern inflow and is drains on the eastern side into the much larger Lake Orzysz. The inflowing creek from Lake Łazduny passes two small and shallow water bodies before entering Lake Rzęśniki. Glaciofluvial sand and gravel deposits dominate the surrounding catchment. A small patch of peat covers the northern side of the lakeshore. The primary soil types are podzols formed from loose sands. There is no settlement in the catchment and nearly the entire catchment is forested with predominantly coniferous trees (Tylmann et al. 2017). An overview of all lake parameters can be found in Table 2.

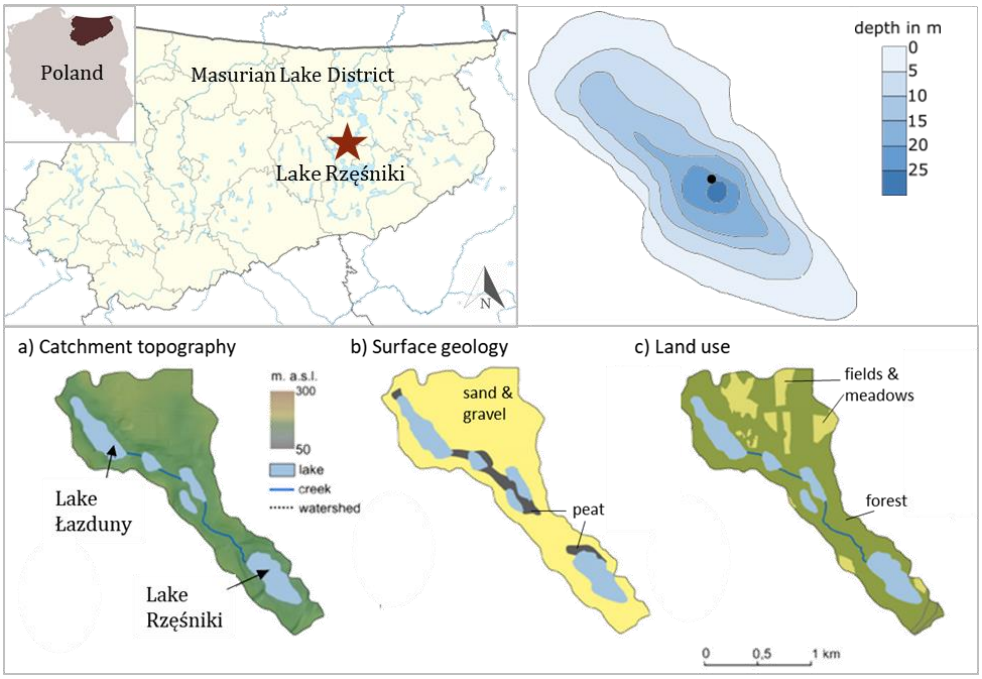

Figure 5: A - Location of Lake Rzęśniki in the Masurian Lake District. B - Bathymetric map of the basin of Lake Rzęśniki with coring site. C – Catchment topography (a), surface geology (b) and land use (c) (modified Tylmann et al. 2017)

Table 2: Catchment and lake morphology parameters (Tylmann et al. 2017)

Catchment and lake morphology			
Coordinates	53° 51.6'/21° 57.2'	Max depth [m]	26
Altitude [m a.s.l.]	125.3	Max. width [m]	280
Surface area [ha]	14.2	Length of shoreline [m]	1700
Volume [tys m^3]	1111.8	Shoreline development index	1.3
Max length [m]	700	Exposure index	1.8
Average depth [m]	7.8	Catchment geology	Sand and gravel

3.3.2. Limnology

Lake Rzęśniki is a dimictic and slightly alkaline [pH = 8.29 at 1m depth] hardwater lake with strong winter. It is summer stratification and is normally covered by ice during the winter season. The lake is currently eutrophic which is shown by hydrochemical measurements (Tylamann et al 2013; Tylmann et al. 2017). Anoxic conditions are observed at a water depth of 7 meters and hypoxia occurs during summer already in shallow water depth. The spring mixing might be incomplete, leaving the hypolimnetic waters anoxic. Oxygen concentrations greater than 1mg dm^{-3} are observed to the depth of 14 m (Tylmann et al. 2017).

Figure 6: Picture of Lake Rzęśniki (photo credit: Paul Zander)

3.3.3. Local settlement and land use history

The Masurian Lake District is one of the least-polluted areas in Europe until eutrophication along with contamination of the lake waters developed as a result of industrial agriculture and mass tourism in the 20th century (Tylmann et al. 2011). Nevertheless, human impact started long before that. Intensified human impact was identified in the Middle Bronze Age [~1400 BC] with the appearance of the Lusatian culture. During this time, plant cultivation and livestock-based production grew significantly. The forest communities experienced a strong

transformation in their composition from oak-hornbeam to spruce-birch-hornbeam forest, but deforestation was only occuring on a small scale. This culture inhabited large settlements mainly on morainic hills until the early Iron Age (~1400 BC – 500 BC) (Wacnik et al. 2012).

The West Baltic Burrow culture emerged from west Baltic tribes and the Lusatian culture in the 6th century (700/600-50 BC). Agriculture was operated as shifted cultivation, burning and fallowing. The overall impact on woodland was more permanent and stronger than under the Lusatian culture. Tumuli, fortified settlements and small lake dwellings are characteristic features of the West Baltic Burrow culture and several remnants were found in the region (closest to study side are Lake Wojnowo and Lake Milkowskie ~15 km north from Lake Rzęśniki).

From the second half of the 2nd century AD to the 6th century AD the Galindai tribes (Bogaczewo culture) populated the area. This period is characterized by diversified farming activities on a greater scale and increased diversity of settlements. Around 600-1000 AD the population decreased, which resulted in secondary forest successions on formerly cultivated patches.

The last phase of strong human impact of the area, which has continued to present times, began in the Middle Ages with the activity of Teutonic Order Knights (~1450 AD). A strong agricultural exploitation with largescale deforestations took place. The onset of deforestation was regionally different and started in the 16th century in the catchment area of Lake Rzęśniki and Lake Łazduny (Fig. 7). The forest cover regenerated in the 20th century as a result of decreasing farming and settlement (Wacnik et al. 2012)

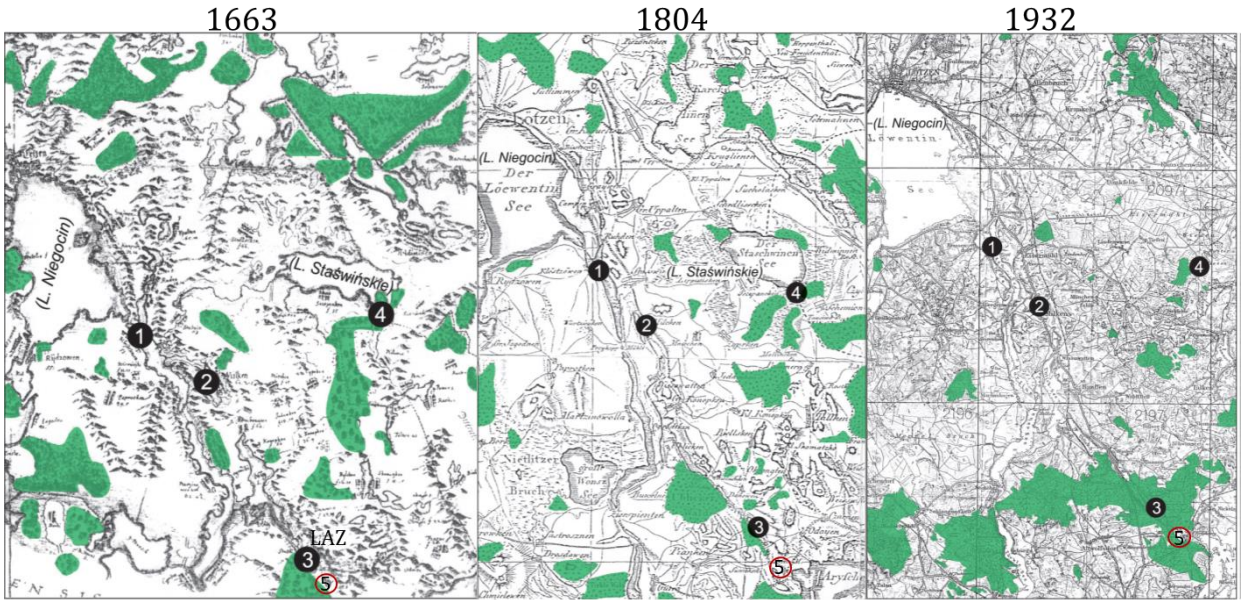

Figure 7: Historical maps showing the strong deforestation in the area from 1663, 1804 and 1932. Forested area is marked in green. (1) Lake Wojnonowo, (2) Lake Milkowskie, (3) Lake Łazduny, (4) former Lake Staswinskie and (5) Lake Rzęśniki in red (Wacnik et al. 2012)

4. Material and Methods

4.1. Coring and sediment description

The coring campaign at Lake Rzęśniki was conducted in September 2017. The cores were retrieved from the deepest point of the lake. Additionally, two surface cores RZE17/6_A and RZE17/6_B were taken. The cores were stored in dark and cool (4° C) conditions until the opening in October 2018. After core opening and core-to-core correlation of the core half, each core was described in detail according to Schnurrenberger et al. (2003). The color was determined using the Munsell® soil color chart.

4.2. Scanning techniques

4.2.1. Multi-Sensor Core Logging (MSCL)

The magnetic susceptibility and bulk density of the un-opened cores of Lake Rzęśniki were determined with the Geotek® MSCL at the Geological Institute of the University of Bern. This non-destructive scanning technique allows us to make a continuous and rapid measurement in high resolution. The magnetic susceptibility of the sediment varies with the content of iron-bearing or ferromagnetic minerals. These are often proxies for detrital input. The bulk density can be calculated with the core thickness and the Compton attenuation coefficient, indicating the density and porosity changes along the core (Last and Smol 2001).

4.2.2. Micro X-ray fluorescence scanning (µXRF)

Micro X-ray fluorescence (µXRF) analysis is a non-destructive and semi-quantitative technique and provides us information about the elemental composition of the sediment. The analysis is based on electrons excitation by incident X-ray radiation, which creates a specific energy emission when electron fall to lower energy level in order to become stable again. The atoms of each element generate a characteristic X-ray fluorescence in terms of energy and wavelength that allows the measurement of the relative abundance of the elements present at the surface of the sediment core. Depending on the X-ray source anode material a different range of elements can be measured (Croudace and Rothwell 2015). For measuring lighter elements (Al, Si, Cl, K, Ca, Ti, Ba) a Cr-Anode-Tube is used and for heavier elements (Mn, Fe, Ni, Cu, Zn, Br, Sr) a Mo-Anode-Tube is used. The most often used elements include Si, Br, S, K, Ca, Ti, Fe, Rb, Sr and Zr. In the form of single element profiles or ratios, many elements have been linked to various environmental proxies such as detrital input, erosion, productivity and redox conditions (Davies et al. 2015). The opened cores of Lake Rzęśniki were scanned at a 2.5 mm resolution with the ITRAX® (Cox Analytical System) micro x-ray fluorescence (µXRF) scanner at the Geological

Institute of the University of Bern. The cores were measured using a Cr-Anode-Tube set to 30kV voltage, 50 mA current and 20 seconds exposure time.

4.2.3. Hyperspectral core scanning

The hyperspectral imaging scanner detects the sediment reflectance from which properties such as mineralogy and organic compounds can be inferred. The method produces semi-quantitative data at a very high spectral resolution of 0.8 nm (reflectance) and a spatial resolution of 38 x 38 µm in a fast and efficient way. A sub-varve scale investigation is possible through this high resolution (Grosjean et al. 2014). Of special interest are the sedimentary pigments with diagnostic absorption bands in the visual and near-infrared range (VNIR) (400 – 100nm), which are diagnostic for productivity and meromixis of the lake (Butz et al. 2017).

The opened cores from Lake Rzęśniki were scanned with the Specim Ltd sediment-core-scanning system (SCS) scanner (Fig. 8). The core scanner consists of a hyperspectral camera (Specim PFD-xx-V10E) and a Schneider Kreuznach Xenoplan 1.9/35 lens as well as a tray that moves the sediment core underneath an illumination chamber and camera (Grosjean et al. 2014; Butz et al. 2015).

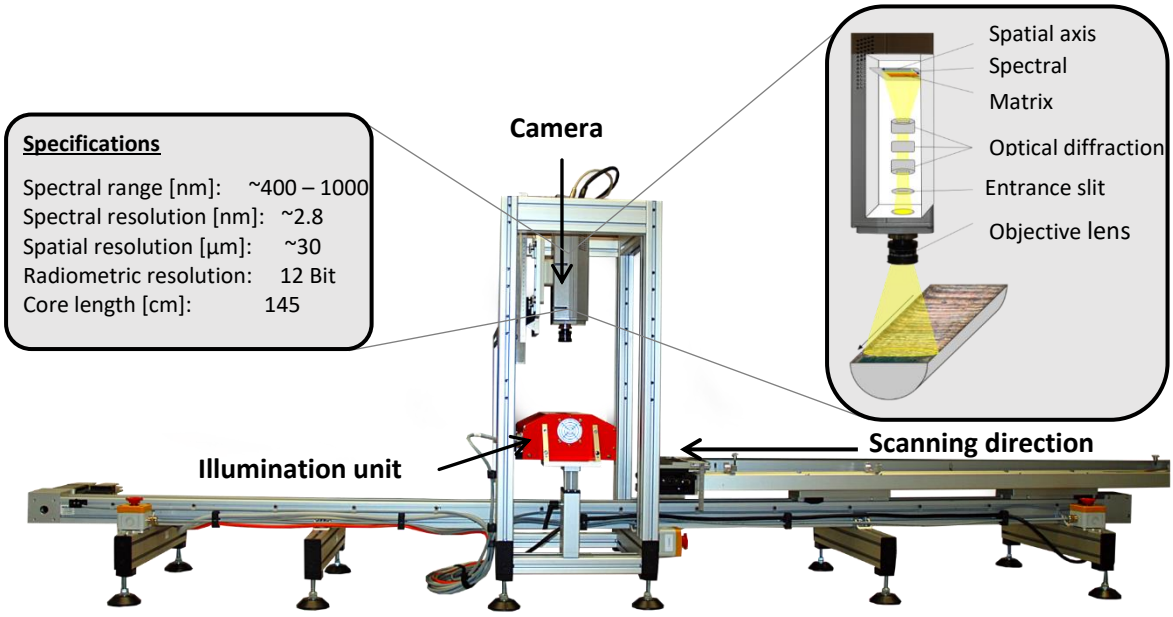

Figure 8: Principle of the Specim Ltd. Hyper-spectral scanner (modified from Butz et al. 2015)

The images are processed in ENVI5.0 software following the methodology of Butz et al. (2015). The diagnostic pigments Chlorophyll and Bacteriopheophytin have major absorption features at 673 and 845 nm , respectively, in the retrieved endmember spectra (Fig. 9). Spectral endmembers are extracted from the dataset, and a continuum removal approach is used to define

the boundaries of absorption features related to the pigments of interest. The relative absorption band depth (RABD) for the absorption band minima at 673 and 845 nm can be than calculated according to formula in Fig. 9. The retrieved indices $RABD_{673}$ (total green pigments) and $RABD_{845}$ (Bacteriopheophytin *a*) are then used to infer semi-quantitative pigment concentrations.

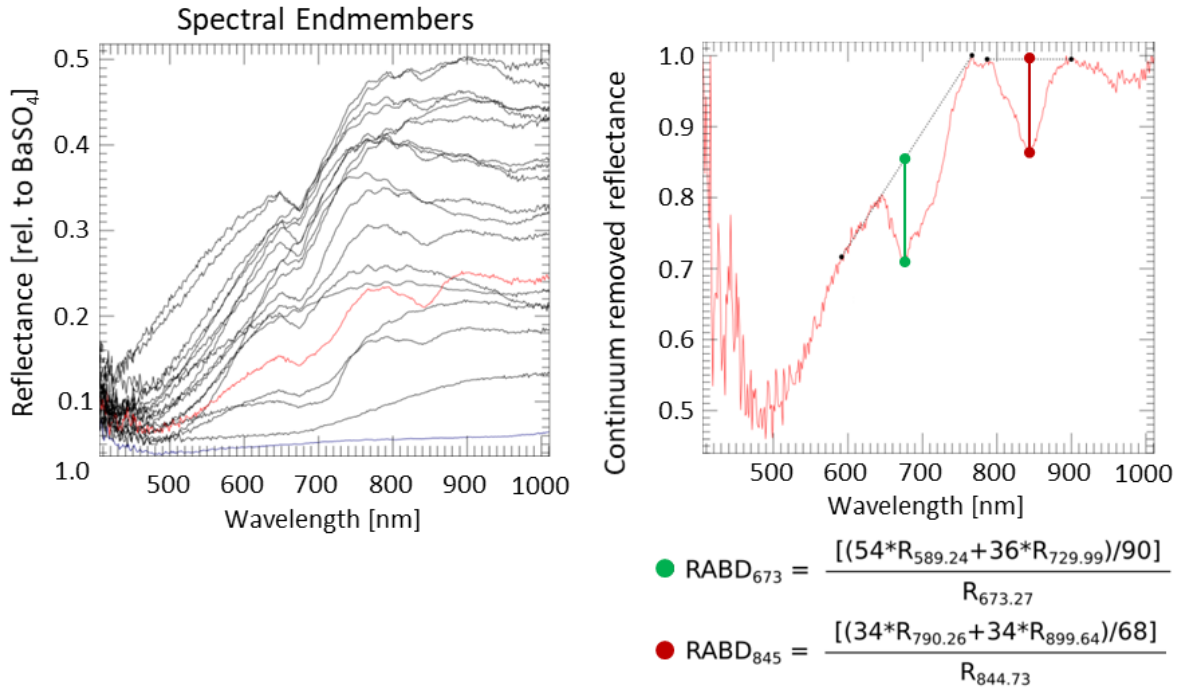

Figure 9: Spectral endmember derived from Spectral Hourglass Wizard. Two diagnostic absorption troughs are visible in the continuum removed spectrum. The relative absorption band depth (RABD) for the absorption band minimum absorption band minima at 673 and 845 nm can be calculated according the formula below the graph (Butz et al. 2015)

In order to transform the spectral indices $RABD_{673}$ and $RABD_{845}$ into absolute pigment concentrations (µg/g), a proxy-to-proxy calibration is performed using extracted pigment samples and measured using High Performance Liquid Chromatography (HPLC) (see 4.3.4.).

4.3. Destructive chemical analyses

4.3.1. Loss on ignition (LOI) and CNS analysis

The organic carbon content is determined according to Heiri et al. (2001). 200 mg of each sample are dried in the oven over night. Subsequently, the organic matter is burnt at 500 – 550 °C to carbon dioxide and ash. The samples are weighed before and after heating. The observed weight loss is proportional to the organic matter content for the sediment. The organic carbon fraction was calculated according to Dean (1974).

CNS (carbon, nitrogen, sulfur, C/N ratio) analysis was used to determine the source (lacustrine or terrestrial) of organic matter in the sediment and gives information about the productivity of the lake. The samples were wrapped in tin-foil and were analyzed on the Vario EL Cube CNS Elementar Analyzer at the Institute of Geography at the University of Bern. The

technique is based on combustion of the material in a pure oxygen environment and detection of different elements by frontal chromatography.

4.3.2. Fourier Transformed Infrared Spectroscopy (FTIRS)

The Fourier Transform Infrared Spectroscopy (FTIRS) technique is a fast and cost-effective technique to analyze changes in paleo-productivity of a lake system through time by estimating biogeochemical properties in the sediment. FTIRS was applied successfully to several lacustrine sedimentary records (Meyer-Jacob et al. 2014; Vogel et al. 2008). The wavenumber-specific excitation of polar bonds in molecules by infrared radiation is used to identify organic and minerogenic components. With the spectral information and an adequate calibration model, it is possible to a quantitatively determine the biogenic silica (BSi) content.

For this purpose, 0.011 g of 71 freeze-dried and powdered/homogenized sediment samples were homogenized with 0.500 g of oven-dried spectroscopic grade potassium bromide (KBr) and analyzed with a FTIR-Spectrometer at the Institute of Geology, University of Bern (Vogel et al. 2016). The Bruker Vertex 70 instrument is equipped with of a liquid nitrogen cooled MCT (mercury-cadmium-telluride) detector, a KBr beam splitter, and a TS-XT accessory unit (multi-sampler). Each sample was scanned 64 times at a wavenumber resolution of 4 cm^{-1} (reciprocal centimeters) for the wavenumber range from 520 cm^{-1} to 3750 cm^{-1} with the aperture set to 8 mm in diffuse reflectance mode. In order to avoid humidification, the samples were stored in a desiccator until the measurement. The sample spectra were normalized by linear baseline correction. BSi concentrations were inferred by using the independent FTIRS BSi calibration (Meyer-Jacob et al. 2014) and a site-specific calibration (Vogel et al. 2008). For the site-specific model, a wet-chemical BSi extraction was applied (see. 4.3.3). These data were square-root transformed and used to calibrate FTIRS spectra using a 2-component Partial Least Square Regression (PLS) model.

4.3.3. Wet-chemical biogenic silica extraction

The absolute BSi concentrations in 19 sediment samples were determined by using a wet alkaline leaching approach and ICP-MS measurement. First, the organic matter was removed by hydrogen peroxide (H_2O_2). In the organic-rich sediment of Lake Rzęśniki several applications of H_20_2 were needed to remove the organic matter completely. Then, 10 ml of the NaOH [1 mol/l; 1N] leaching solution was added to each sample. For 3 h, the samples were placed into the drying chamber at 90°C. After each hour, the sample tubes were shaken, placed into the ultrasonic bath, and put back into the oven (Ohlendorf & Sturm 2008). The supernatant solution was then measured with the inductively coupled plasma mass-spectrometer (ICP-MS) at the Institute of Geography, University of Bern.

4.3.4. Pigment analysis – High Performance Liquid Chromatography (HPLC)

The applied methodology for pigment extraction is based that on Reuss et al. (2005), refined by Sanchini et al. (2019, submitted) (Fig. 10). Due to the labile nature of pigments, cores should be stored under dark and cold conditions in order to prevent pigment degradation. The samples and extracts should be protected from light whenever possible.

Overall, 39 samples were analyzed along the entire composite core from Lake Rzęśniki with a discrete sampling resolution of 20 cm. For pigment extraction, 0.5g of freeze-dried and homogenized sediment was used. The extraction included three sequential extraction cycles. Firstly, in order to sufficiently extract pigments, 5 ml of acetone 95% solvent was added to the samples, followed by a vortex (1min), sonication (1 min) and centrifugation (10min) step. After centrifugation, the supernatant was removed with a glass pipette and stored in a glass vial. This step was repeated three times. Afterwards, the water in the supernatant was removed by passing it through a 10 ml column filled up with glass wool, 3 g of Dionex™ ASE ™ Prep DE, 1 g of Dionex™ ASE ™ Prep MAP, 1 g of Dionex™ ASE ™ Prep DE and glass wool (from bottom to top). The vials were rinsed three times with 1 ml acetone 95%. The column was pre- and post-conditioned with 10 ml of acetone HPLC grade 95%. The third step includes the concentration and reconstitution of the water free supernatant. For this, the supernatant was placed under a N_2 evaporator on a heating plate (35°C) to speed up the solvent pre-concentration. The obtained dry crust of pigments was reconstituted with 2 ml acetone HPLC grade 100% and filtered (0.2 um Nylon fisher Brand). The final solvent was stored at -20 °C until further analysis.

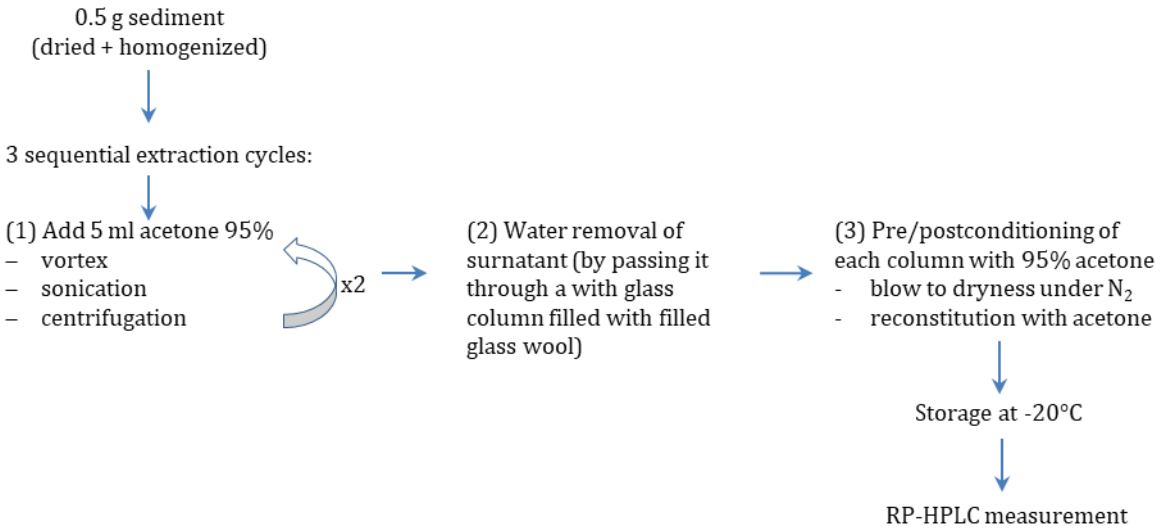

Figure 10: Schematic overview of the pigment extraction method

The final supernatants were quantified by reversed-phase high performance liquid chromatography (RP-HPLC). The instrument (Agilent Infinity 1260 series) was equipped with a G7117C photodiode array detector (DAD) and a G7121A fluorescence detector (FLD). 25 µL of the extracted sample in acetone 100% was injected onto Ominsphere (250 nm x 4.6 mm, 5 µm) through an Omnisphere replacement guard column (10 mm x 3nm). In order to accurately identify sedimentary pigments, the retention time and absorption spectrum of unknown pigments are crucial (Reuss et al., 2005). Pure and mixed pigment standards were used. Pigments were identified and quantified by setting the DAD detector at different wavelengths of absorption. For instance, the sensitivity is highest at 365 nm for Bphe-*a*, 432 nm for Chl-*a*, at 468 nm for Chl-*b*, 408 nm for pheopigments-*a* and 450 nm for carotenoids. The FLD detector was used to double check the identified pigment peaks in the chromatograms. Pigment preservation indices (CPI and Chl-*a* index) were calculated according to Buchaca and Catalan (2008). Total phosphorus inferred from total carotenoids was calculated using the calibration model reported by Guilizzoni et al. (2011).

4.4. Chronology - Radiocarbon dating

In paleolimnological studies radiocarbon dating is often the primary method of choice. Radiocarbon (^{14}C) is formed by the bombardment of nitrogen isotopes (^{14}N) by neutrons in the atmosphere. ^{14}C is oxidized to $^{14}CO_2$, which is used in the plant photosynthesis. The molecule then becomes incorporated into the tissue of organisms with a certain $^{14}C/^{12}C$ ratio close to the atmospheric ratio at the time of absorption (Blaauw and Christen 2005). After the organism dies, this ratio becomes unstable and begins to decrease. Determining a radiocarbon age is then possible by measuring the ^{14}C activity and calculating the percent modern carbon (pMC) ($\lambda_{1/2}$ = 5,730 years) (Cohen, 2003). These radiocarbon ages need to be calibrated into years before present (BP) with an appropriate calibration curve, because radiocarbon and calendar years have a non-linear relationship. This is due to variations in the ^{14}C production and the $C0_2$ concentration in the past (Cohen 2003).

25 macrofossil samples were measured to estimate the age of the sediment material in Lake Rzęśniki. In order to avoid reservoir effects only terrestrial plant macrofossils were used (Cohen 2003). The samples are measured by Accelerated Mass Spectrometry (AMS) at the MICADAS ^{14}C AMS at the University of Bern (Synal et al. 2007). In order to calculate the age-depth model, the bayesian BACON modelling approach (Blaauw and Christen 2011) was used (rbacon package 2.3.9.1). For calibration, the IntCal13 calibration curve for the northern hemisphere was applied.

4.5. Statistical analyses

The data analysis includes descriptive and multivariate approaches. A principle component analysis (PCA) was performed on the XRF and pigment datasets for tracing the major underlying trends and identifying compositional assemblages in the sediment core. Both datasets were standardized (mean= 0, standard deviation= 1) before analysis. The pigment data was square root-transformed and a logarithmic transformation was applied on the XRF dataset. A broken stick model assessed the PCA significance. PCA scores were considered as elemental and pigment temporal variability in the sediment core.

Constrained hierarchical clustering methods were then used to subdivide the time series and facilitate the description and comparison of the clusters. Biostratigraphic zones in the pigment data set were detected by Constrained Incremental Sum of Squares cluster analysis (CONISS) (Grimm 1987). Clustering was performed on the standardized and square root-transformed data set. In order to identity statistically different zones in the XRF data and geochemical sediment composition, a CONISS linkage method was applied. The data set was standardized and log-transformed. The statistical significance of zone boundaries was tested by a broken stick model (Bennett 1996). All statistical tests were performed using R version 1.1 463 statistical software (R Development Core Team).

5. Results and interpretation

5.1. Sediment description

In order to characterize the lake sediment core from Lake Rzęśniki a visual description was done before subsampling on fresh sediment. The lithological description revealed five facies. The definition for each facies is given in Fig. 11. A detailed sediment description table can be found in the attachment (Table A.1.1.).

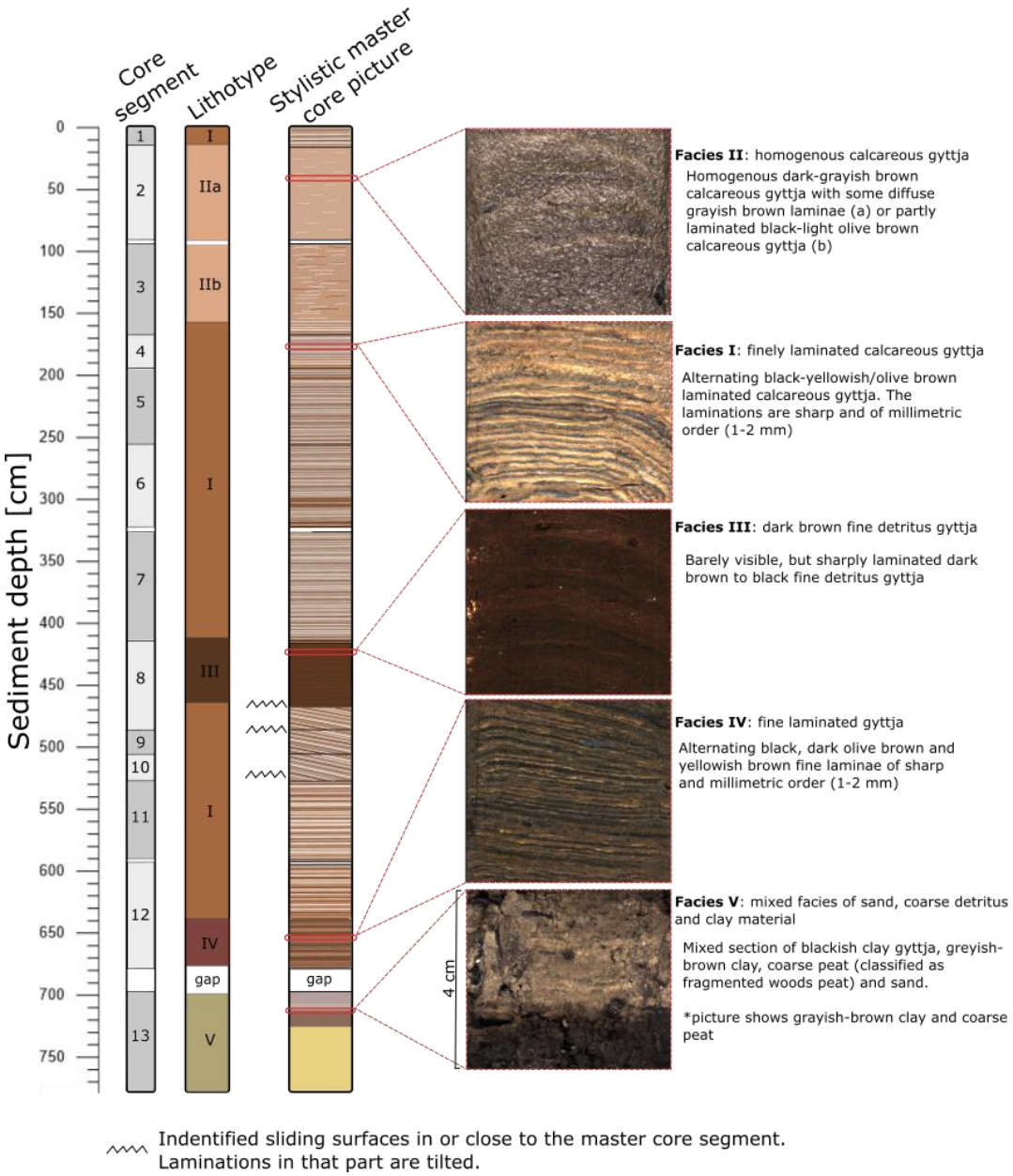

Figure 11: Sediment description of the master core of Lake Rzęśniki. A stylistic core picture with the defined facies and their definition is shown. For each facies, a sediment picture example is given. In order to see the lamination, the picture of facies III is color adjusted.

The sediment of Lake Rzęśniki is laminated throughout almost the entire core. Background sedimentation is characterized by sharp laminations at a millimeter scale, which are composed of an organic dark and a calcareous white lamina (facies I). The color of the laminae changes slightly along the core.

The core bottom (771 - 695 cm) appears very different compared to the rest of the sediment. Peat and a light and dark clay overlay coarse sand (facies V). Olive-brown fine laminations are described in a sediment depth of 674 and 638 cm (facies IV). Above this segment, between 637 and 470 cm, the sediment shows again characteristic background sedimentation with alternating fine light and dark laminae. In this core segment, laminations are tilted and show deformation or sliding features in and outside the defined master core segments. Between 469 and 417 cm, the sediment is much darker in color (facies III). The texture is dense and fine-grained. Barely visible dark laminations can be recognized. The transition between background lamination and this segment appears very sharp. A clear sliding surface is observed on the bottom of this segment. Right above, a second 1 cm thick dark layer is visible. Above this segment, background sedimentation with fine laminations (416 - 170 cm) is present. The core segment between 15 and 169 cm is poorly laminated. Between 92 and 169 cm the sediment shows weak and often disturbed laminations (facies IIb). Between 15 and 91 cm the sediments are nearly homogenous, with only some diffuse light laminae (facies IIa). The top 15 cm of the sediment is again laminated.

The fine biogenic and calcareous laminations in Lake Rzęśniki can most likely be described as biogenic varves (annually laminated sediment). The dark organic lamina is deposited in fall and winter. The light calcareous layer is deposited in spring and summer (Tylmann et al. 2013). When laminated sediment is under anoxic bottom water conditions, no bioturbation can affect the sediment preservation (Zolitschka et al. 2015). Therefore, periods of laminated sediment in Lake Rzęśniki can be interpreted as an indication of seasonal or permanent anoxic conditions in the bottom waters. Furthermore, the disappearance of those laminations could indicate better oxygenation of the bottom waters. The observed homogenous section in the sediment record of Lake Rzęśniki most likely represents a time with better oxygenation of the bottom water. The coarse section at the bottom of the core can be identified as a terrestrial phase before the lake developed. After deglaciation of the area, the environment was highly dynamic and a lot of glaciofluvial material (sand) covered the dead ice block. The peat was most likely formed on top of dead ice block (Tylmann et al. 2017). After the ice block melted, sand and peat deposited in the basin and gyttja accumulated atop glacio-lacustrine clays, which indicates the start of lake development.

Deformed and tilted sediments as observed in Lake Rzęśniki are often indications of mass movements in the lake basin. Sliding surfaces represent the contact zone between the moving sediment block and underlying sediment where erosion might take place, which can appear as a sediment hiatus in the chronology. Therefore, the tilted sediments are most likely originating from a different part of the basin and were transported as a slump to the lake center. The dark brown sediment on the top of these sections is interpreted as a second slump event from the littoral part of the lake basin. The clear sliding surface at the bottom and the fine dark layer on top, which likely formed from suspended material afterwards, can be taken as evidence for a second slump event. Nevertheless, the appearance of laminations and its dense and fine composition is unusual. Slumped sediment parts do not represent in-situ formation processes that are the focus of environmental and climate reconstructions. Therefore, the sections identified as slump material are excluded from the following analysis of the sediment record of Lake Rzęśniki.

5.2. Chronology

Radiocarbon dated samples were used to build the age-depth model with the Bacon modelling routines. Because one single model run was not able to sufficiently capture the sediment features, the illustrated age-depth model is constructed out of two separately calculated models (same settings; except adjusted accumulation rates), separated by the slump sequence. The prior definition of the slump was based on the lithological description. The slump ages were excluded from the final model calculation. Performance plots of the two model runs and ^{14}C macrofossil sampling are included in the attachment (Fig. A.2.2. Tables A.1.2 and 2.1).

Fig. 12 shows the age-depth model used for the reconstruction. The oldest sediments from Lake Rzęśniki are around 10 900 cal yr BP old. The slope of the plotted lines represents the sedimentation rate. Higher sedimentation rates are found at the top and at the bottom of the core sequences. The middle part of the core sequence shows a constant rate of sedimentation. Around a depth of 500 cm, age reversals are visible within the previous slump region that creates a gap of around 4800 years.

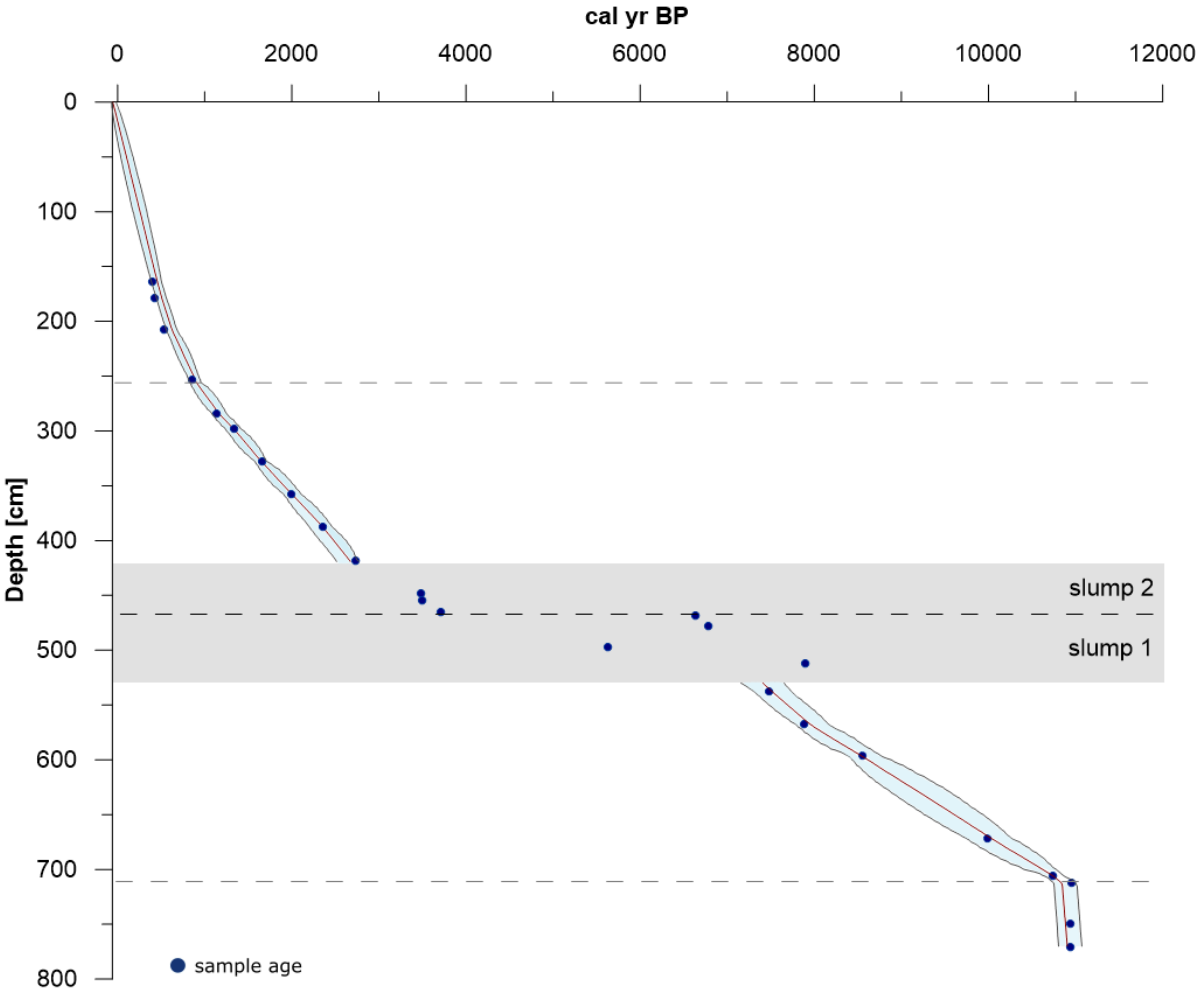

Figure 12: Age-depth Bacon model used for the reconstruction of Lake Rzęśniki. The age-depth model was calculated using Bacon 2.3.9.1 modelling routines with the IntCal13 calibration curve. The red lines indicate median ages modelled for each centimeter along the core. Calibrated ^{14}C dates are shown as blue dots. The 95% confidence interval of the modeled age-depth relationship is shown in blue. Two slumps are indicated in grey, whereas boundaries with changing accumulation rates are indicated as grey dashed lines. Sample ages from the slump area were excluded from the model calculation.

The radiocarbon dates reveal that the sediment record from Lake Rzęśniki covers nearly the entire Holocene. The lake developed in the early Holocene around 10 800 cal yr BP. The very high sedimentation rates at the base of the core can be interpreted as lithogenic sedimentation before the lake developed. The abrupt change in sedimentation indicates that the lake emerged relatively fast and quickly reached a sufficient depth to allow constant and fine-grained sedimentation. A slower lake development or lake level fluctuations during that period would probably appear as more dynamic sedimentation rates. These stable conditions remained until the Late Holocene. The sedimentation rate increased remarkably, which is interpreted as a change in the catchment conditions bringing more detrital material into the lake.

Age reversals are often indicative for slump events transporting older material from shallow parts of the basin to the deeper parts of the basin. Recently deposited sediment material is then overlaid by older sediments. In the case of Lake Rzęśniki, the slump might be more

complex, because the radiocarbon measurements revealed two age reversal on top of each other. One explanation could be that a massive sediment block slid down, broke into smaller parts and/or rotated, exposing old material on top of young material. The upper part of the slump instead shows constant sedimentation rates. Only according to the chronology, this part would be defined as "normal" sedimentation. Between the two parts (469 cm), a large jump in ^{14}C ages appears, suggesting a hiatus. The issue about the slump will be discussed further in detail in the discussion (chapter 6.4).

5.3. Geochemical composition

Geochemical analyses include data from high-resolution µXRF, LOI and CNS analyses (Fig. 13). The sampling resolution of the LOI and CNS dataset is 5 cm. Because of the amount of data, a selection of the most representative data is presented here. The complete LOI and CNS dataset is shown in the attachment (Fig. A.3.1). The XRF data is reported in absolute values, because the water content is quite stable over the core sequence, which makes the use of absolute values possible. The XRF dataset reported as element ratios (normalized against Ti) is shown in the attachment (Fig. A.3.2). The results of the constrained clustering and PCA analysis are shown in Fig 13. Fig. 14 and 15 present the results of the principle component analysis. Values within the slump were excluded from statistical analysis.

Fig. 13 shows the biochemical composition of the sedimentary record from Lake Rzęśniki relative to depth. The constrained clustering revealed four stratigraphic zones. In *cluster I* (770 - 720 cm) the sediment composition is dominated by high Ti and Si. Other elements show very low counts. The PCA scores reveal positive values for PC1 and negative values for PC2. *Cluster II* (720 - 190 cm) covers a long part of the sediment record. It is generally characterized by enhanced levels of Ca, Fe, S, Br, a higher Mn/Fe ratio and low Ti and Si counts. Ca counts increase in the first half of the cluster (bottom to slump), whereas Fe and Mn show high values at the bottom of *cluster II* and then steadily decrease. The S content fluctuates in this part. The second half of *cluster II* shows high contents of Ca and Fe. Some confined peaks of Mn are visible. Si, Ba, S and the ratios Si/Ti and Fe/Mn show constantly high levels. The Ti level in *cluster II* is constantly low. The scores of PC1 are negative, whereas the PC2 scores are fluctuating around 0. *Cluster III* (190-115 cm) is dominated by a remarkable increase of Ti values, while Fe, Ca and Mn levels decline. The S content and the ratios Si/Ti and Fe/Mn decrease to very low values. The scores of PC1 and PC2 turn positive. In *Cluster IV* (115 – 0 cm) Ca, Fe, Mn, S and Si/Ti continue to be low. Fe/Mn is highly variable. Ti is high at the bottom of *cluster IV* and decreases towards the top. The Br level, which

was rather constant over the whole record, peaks at the top of the record. The scores of PC1 become more positive. The PC2 scores instead decrease to less positive values.

Moreover, LOI_{550} and TC are remarkably stable along the core sequence (with the exception of much higher values in the peat and the top of the slump) and show average values of 25 % and 15 %. The TOC/TN ratio moderately decreases from 15 (*cluster II*) to 10 (*cluster IV*). The slump sequence has elevated Ti values, and elevated Ca in the lower portion. The upper portion contains almost no Ca and extremely high Si values.

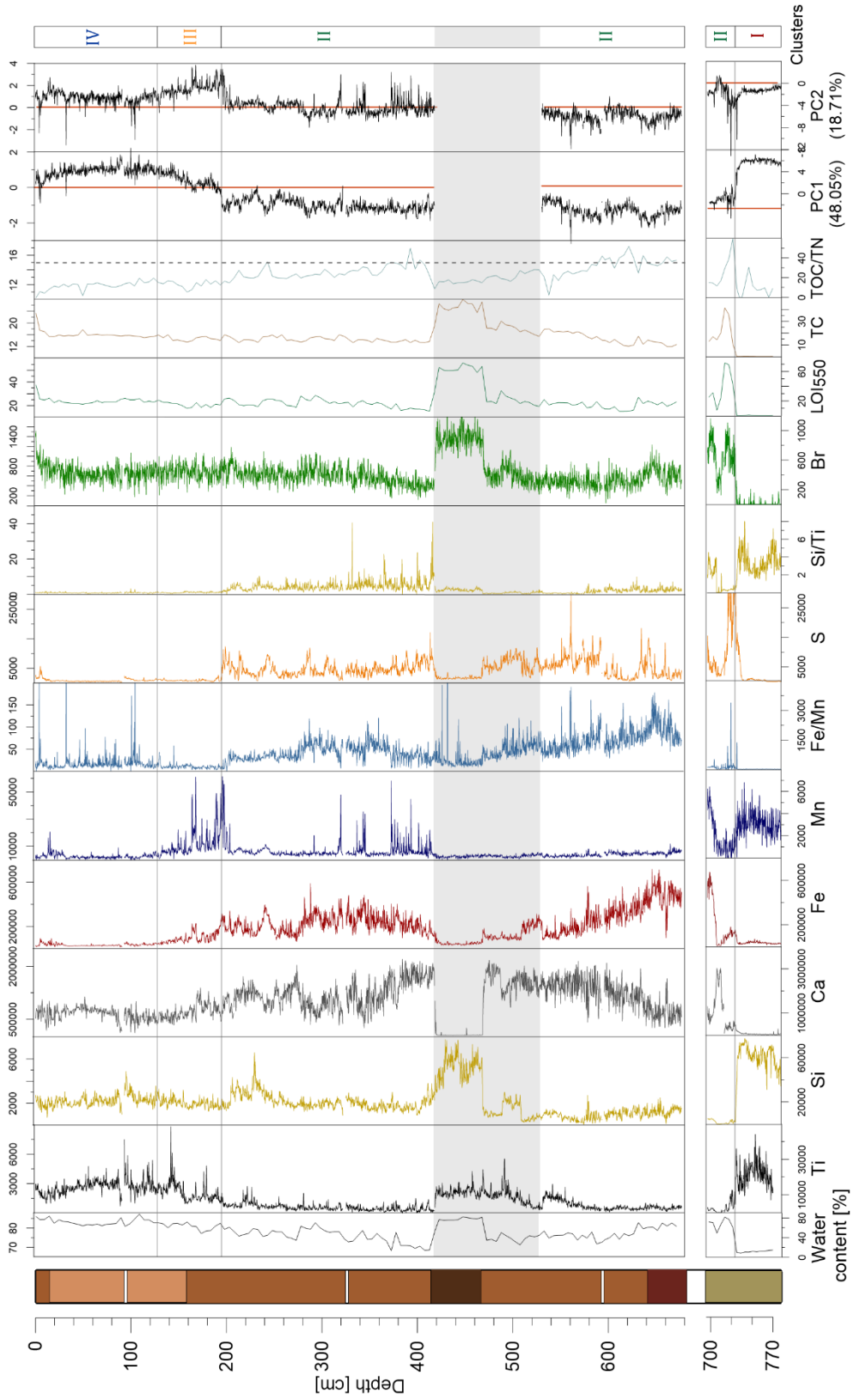

Figure 13: Geochemical composition of the sediment record from Lake Rzęśniki showing a selected dataset from XRF, LOI and CNS analyeis is shown in terms of depth. Additionally, the score values from principle component 1 and 2 are illustrated. Different scales were used for the upper section (0-680 cm) and the bottom section (700 -770cm). The slump is highlighted in gray. The gray lines show the stratigraphic zones according to constrained clustering conducted on the XRF data.

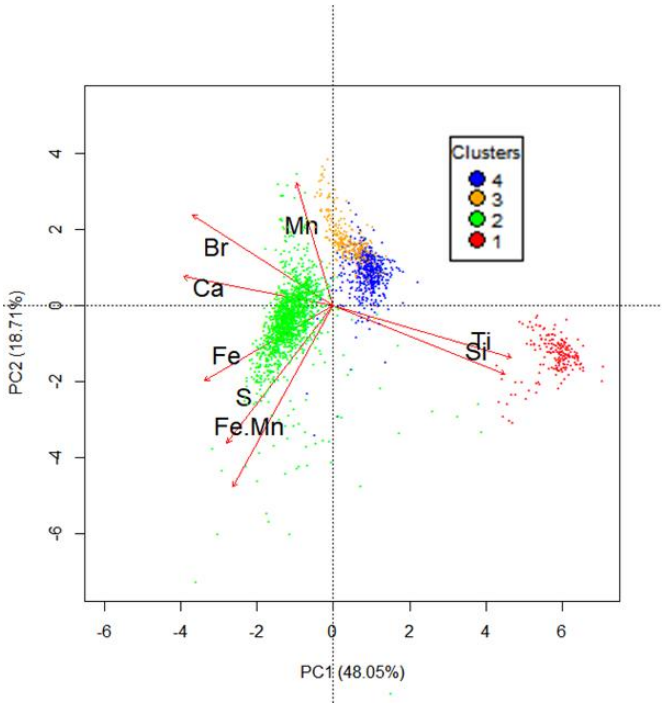

Figure 14: Biplot of the PCA with the XRF data set showing principle component 1 and 2.Indvidual sample points are shown according to their cluster affiliation.

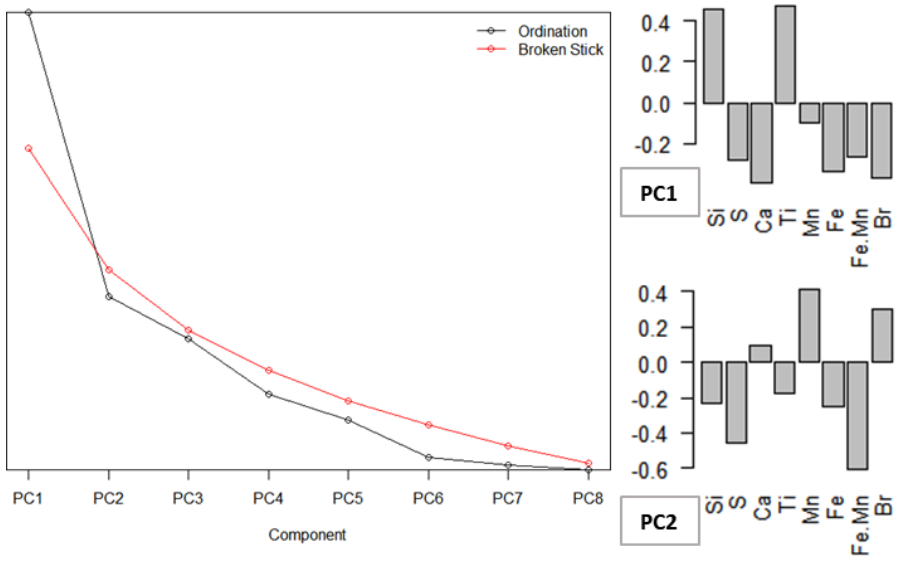

Figure 15: Broken Stick model for the PCA on the XRF dataset indicating one significant component. Additionally, the loadings for PC1 and PC2 are shown.

Fig. 14 and Fig. 15 show the results of the principle components analysis conducted on the XRF data set. According to the broken stick model only one principle component (PC) is significant, whereas the elbow structure (Thorndike 1953) in the scree plot indicates two principle components explaining most of the variance (Fig. 15). Indeed, PC1 explains 48.05 % of the variability, and PC2 an additional 18.71 %. The biplot and the PC-loadings reveal a clear clustering of the elements. PC1 is positively related to Ti and Si, which are found to be linked to the stratigraphic *cluster I*. PC2 shows a more diverse picture and samples from *cluster II* are spread along the second component. The elements Mn, Br and Ca are positively correlated and associated to *cluster II, III* and *IV*. Fe, S, and the Fe/Mn ratio are grouped highest in *cluster II* and show negative correlations to PC2.

The geochemical composition of the sediment and statistical analyses reveal fourclear lake stages where PC1 represents erosional processes and PC2 represents the changes in water column oxygenation. *Cluster I* represents the glacio-fluvial phase before the lake developed. Ti and Si show high values characteristic for enhanced catchment erosion during that period. The low organic matter content is indicated by low Br, TC, LOI_{550}. Overall sediment composition indicates allochthonous origin, represented by a positive PC1 contribution.

The transition from clastic sedimentation to biogenic sedimentation (*Cluster II*) is represented by a rapid decrease in Ti and Si. In turn, in-lake processes become more dominant (neg. PC1 scores). In addition, the decreasing TOC/TN ratio is an indication for an increase in aquatic production contributing to the organic matter pool (Meyers and Teranes 2001). The Fe/Mn ratio, used as a proxy for bottom water oxygenation (Naeher et al. 2013), indicates anoxic conditions. This coincides with low Mn values, because Mn is only deposited in the sediment if the hypolimnion is oxygenated (Hamilton-Taylor and Davison 1995). Negative contribution to PC1 indicates that Fe and Si are mainly deposited through in-situ processes and without significant contribution from detrital siliclastics through soil erosion. The abundance of Fe and S in the sediment suggests iron deposition as sulfide minerals (greigite, pyrite). The increasing Ca values are due to carbonate precipitation and deposition likely as a result of an increase in productivity possibly in combination with increased dissolved load inputs from soil weathering in the first half of *Cluster II*. Increased productivity is supported by the close correlation with Br indicated in the PCA. The simultaneous decrease of Fe might be a result of calcite dilution (Naeher et al. 2013). The Si/Ti ratio, which is diagnostic for biogenic silica formation, indicates a high contribution of BSi in the second half of *Cluster II*. Local Mn peaks beginning after the slump unit (417 - 320 cm) indicate sporadic mixing of the water column, until more permanent anoxic conditions seem to establish around 320 cm. In turn, the geochemical profiles of Fe and S indicate distinct periods of strong lake stratification and anoxia, where stable Fe-sulfides are formed and deposited in the sediment. Ca shows local low values during these periods, which might be explained by pH mediated Ca-dissolution during anoxic conditions (Gulati 2017). However, a matrix effect between Fe and Ca as observed in the bottom part of the core might also be a triggering these changes.

Increasing catchment erosion (*Cluster III*) is indicated by a rise in Ti and coincides with a decline of the Fe/Mn ratio and a high abundance of Mn, suggesting the establishment of oxic bottom water conditions. Simultaneously, deposition of Fe and S is reduced due to regular oxygenation of the bottom water. The dominance of erosional processes and oxic conditions is also indicated by a change in the PC scores. Unlike Ti, the relatively stable Si counts do not give an indication of lithogenic Si input.

Similar sediment and lake conditions are observed in *Cluster IV*. The high variability of Fe/Mn is mostly due to very low Fe or Mn counts and might be not diagnostic for bottom water oxygenation. A decline in Ti indicates an overall decline in catchment erosion, whereas the modern eutrophication of Lake Rzęśniki is represented by high Br, LOI_{550} and TC values at the very top of the sequence (above 15 cm). In addition, Br, LOI_{550} and a decreasing TOC/TN ratio, represent a moderate increase in lake productivity over the whole sediment sequence.

5.4. Pigment stratigraphy and biogenic silica

Changes in the sedimentary pigment stratigraphy (Fig. 16) illustrate changes in the trophic state and algal community in the lake. A few pigments with very low concentrations or isolated high abundances in the slump section are not included in the stratigraphy plot. The pigment peaks of zeaxanthin and lutein could only be separated in the first few samples on the chromatogram and are shown as a sum of both pigments. All HPLC derived pigments were expressed in nanomoles per gram sediment organic matter (nmol g^{-1} OM) in order to avoid dilution effects of clastic material from the catchment (Guilizzoni et al. 1983; Leavitt 1993a). HSI-inferred pigments are reported in µg g^{-1}. In addition, biogenic silica was measured by FTIRS. Constrained clustering and principle component analysis was conducted on the dataset (Fig. 16 and 17). Additionally, the HPLC data is used to infer absolute concentrations from hyperspectral indices (Fig. 19 and 20). The calibration model for FTIRS inferred BSi is shown in Fig. 21.

The CONISS-analysis resulted in five significant pigment zones (Fig. 16). *Zone I* (770 - 720-cm) is characterized by low pigment concentrations overall. HSI inferred Bphe-*a* shows high concentrations at the top of Zone I, which is not reflected in the HPLC-measured Bphe-*a* values. *Zone II* (720 - 525cm) illustrates overall low pigment concentrations. Bphe-*a*, pheophytin-*b*, cyanobacteria (zeaxanthin, canthaxanthin, echinone) and chromophyte (diadinoxanthin, diatoxanthin, fucoxanthin and alloxanthin) pigments appear in the record but stay at low concentrations. The carotenoid-inferred TP concentration is low in this zone (~7.5 ug/l). *Zone III* (418 - 190 cm) reveals a high abundance of cyanobacteria pigments, pheophytin-*a* and Bphe-*a*. The high resolution HSI data show that Bphe-*a* fluctuates around a high level, including pronounced periods with high Bphe-*a*. Green algae pigments (violaxanthin, antheroxanthin) appear for the first time in the stratigraphic record and TP concentrations are stable at a high level. A moderate increase of total green pigments and Chl-*a* derivatives can be observed. *Zone IV* (190-20 cm) is characterized by an abrupt decrease of Bphe-*a*, pheophytin-*a*, green algae and cyanobacteria pigments as well as TP concentrations at the bottom of *Zone IV*. Chl-*a*, pheophytin-*a* and pyropheophorbide-*a* instead show local high concentrations. The increasing trend in

chromophyte pigments and biogenic Si from *Zone III* continues also in *Zone IV*. Biogenic Si in particular reaches high values. *Zone V* (20 - 0 cm) shows the highest pigment concentrations. Green pigments, chlorophyll derivatives, and green pigments show the strongest increase. It is noteworthy, that Bphe-*a* increases again to high concentrations. Chromophyte pigment concentrations stay constantly high except for alloxanthin that shows a pronounced peak.

In general, chlorophyll a and its derivatives increase constantly over the record. Bphe-*a* and pigments associated with cyanobacteria and chromophytes appear earlier in the sediment than other pigments and dominate the pigment composition throughout the sediment record of Lake Rzęśniki. The different pigment ratios appear with some variability, quite stable over the record. Furthermore, the apparent dual composition in pigments of the slump sequence is worth mentioning. In the first part of slump sequence, quite similar pigment compositions are observed compared to the underlying sediment. High carotenoid concentrations (green algae, cyanopigments, chromophyte pigments) and a high biogenic silica content are found in the second part of the slump.

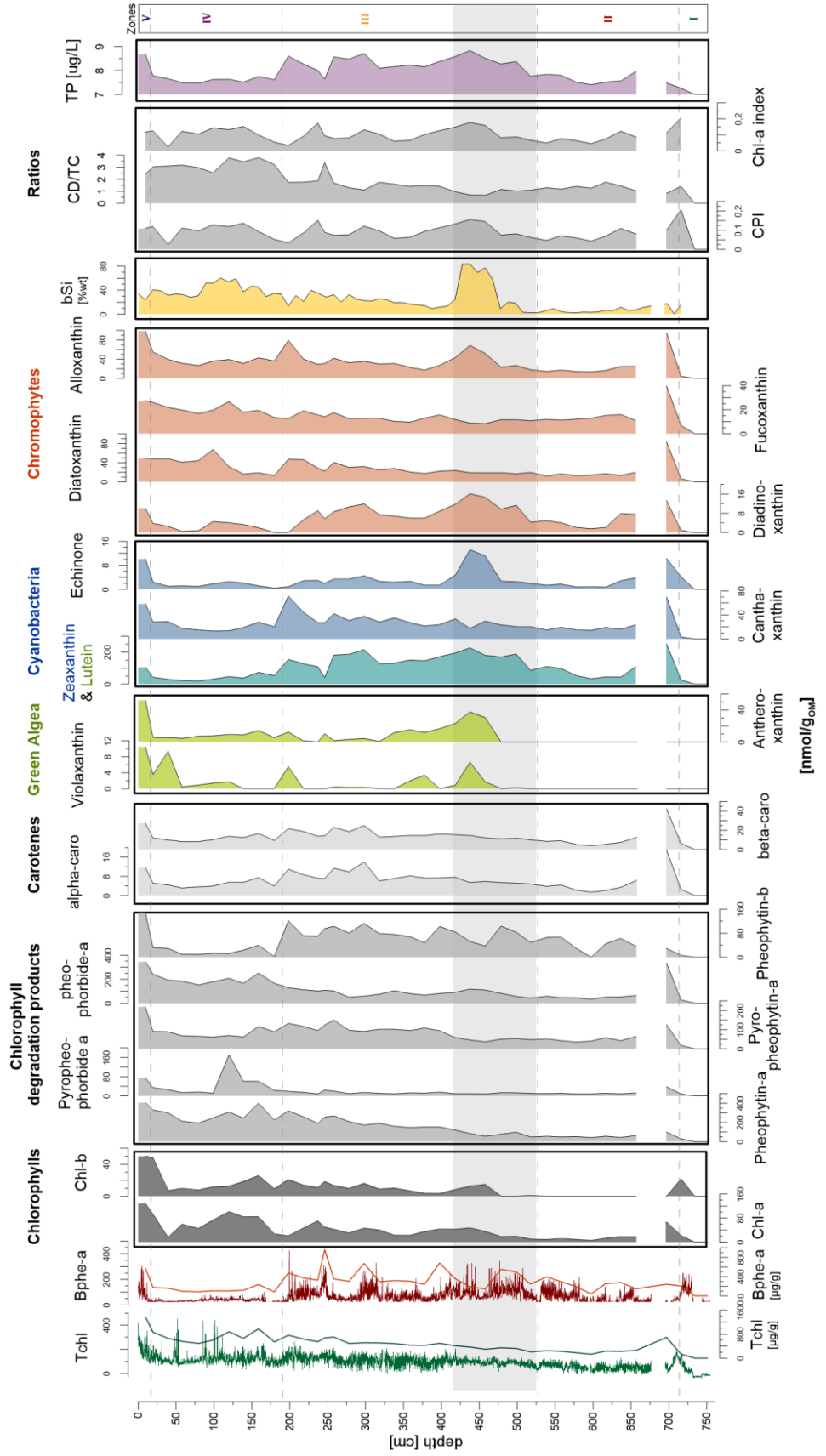

Figure 16: Pigment stratigraphy showing HSI-inferred pigments values in high resolution and HPLC-derived measurements plotted by depth. Pigment ratios and TC-inferred total phosphorus concentrations (TP) are illustrated at the right hand side. The slump region is highlighted in grey. Stratigraphic zones (dashed lines) were defined by constrained clustering.

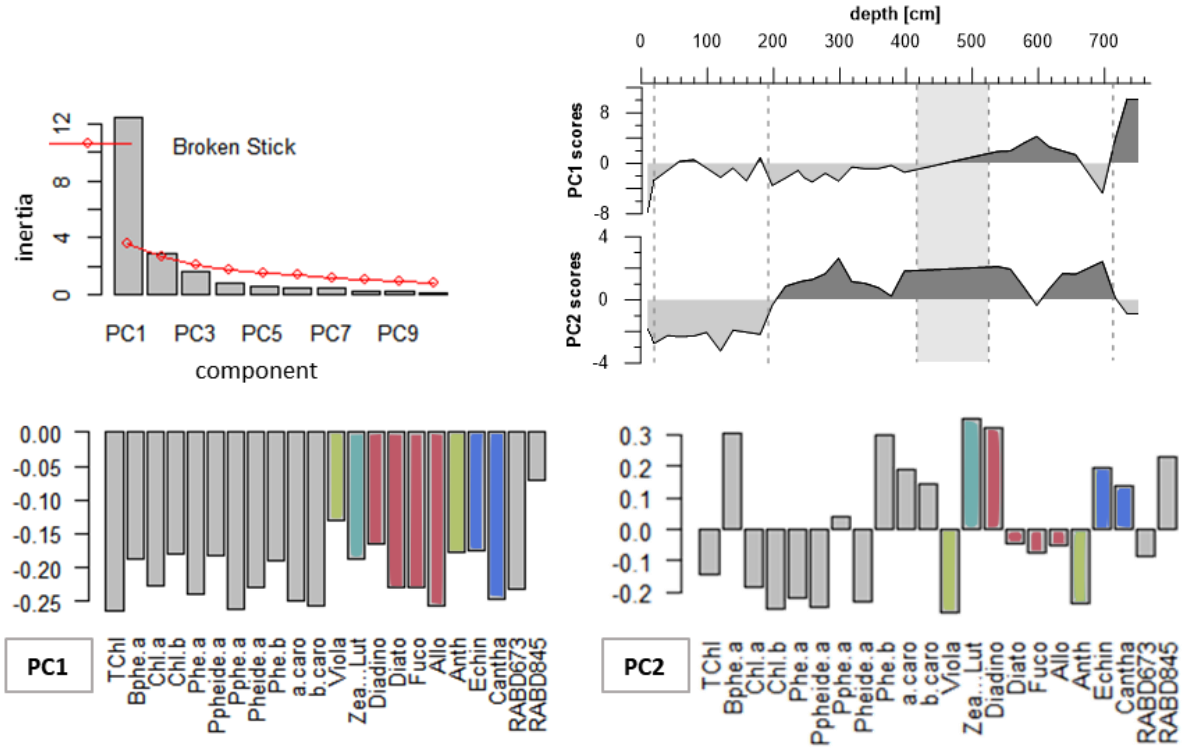

Figure 17: Screeplot with broken stick, loadings and scores of the first two principle components of the PCA applied on the pigment data set. Dashed lines in the score profiles indicate the cluster boundaries. Coloring of loadings was done according to the pigment groups.

The statistical analysis revealed two significant principle components (Fig. 17). PC1 explains 60 % of the variance. All analyzed pigments are negatively correlated to PC1. The second component shows a more diverse structure and explains 13.9 % of the variance of the pigment assemblage. Pigments with strong positive loadings include Bphe-*a*, pheoporbide-*b*, Zeaxanthin and Lutein, and Diadinoxanthin. Chl-*a* and its degradation products show negative loadings.

These clusters are also displayed in the PC scores (Fig. 17) and biplot (Fig. 18). Pigments that are positively correlated to PC2 generally correspond to *Zones III* and *II*, which are dominated by pigment assemblages of cyanobacteria and the chromophyte pigment diadinoxanthin. Pigments that are negatively correlated to PC2 are associated with *Zones IV* and *V*, where green algae and chromophytes pigments are dominant. *Zones II* and *I* are associated with positive PC1 scores. PC1 scores follow a gradual decrease from bottom to top of the record, corresponding to a gradual switch from positive to genitive values. PC2 scores show a rapid shift from positive to negative values from bottom to top.

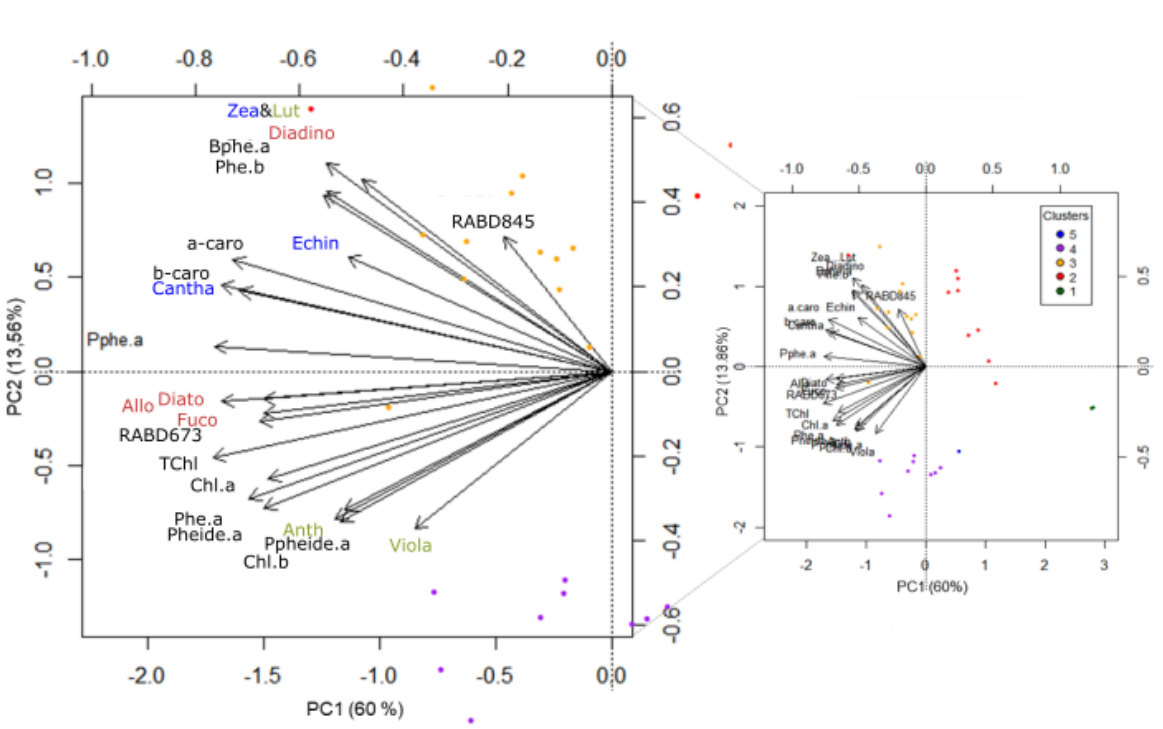

Figure 18: PCA biplot with the first and second principle components. The sample points are included according to the stratigraphic clusters. A close up on the left shows the pigment names according to their affiliation.

The pigment stratigraphy reveals distinct phases of productivity changes and related phytoplankton assemblages in Lake Rzęśniki. In the early phase of the lake (*Zone II*), sedimentary pigments indicate low productivity and oligotrophic conditions. The pigment concentrations are low overall and the low TC-inferred total phosphorus (TP) concentration suggests oligotrophic conditions. No pigments were found in the terrestrial phase (*Zone I*). All identified pigments had negative contributions to PC1, indicating that the majority of the variance in the dataset is driven by overall lake productivity. A continuous increase of primary production and total biomass since the early phase of the lake is indicated by long term positive trends for TChl, chlorophyll α, pheophytin-α and ββ-carotene (Leavitt and Hodgson 2001).

Zone III represents a period of high productivity dominated by cyanobacteria and the chromophyte pigment diadinoxanthin (Diadino), displayed in a positive contribution to PC2. Diadino is generally associated with the presence of diatoms and dinoflagellates, but can be a present compound in many other groups. Therefore, its presence might not be a clear indication for diatoms or dinoflagellates. Indeed, PCA analysis suggest a closer association with anoxic and eutrophic conditions. Cyanobacteria are associated generally to more nutrient-rich conditions (Wetzel 2001). Cyanobacteria have a competitive advantage in eutrophic and anoxic waters, because of their capability to fix atmospheric N_2 and migrate quickly through the water column (buoyancy alteration) (Wetzel 2001). Filamentous and colonial cyanobacteria are suggested by

canthaxanthin (Catha) abundance and N_2-fixing filamentous cyanobacteria are indicated by echinone (Echin) (Waters et al. 2013; Deshpande et al. 2014).

Zeaxanthin (Zea) and lutein (Lut) are presented together and represent, therefore, a mixed signal of colonial cyanobacteria (Bianchi et al. 2002) and green algae (Waters et al. 2013). However, Zea can also be present in crysophytes and dinophytes or as a minor pigment in green algae (Roy et al. 2011). Consequently, the profile of Zea+Lut might not give a clear interpretation for a specific phytoplankton group. Furthermore, the various sources explain the high concentrations found in the profile. Violaxanthin (Viola), antheroxanthin (Anth) and chlorophyll-β (Chl-β) present green algae dynamics (Leavitt and Hodgson 2001; Waters et al. 2013). Their highly fluctuating abundance in *Zone III,* specifically Viola and Anth might be an indication for competitive replacement by cyanobacteria (Wetzel 2001). However, these compounds are highly labile and selective grazing by zooplankton might even affect green algae abundance in the sediment record. This cannot be excluded or validated, because the CP and Chl-α indices, which assess changes in preservation, are quite variable during that time.

The abundance of bacteriopheophytin α (Bphe-*a*) is an indication for the presence of anaerobic sulfur bacteria, which occur at the chemocline of permanent or seasonally stratified lakes (Van Gemerden and Mas 2004). The two pronounced peaks at 250 and 300 cm, with very high Bphe-*a* concentrations are evidence that the water column was permanently stratified during these periods (meromixis). Occasional mixing and oxygenation of the water column, higher turbidity of the water or too low an anoxic layer not reaching the photogenic zone reduces the Bphe-*a* immediately (Parkin and Brock 1980). The nutrient-rich conditions indicated by the phytoplankton assemblages coincide with enhanced TC-inferred TP concentrations.

The transition of *Zone III* to *Zone IV* represents an abrupt disappearance in meromictic conditions, where a rapid decrease of Bphe-*a* is observed. This fast transition from meromictic to holomictic conditions led to a pronounced change in the phytoplankton community. Chromophytes and green algae replaced cyanobacteria as the dominate species. Chromophytes, including bacillariophyta (diatoms), dinophyta (dinoflagellates), and crysophyta (golden algae), are ubiquitous and fast-growing compared to cyanobacteria giving them a competitive advantage. Diatoms and dinoflagellates show the highest abundance in less productive conditions (Wetzel 2001). The high diatom occurrence is indicated by the pigments fucoxanthin (Fuco) and diatoxanthin (Diato) and generally high values of BSi. A high CD/TC ratio and a decrease in TP represents the establishment of mesotrophic conditions in *Zone IV*. Enhanced zooplankton grazing at the transition event is shown by local decrease in Chl-*a* and the simultaneous increase of its derivative pigments pheophytin *a* and pheophorbide *a*. In addition, enhanced transformation to colorless compounds is indicated by a local decline in the preservation indices

(CPI and Chl-*a*). Despite the regular oxygenation of the bottom waters, the conditions of preservation seem to be still sufficient to preserve labile pigment compounds in the sediment, e.g. Chl-*a* (Leavitt and Hodgson 2001). Stable Chl-*a* and CP indices confirm this observation. The higher variance observed in the TChl concentration retrieved by HS imaging presents pronounced seasonal changes in productivity related to regular mixing of the water column (Wetzel 2001). Peaks in TChl can be interpreted as algae blooms.

Zone V represents a re-eutrophication and the strengthened stratification. Overall high pigment concentrations and TC-inferred TP concentrations indicate a rise in trophic state. The statistical analyses reveal that this cluster is dominated by the rise in Bphe-*a*, a pigment associated to permanent stratification of the water column (Butz et al. 2016). The high concentrations of pigments in *Zone V* might have additionally been caused by overall better pigment preservation, as shown by enhanced concentration of labile pigments (e.g. chlorophyll a, violaxanthin, neoxanthin, peridin) (Leavitt and Hodgson 2001). In contrast to chloropigments and other carotenoids, diatoxanthin (Diato), fucoxanthin (Fuco) and FTIRS inferred BSi are not increasing in the uppermost zone. This might be caused by light-limitation, by other phytoplankton taxa or the rising silica-limitation through the phosphorus enrichment in the water column, which in turn initiated the diatom production (Schelske et al. 1987).

In general, the CD/TC ratio matches the TC-inferred TP concentrations very well in *Zones III* and *IV*, whereas the CP and Chl-*a* indices give a more inconsistent picture. Due to the labile structure of chlorophylls, the chlorophyll derivatives pheophytin *a* and pheophytin *b* show generally higher concentrations than their parent components. They are typical pigments of decaying communities (Buchaca and Catalan 2008). The abundance of pyropheo-pigments (pyropheophorbide *a* and pyropheophytin *a*), associated to dinoflagellates, diatoms and crysophytes (Buchaca and Catalan 2008), correspond with detected chromophytes carotenoids and BSi content. The Chl-derivative pheophorbide *a* is commonly used as grazing indicator (Leavitt and Hodgson 2001; Reuss et al. 2005). It steadily increases from *Zone III* to *V* proportional to Chl-*a* and does not indicate significant changes in grazers community.

Spectral indices $RABD_{673}$ and $RABD_{845}$ calibration

The calibration of the HSI indices ($RABD_{673}$ and $RABD_{845}$) with absolute concentrations of total green pigments and bacteriopheophytin *a* determined by HPLC are shown in Fig. 19. The proxy-proxy calibration for total green pigments resulted in a Pearson correlation of r = 0.88 ($p < 0.001$) and a coefficient of determination of $R^2_{adj} = 0.77$ ($p < 0.001$). The root mean squared errors of prediction (RMSEP) varies between 26.66 (k-fold) and 26.79 µg/g (bootstrapped) with corresponding uncertainty of around 10%. Normality distribution of the residuals was tested with the Shapiro-Wilk-test and the Kolmogorov-Smirnov-test. Both tests indicate normal distribution of the residuals, making interferences with this calibration model possible. Corresponding residual plots are in the attachment (Fig. A.3.3).

The linear regression model for bacteriopheophytin *a* resulted in a Pearson correlation of r = 0.93 ($p < 0.001$) and a coefficient of determination of $R_{adj} = 0.87$ ($p < 0.001$). The root mean squared errors of prediction (RMSEP) varies between 18.71 (k-fold) and 16.27 µg/g (bootstrapped). The corresponding uncertainty lies around 7.7 %. The Kolmogrorov-Smirnov test indicates normal distribution of the residuals, whereas the Shapiro-Wilk normality test rejects that the residuals originate from a normal population. Residual analysis revealed that samples 1 and 17 cause a tailing in the normal QQ-plot (Fig. 20b) and higher leverage (Fig. 20d). A weak heteroscedastic pattern is visible in Fig. 20c. Based on the Kolmogorov-Smirnov-test interferences from this model are valid.

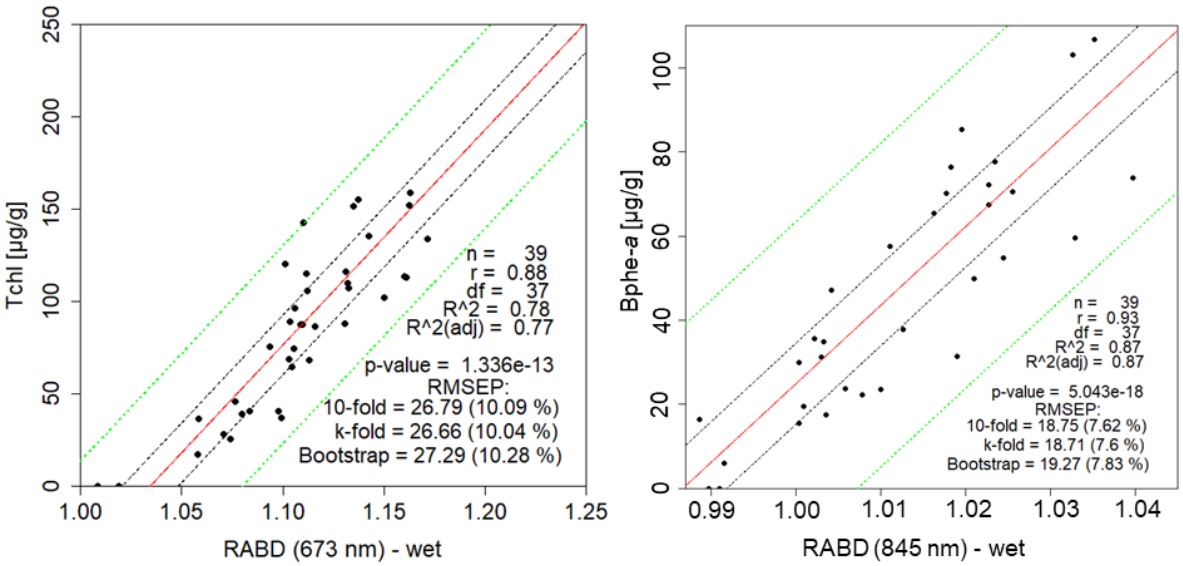

Figure 19: Linear regression model of $RABD_{673}$ with green pigment concentrations (A) and of $RABD_{845}$ with Bphe-a concentrations (B). The black points represent the 39 samples, the dashed lines show the 95% confidence intervals for the regression function (black) and predicted values (green).

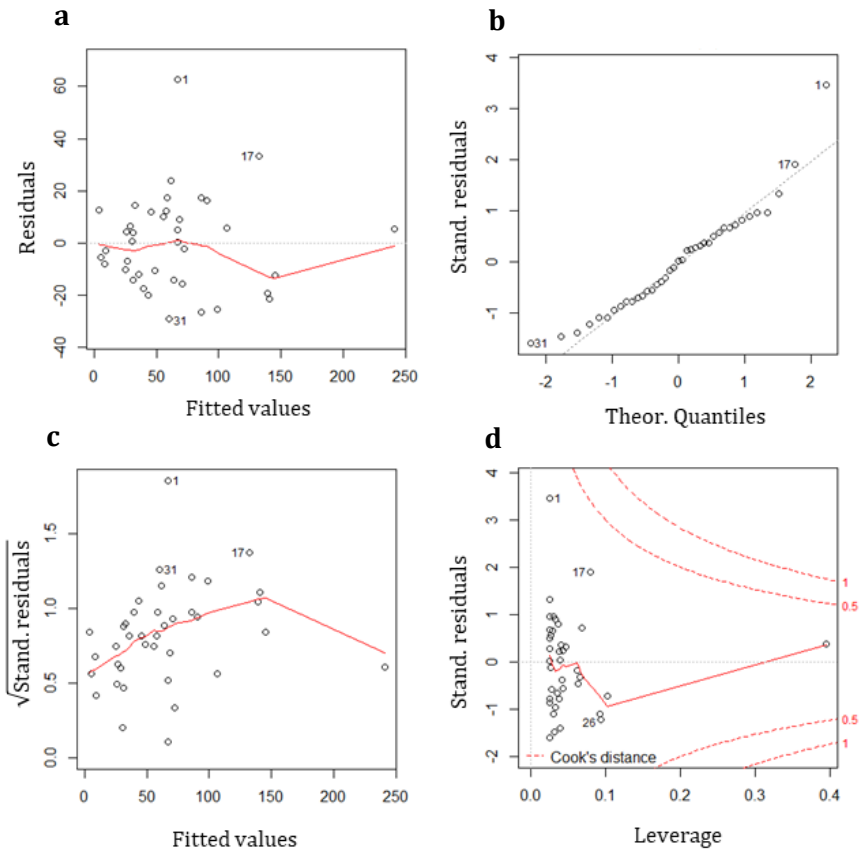

*Figure 20: Different residual plots of the linear calibration model of $RABD_{845}$ with absolute Bphe-a concentrations are shown in **a)** residuals versus fitted values, **b)** standardized residuals versus theoretical quantiles, **c)** scale-location plot and **d)** standardized residuals versus leverage plot.*

BSi calibration

The calibration of FTIRS data using the site-specific calibration model is shown in Fig. 21. The resulting cross-validated (CV) coefficient of determination (R^2_{CV}) of 0.86 and a root mean square error of cross-validation ($RMSE_{CV}$) of 10.03 (% BSi), resulting from 7-fold validation show that the FTIRS was successfully calibrated to determine BSi in Lake Rzęśniki sediment samples. The independent FTIRS BSi calibration shows similar results, whereas the site-specific calibration using the ICP-MS Al-corrected data lead to much lower FTIRS values.

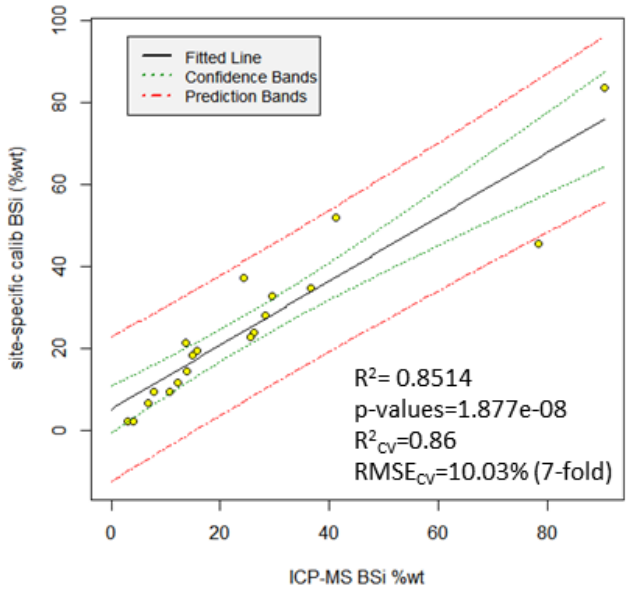

Figure 21: Calibration model of site-specific calibrated FTIR data with ICP-MS (uncorrected) BSi (% wt) data. The fitted line is shown in black, confidence and prediction bands in green and red. The yellow points indicate the 19 samples, used for calibration.

6. Discussion

This chapter discusses the major results of the present thesis. After the development of the lake with regard to regional climate conditions and deglaciation, changes in productivity and lake trophy are discussed. Furthermore, the stratification and mixing regime of Lake Rzęśniki and their linkage with catchment dynamics are shown. Next, the origin and causes of the slump events in Lake Rzęśniki are discussed in more detail. Finally, the data treatment is reviewed.

6.1. Development of Lake Rzęśniki

Lake Rzęśniki developed at the beginning of the early Holocene around, 10 800 cal yr BP, which confirms previous assumptions, that the lake formed by melting dead ice at the onset of the Holocene (Tylmann et al. 2017). A similar time of lake formation was determined for lake records in the Masurian Lake District (e.g. Lake Łazduny and Żabińskie, unpublished). These findings agree with regional climate reconstructions for the Holocene period, which proposed that cold conditions persisted after the Late Glacial in the south-eastern Baltic region and the characteristic Holocene warming was delayed compared to central Europe (Lauterbach et al. 2011). These conditions, which are thought to be caused by the anticyclone circulation around the Scandinavian ice sheet (Wohlfarth et al. 2007; Subetto et al. 2002) enabled a long persistence of dead ice blocks forming the basin of Lake Rzęśniki. The insulation provided by sand and peat had an additional conservation effect.

The observed sediment lithology composed of sand overlain by peat and then covered by a layer of clay, is found in many lakes in northern Europe and the Baltics (Gałka and Sznel 2013; Milecka et al. 2011) and is consistent with the initial formation of Rzęśniki (10,900-10,530 cal yr BP). The accumulation of fine detritus gyttja marks the start of limnic and biogenic sedimentation around 10,500 cal yr BP. Although the establishment of vegetation in the region was also reported to be delayed in comparison to Western Europe (Lauterbach et al. 2011), the catchment soils were already fully stabilized by forest according to the palynological record form nearby Lake Łazduny (Wacnik et al, unpublished). This agrees with other regional reconstructions (Milecka et al. 2011; Stančikaitė et al. 2009). Therefore, the erosional sediment influx decreased shortly after lake development and aquatic processes dominated the geochemical sediment composition. Overall, the lithogenic input to Lake Rzęśniki was at a very low level (low Ti, K and lithogenic Si) until 600 cal yr BP (16th century), when anthropogenic impact on the catchment vegetation increased remarkably (Wacnik et al. 2012). Almost permanent anoxic bottom water conditions are represented by redox-sensitive elements like Fe and Mn (Hamilton-Taylor and Davison 1995), the presence of Bphe-*a* and the formation of laminated sediment throughout the sediment record

(Fig. 22). The absence of phosphorus in the sediment is a further evidence for anaerobic conditions.

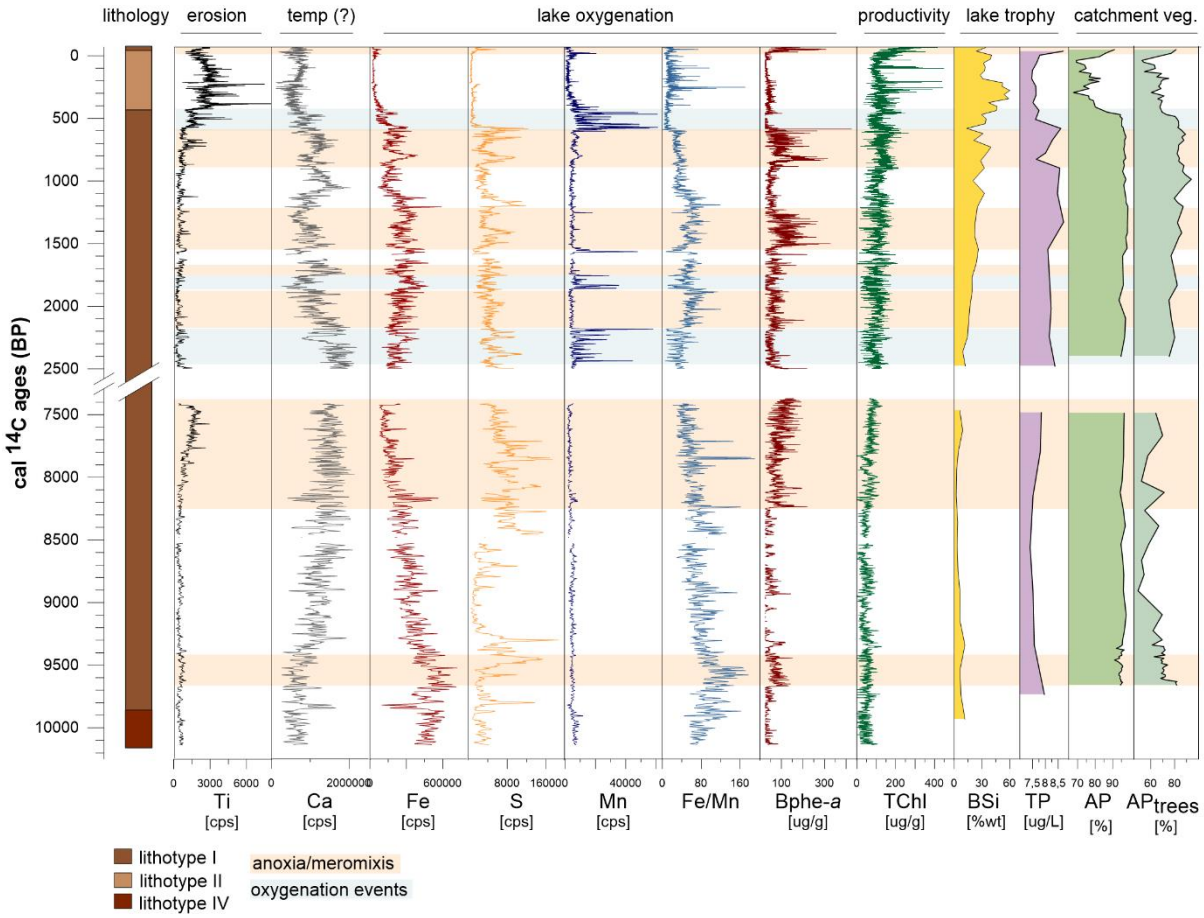

Figure 22: Summary stratigraphy with XRF, HSI indices, BSi, TC-inferred TP in comparison with arboreal pollen (AP) sums from the nearby Lake Łazduny (Wacnik et al. 2012, Wacnik et al. unpublished). AP (%) reflects the total pollen sum of trees and shrubs, whereas AP_{trees} (%) shows the sum of tree pollen. Pronounced oxygenation events and anoxic (meromictic) bottom water conditions are highlighted in blue and orange, respectively. The terrestrial phase is not shown in this graph.

6.2. Reconstruction of trophic state and paleoproductivity

Overall, a general increase in aquatic productivity is observed since 8000 cal yr BP with a peak at the top of the record indicating modern eutrophication. This observation is consistent over the whole data set and is represented by increasing values in Br, TChl, Chl-*a*, and LOI_{550}. In addition, the gradual decrease in PC1 of the pigment dataset indicates an increase of productivity (Fig. 17). The decreasing trend in the TOC/TN ratio in the late Holocene reflects that organic matter composition remains unaffected by erosional input and changes in the catchment (Fig. 13). Moreover, this gives evidence that the observed changes in the phytoplankton community or the inferred trophic state in Lake Rzęśniki reflect responses to processes that shape algal community structure rather than overall changes in of paleoproductivity (Carpenter et al. 1986). Furthermore, the analyses clearly show that lake stratification and phytoplankton community composition are closely linked, whereby the pigment stratigraphy and biochemical data correspond well.

Overall, less productive conditions with low pigment concentrations were observed after lake formation and during the mid-Holocene (10,530 - 7311 cal yr BP). Nevertheless, both PCA analyses of geochemical and pigment data indicate anoxic conditions of the hypolimnion (Fig. 13, 16 and 22), which agrees with the early (relatively low) abundance of cyanobacterial pigments (Fig. 16). Between 2725 and 600 cal yr BP increased dominance of cyanobacteria indicates a shift to more eutrophic conditions and bottom water anoxia. The TC-inferred TP and Bphe-*a* are correspondingly high. A remarkable transition around 600 cal yr BP to more mesotrophic conditions is indicated by the dominance of chromophyte species, especially diatoms. The diatoms pigments and FTIRS-inferred BSi correspond well, whereas diatoms associated pigments indicate a major contribution of diatoms to the biogenic silica fraction during that time. However, it is reported that dinoflagellates are often underrepresented in the sediment record due to their higher lability (Buchaca and Catalan 2008). Modern eutrophication (~1950) is poorly recorded in the pigment statistical analysis, because this cluster is composed only of one single sample point. However, the trend is reflected among other productivity proxies (HSI-inferred TChl and Br) and visually in the peak of all pigment concentrations.

In general, much lower pigment concentrations (in the HPLC data as well in the HSI-inferred pigment concentrations) were observed in Lake Rzęśniki than in Lake Łazduny (Sanchini, in preparation). This is contradictory to the reported current trophic state of the two lakes. Lake Łazduny is classified as currently mesoeutrophic whereas Lake Rzęśniki is eutrophic (Tylmann et al. 2017). Furthermore, the total carotenoids-inferred phosphorus (TP)

concentrations do not indicate eutrophic conditions in the most recent sediments. However, the inferred TP concentration seems to underestimate phosphorus concentrations. The calculated concentrations indicate values between 7 and 9 µg/L which, according to Wetzel (2002), can be classified as oligomesotrophic conditions, despite the pigment stratigraphy and biochemical proxies clearly indicating periods of eutrophic conditions. Nevertheless, the inferred TP can be used as qualitative indicator of changes in the trophic state, and it works sufficiently to support information of other paleoproductivity proxies.

The difference in trophy and pigment concentrations between Lake Łazduny and Lake Rzęśniki likely represents rather the different lake characteristics such as basin morphology and the importance of sediment focusing (Hilton et al. 1986; Larsen and MacDonald 1993). Indeed, it is known that the amount of pigments depends on several decay factors, which in turn depends on lake morphology (e.g. lake depth, depth of photic and oxic zones or lake size). Sediment focusing also appears to have an impact on sedimentary pigment concentration. But this still needs to be assessed in more detail (Leavitt 1993b).

Climate responses

Because of the multiple effects on lakes' biogeochemical cycles and productivity, climate impacts over the Holocene are often difficult to quantify. However, it is assumed that the Ca precipitation in Lake Rzęśniki mainly reflects the temperature increase at the onset of the Holocene and Mid-Holocene, and is only driven to some extent by enhanced productivity, because other productivity marker (e.g TChl, fossil pigments) indicate low productivity during that period in Lake Rzęśniki. A moderate increase of biogenic productivity (LOI_{550}, TChl and Br) is detected between 8000 and 7300 cal yr BP in the Mid-Holocene. The steep rise of Ca counts around 9500 cal yr BP coincides with reported climate amelioration at the onset of the Holocene, when warm and moist climate conditions established in eastern Poland after the final decay of the Scandinavian ice sheet between 10 000 and 9 500 cal yr BP (Yu and Harrison 1995; Lundqvist and Mejdahl 1995). The simultaneous decrease of Fe between 9 500 and 7 500 cal yr BP is interpreted as a Ca dilution effect in the XRF data, because other elements such as S or Mn do not indicate major changes in lake conditions. The characteristic short-term cooling event around 8.2 k yr BP observed in many paleoecological datasets in the Baltic region (Lauterbach et al. 2011; Bjerring et al. 2013), could not be recognized in Lake Rzęśniki. Simultaneously occurring variability in the Bphe-*a* content and some elements (Fe, Ca and S) (Fig. 22) might be related to this cold event.

The sediment record form Lake Rzęśniki exhibits major slump events (further discussion in 6.4), which led to a sediment hiatus from 7331 to 2725 cal yr BP. Thus, responses in

sedimentary composition or the phytoplankton community to environmental changes (e.g the Holocene Thermal Maximum (Ilvonen et al. 2016)) cannot be detected during this period.

Pigment degradation and preservation

Using fossil pigments to reconstruct primary production and phytoplankton assemblages should be done carefully and in consideration of the multiple degradation processes affecting fossil pigment amounts. Production, pigment deposition and sedimentary concentration are expected to be proportional as long there is no change in the environmental conditions affecting pigment degradation pathways such as changes in stratification, deep water oxygenation or light penetration (Leavitt et al 1993). Such changes are expected when analyzing fossil pigments over longer time scales such as in case of Lake Rzęśniki. It is expected that the variability in the applied preservation indices (CPI and Chl-*a* index) (Fig. 16) in the Late Holocene reflects dynamic preservation and degradation conditions, due to changes in mixing, turbidity and oxygenation of the water column. Nevertheless, from the pigment stratigraphy alone it is not clear which factors are controlingin changes of the ratios. Moreover, the CD/TC pigment ratio reflects only partly the changes in lake trophy (Fig. 16) and captures only the change to more oligotrophic conditions during the time of holomixis in the late Holocene. Overall, the applied pigment indices tend to be inconsistent looking at the whole core sequence, which makes general interpretation challenging. However, it is reported that they are probably more valid for more oligotrophic and alpine lakes with high secchi depth (Buchaca and Catalan 2008).

Furthermore, pigment-selective preservation has to be considered in the interpretation of pigment data. For example, the very low observed concentrations of the pigments peridinin, neoxanthin or dinoxanthin (not shown in graph) as well as the highly variable abundant green algae pigment violaxanthin (Fig. 16) agree with the reported high lability and weak sedimentary preservation (Buchaca and Catalan 2008; Hurley and Armstrong 1990). In the cases of perdinin, neoxanthin and dinoxanthin, the signal was fully lost in the downcore sediment of Lake Rzęśniki.

6.3. Mixing and stratification in Lake Rzęśniki

The pigment stratigraphy and geochemical analysis show that meromictic conditions or strong seasonal anoxia are present naturally for a long time period in Lake Rzęśniki. The fast lake development suggesting a rapid water level increase and the morphology of the lake basin with a proportionally much bigger productive epilimnion and a small hypolimnion makes the lake prone to bottom water anoxia. The bacteriochlophyll derivative Bphe-*a*, used as proxy for meromixis (Butz et al. 2016), is abundant over most core sequences indicating a permanently stratified water column (Fig. 22). This is supported by the early abundance of cyanobacteria in the pigment stratigraphy, abundant S and Fe minerals and a high Fe/Mn ratio all indicating anoxic conditions.

Already, after lake formation in the early Holocene seasonal anoxia is indicated by Bphe-*a* abundance. However, the hypolimnetic anoxia was likely weak; low levels of Bphe-*a* suggest no mass development of purple sulfur bacteria. The sporadic abundance of the pigment between 9400 and 8250 cal yr BP indicates irregular establishment of a chemocline. A possible reason might be the change in catchment vegetation suggested by low tree pollen sums (AP_{trees}) during that time (Fig. 22). This period also corresponds to low S amount in the sediment. However, the abundance of laminations and low Mn values in the sediment still indicate bottom water anoxia (or hypoxia) (Fig. 22), which was probably not sufficient to preserve sulfide minerals in the sediment which mostly form under strict anoxic conditions (Hamilton-Taylor and Davison 1995). From 8250 cal yr BP to 7331 cal yr BP, a strengthening of lake stratification is recorded in the sediment record. A simultaneous rise in productivity (e.g TChl and Br) is also recorded. The dominance of cyanobacteria-associated carotenoid pigments (Fig. 16) in the Late Holocene period (2500-600 cal BP) support the interpretation of eutrophic and anoxic conditions during that time. However, a clear relationship between Ca dissolution (decrease of Ca counts) and under enhanced hypolimnetic anoxia (high Bphe-*a*), which is often reported for meromictic lakes (Gulati 2017) could not be observed in Lake Rzęśniki. The two pronounced periods of enhanced Bphe-*a* concentrations in the Late Holocene (1520-1210 and 820-600 cal yr BP) are suggested to be internally driven strengthened by lake stratification and establishment of meromictic conditions. No evidence for external driving factors is found in the dataset and the literature, regarding catchment vegetation dynamics or regional climate variability. However, a more detailed literature review is needed to exclude possible climate variability during that time. Sporadic oxygenation events of the water column are indicated by spikes in Mn abundance and a simultaneous decrease of Bphe-*a*. This relationship is explained by most photrophic sulfur bacteria being strictly anoxic and unable to survive under oxic conditions (Van Gemerden and Mas 2004). A disappearance of meromixis indicators occurs around 600 cal yr BP and correlates with anthropogenic impact (further discussion in 6.3.1).

Bphe-*a* as proxy for meromixis

The use of Bphe-*a* as a diagnostic biomarker for meromixis (Butz et al. 2016) might be controversial, because it is reported in literature that bacteriopheophytin *a* can also be produced under non-permanent anoxic conditions during strong summer stratification (Dreßler et al. 2007). Another important parameter, which has to be considered, is the light availability and vertical structure of lake ecosystems. Phototrophic sulfur bacteria are strictly depending on light (Van Gemerden and Mas 2004). This implies that, if the chemocline is too deep and located below the phototrophic zone, no Bphe-*a* is produced and preserved in the sediment, despite the presence of meromictic conditions. Additionally, a negative correlation exists between

phytoplankton biomass in the mixolimnion and the purple-sulfur bacteria at the chemocline, so that high biomasses in the photic zone can decrease water transparency (Rogozin et al. 2012). In a comprehensive model-study, Rogozin et al. (2012) demonstrated the interplay of water-weather conditions, column stratification and food web structure. The study revealed that weather conditions and biological processes control detrimentally the chemocline position and thus sulfur bacteria biomass. However, changes in light conditions (i.e secchi depth) are difficult to reconstruct based on fossil pigments due to their photosensitive degradation (Leavitt and Hodgson 2001) and only detailed limnological monitoring could answer this kind of question.

Because of these issues, the presence of Bphe-*a* might not only be associated to meromictic conditions and represents strong water column stratification with bottom water anoxia and the development of a chemocline. These conditions are often associated to meromictic conditions, but can also be present in holomictic lake systems. Periods of enhanced Bphe-*a* concentrations represent most likely periods of meromictic conditions (as indicated in Fig. 22), because bacteriochlorophyll-producing bacteria reach much lower biomasses during seasonal stratification and cannot explain such stable high values in Bphe-a concentrations (Gulati 2017).

Lake stratification and catchment dynamics

Water column stratification and catchment vegetation dynamics are closely related in Lake Rzęśniki. The disappearance of meromixis and bottom water anoxia, indicated by a rapid decline of Bphe-*a* concentration, around 600 cal BP, coincides with e time of large anthropogenic deforestation and agricultural exploitation of the catchment in the 16th century by Teutonic Order Knights (Wacnik et al. 2012) (Fig. 23). The offset of 100 years between the decrease of AP at Lake Łazduny and Bphe-*a* in Lake Rzęśniki suggests that the anthropogenic deforestation around Lake Rzęśniki occurred earlier than at Lake Łazduny. The rapid deforestation caused high erosional influx and oxygenation of the bottom water reflected by high Ti and Mn abundance in the sediment and poor preservation to even disappearance of sediment laminations (Fig. 22). A change in the mixing regime is also displayed in the phytoplankton assemblages, which show a significant change from cyanobacteria to chromophytes dominance and a peak of BSi (Fig. 16). It is expected that opening of the vegetation enhanced the wind mixing of the water body and turned the lake system into holomictic conditions (Stevens et al. 2000). Wind stress on a lake surface is known to be a determining process for water column mixing and, thus, the ecology of and geochemical cycles of a lake (Imboden et al. 1995). Indeed, simulation studies reported that continuous canopy (forest) surrounding the lake has a substantial sheltering effect, and this effect is more pronounced in small lakes with smaller surface area (Markfort et al. 2010).

The same process is also observed in the last century, where regeneration of the forest communities as a result of depopulation of the area (decrease of cultural pollen indicators) (Wacnik et al. 2012) led to re-establishment of meromictic conditions (Fig. 23). Although the first significant human impact on vegetation in the region already began during the Middle Bronze Age (~1400 BC) (Wacnik et al. 2012), the forest communities experienced mainly composition transformations, and palynological data do not indicate a decline of total arboreal pollen (AP) (Fig. 22). Consequently, permanent lake stratification persisted in Lake Rzęśniki. Furthermore, the relationship seems to be also valid for the Mid-Holocene, where pronounced meromictic periods and the absence of meromixis seem to coincide with total AP_{trees} fluctuations (Fig. 22). However, low resolution of the pollen data in the early to Mid-Holocene does not allow a specific correlation of these events.

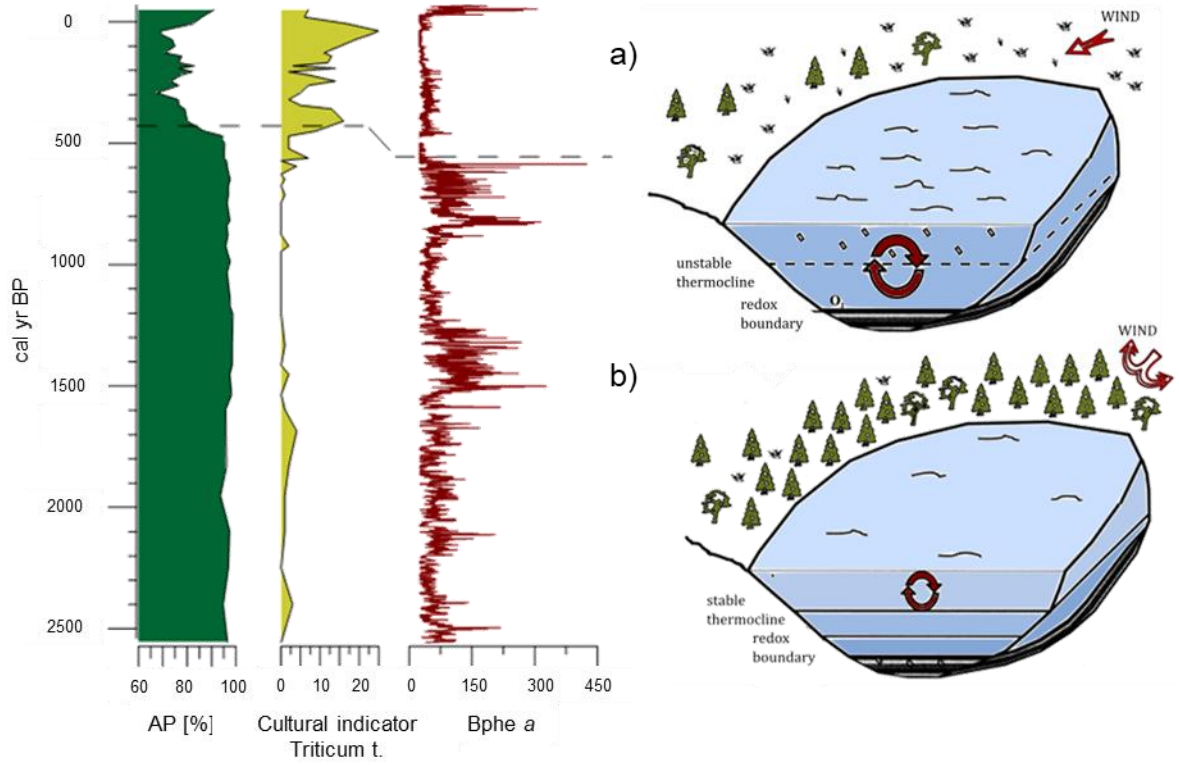

Figure 23: Sum of arboreal pollen and Triticum T. counts used as a cultural indicator of the catchment of Lake Łazduny (Wacnik et al 2012) next to the HSI-inferred Bphe-a concentration from Lake Rzęśniki in terms of ages. The abrupt decrease of arboreal pollen corresponds to the disappearance of meromixis and is associated to the large-scale deforestation by Teutonic Order Knights in the 16th century. The two schemes on the right illustrate the relationship between lake mixing and vegetation cover. a) With open vegetation, wind can influence the lake stratification by effectively mixing the water column. B) The densely forested catchment shields the lake basin from wind and the lake is stratified (redrawn from Stevens et al. 2000).

The same linkage of lake mixing and catchment vegetation was observed in Lake Moos in Switzerland (Makri, in preparation) and Lake Żabińskie in NE-Poland (Zander, in preparation). Interestingly, the observation could not be retrieved in the close-by Lake Łazduny (Sanchini, in preparation). However, the catchment topography of this lake is dominated by steep hills, which might have an additional wind sheltering affect.

6.4. Slump events

The slump sequence is a very distinctive feature in the sediment record of Lake Rzęśniki. The geochemical and pigment stratigraphy confirm the preliminary interpretation of the sediment description of the slump sequence suggesting two separate slumps from different parts from the lake basin.

The first part of the slump can be easily identified as a slump deposit. It shows characteristic features such as shifted and deformed laminae, sliding surfaces or an increased erosional signal (Ti) (Fig. 13). The dark-brown sediment on top of it appears to be of littoral or sub-littoral origin according to its geochemical and pigment composition. The high pigment concentration (Fig. 16) and high organic content (Fig. 13) support a littoral/sub-littoral origin. Higher deposition of organic matter and better preservation of pigments due to faster incorporation into the sediment is expected in littoral zones (Leavitt 1993b). In addition, smear slides taken in this part of the core indicate an abundance of phytoliths instead of diatoms. Indeed, no specific contribution of diatom associated pigments diatoxanthin and fucoxanthin to the FTIRS inferred BSi is observed. Pytholiths are composed of opal biogenic silica produced by many grass and sedge species (e.g. poaceae) (Piperno 2001) and are mainly transported by water from the catchment. Therefore, they are found in much higher abundance in littoral or sub-littoral lake sediments (Fearn 1998).

The abundance of Bphe-*a* in this part of the core seems to be surprising (Fig. 16), because the production of this pigment is associated with anoxic photogenic sulfur bacteria which are located at the chemocline of stratified lakes (Van Gemerden and Mas 2004). Nevertheless, such a high position of the chemocline in the water column and an anoxic layer reaching up to the sublittoral zone may be possible considering that the current limnological data reported hypoxia at around 7 meters water depth (Tylmann et al. 2017). In addition, the pigment echinone, a pigment associated specifically to N_2-fixing filamentous cyanobacteria (Deshpande et al. 2014) occurs in the stratigraphical pigment record. However, it can be assumed that the dark color of this sedimentary unit to some degree affects the hyperspectral scanning quality and the HPLC-derived Bphe-*a* show lower concentration.

A drastic lake level change leading to such an abrupt shallow-water facies formation instead seems to be unrealistic when considering the abrupt and clear transition in the sedimentology and the long formation time of around 1000 years. A damming of inflow or an erosional event at the outflow provoking such a drastic reduction of lake level seem to be impossible when considering the geomorphic situation. However, a specific trigger for the slump could not be identified. An over steepening and instability of the slope in the basin appears to be

the most reasonable cause, since no earthquakes are reported for that region and time period, and the Łazduny record does not show any evidence of mass movements at the same time.

6.5. Data quality and validation

BSi calibration

The site-specific BSi calibration model using Al-corrected values leads to unreliable low values. These very low values are contradictory to the much higher BSi contribution calculated by the independent FTIRS BSi calibration model and the dominance of chromophyte pigments in the stratigraphy. The high abundance of diatoms seen in smear slides also indicate overall much higher biogenic silica values. In addition, the site-specific calibration model and the independent FTIRS BSI calibration give much more reasonable results without applying Al-correction on the ICP-MS measured Si concentrations. This is an indication that a simple application of an Al correction factor might not record the true lithogenic input. Beside in clay, Al is also naturally incorporated in diatoms cell walls and secondary Al uptake after sedimentation can additionally increase the natural Al concentrations in diatoms (Koning et al. 2007). According to Chapligin et al. (2012) Al_20_3 concentrations, greater than 1 % are a reliable indication of lithogenic clay input. Since the Al values in the sediment of Lake Rzęśniki are very low (<1 %), applying of an Al-correction factor would underestimate the sedimentary BSi fraction. In order to assess the precise correction factor, a separate sequential extraction of contributing silica fractions should be done for each individual sample (Ohlendorf and Sturm 2008; Swann and Patwardhan 2011). In addition, the Si cycle and its biogenic and lithogenic linkages are still not well understood (Tallberg et al. 2015) and the contribution of lithogenic processes and their interaction with biogenic Al incorporation is difficult to assess.

HSI calibration

The calibration model for Bphe-*a* differs from the model from TChl in its outcome of the residual normality tests (Fig. 19 and 20). Excluding the sample value 1 from the calibration data set would solve this issue. However, the high pigments concentrations in the first sample are valid and result from enhanced productivity and overall better preservation in the surface sediments. Therefore, the sample cannot be treated as an outlier. The different outcomes of the two normality tests are a result of their different sensitivities of each test towards outliers. The positive Shapiro-Wilk test is more sensitive towards outliers, whereas the Kolmogorov-Smirnov test is more general and robust (Ahad et al. 2011). Consequently, making inferences using the calibration model seems to be still valid. Negative values in the HIS-inferred TChl concentrations

might be a result of a matrix effect on the absorbance feature between the reflectance at the wavelengths 590 and 730 nm.

XRF data

Changes in organic or water content can create changes in the element counts, which are unrelated to true sediment geochemical composition. This masking effect is well described for lighter elements such as Si or Al. In order to avoid this closed sum effect, it is recommended to normalize the raw data (Davies et al. 2015) . Several normalization techniques are proposed in the literature such as logarithmic ratios (Weltje and Tjallingii 2008), ratios with Al or Ti (Löwenmark et al. 2011).

In case of the sediments of Lake Rzęśniki, the water content is not very variable. Indeed, Si counts at the top of the sequence do not show any indications of masking. Changes in TOC content or weathering are also reported to bias elemental counts (Löwemark et al. 2011), but those changes could be observed neither in the XRF data nor in the stable TOC content in Lake Rzęśniki. Furthermore, another issue is the striking discrepancy between absolute Si counts, the Si/Ti ratio and FTIRs-inferred BSi concentrations. Although the Si/Ti ratio is widely used as proxy for changes in biogenic silica content (Davies et al. 2015; Brown et al. 2007) and is reported to correlated very well with TC, TOC and BSi (Liu et al. 2013). This ratio does not seem work in the case of Lake Rzęśniki. In fact, the absolute Si profile instead corresponds much better with the inferred BSi concentrations and observed chromophyte pigments. Conclusively, based on the observation that water content does not seem to affect the downcore element profile (Davies et al. 2015) and that the absolute values are more consistent with the other methods it was decided that it is valid to present the XRF data in absolute values.

Another issue is the compositional character of XRF data. Almost all data in geochemistry are closed data (closed sum effect), which means that they sum up to a constant (e.g. 100 %). This is also the case for XRF retrieved datasets. An increase of one compound leads to decreasing values of other compounds, which might bias the correlation of different elements and an application of principle components is not valid (Miesch 1969). In a strictly statistical sense, due to the compositional nature of XRF data, PCA should not be carried out without appropriate transformation (Filzmoser et al. 2009). However, it is widely accepted in the community to apply PCA analysis on XRF data without big constraints.

7. Conclusion

The aim of this thesis was to investigate the history of Lake Rzęśniki with a special focus on paleoproductivity and meromixis. The sediment record proved to be a valuable archive to study the relationship of productivity and mixing regime changes. To conclude, major findings in respect to the research questions are reported below.

Main findings:

- Lake Rzęśniki developed in the early Holocene. The sediment record covers the last 10,500 cal yr BP. The delayed lake formation is in accordance with other paleolimnological records in the Masurian Lake district, and supports the view of a delayed onset of Holocene warming reported for the southeastern Baltic region.
- Meromictic conditions occurred naturally in Lake Rzęśniki and are observed almost over the whole sediment record. Sedimentary redox-sensitive elements (Fe, Mn) and bacteriochlorophyll derivative Bphe-*a* are the most diagnostic indicators for pronounced anoxic periods.
- Meromixis, catchment dynamics and lake trophy are closely related in Lake Rzęśniki. A pronounced reduction of bottom water anoxia is associated to intense anthropogenic deforestation of the catchment by Teutonic Order Knights in the 16th century. In turn, the re-establishment of meromictic conditions correlates with the afforestation of the catchment in the recent decades. Inferred trophic conditions change remarkably with the transition from meromixis to holomixis, and are reflected by major changes in the phytoplankton assemblages.
- Wind stress could be identified as a main driving factor of mixing and stratification of Lake Rzęśniki. During the time of anthropogenic deforestation, wind stress could act sufficiently on the lake surface and destabilized the permanent stratification.
- The aquatic phytoplankton community is composed of diatoms and dinoflagellates, golden-brown algae, green algae and cyanobacteria, whereas cyanobacteria dominate during permanent stratification periods and chromophyte assemblages gain dominance when the water column is well oxygenated. More local fluctuations of the abundance of fossil pigments reflect the multiple processes shaping the preservation and degradation of pigment in the lake water and sediment. In addition, biogenic silica concentrations correspond well with the pigment stratigraphy. Diatoms can be identified as major contributors to the BSi peak in the late Holocene.

8. References

Adrian, R., C. M. O'Reilly, H. Zagarese, S. B. Baines, D. O. Hessen, Wendel Keller, D. M. Livingstone, et al. 2009. 'Lakes as Sentinels of Climate Change'. *Limnology and Oceanography* 54 (6): 2283–97. https://doi.org/10.4319/lo.2009.54.6_part_2.2283.

Ahad, N. A., A. Rahman Othman, T. Sin Yin, and C. Rohani Yaacob. 2011. 'Sensitivity of Normality tests to Non-Normal Data'. *Sains Malaysiana* 40 (6): 637–41.

Ansari, A. A., S.t S. Gill, and F. A. Khan. 2011. 'Eutrophication: Threat to Aquatic Ecosystems'. In *Eutrophication: Causes, Consequences and Control*, edited by Abid A. Ansari, Sarvajeet Singh Gill, Guy R. Lanza, and Walter Rast, 143–70. Dordrecht: Springer Netherlands. https://doi.org/10.1007/978-90-481-9625-8_7.

Bennett, K. D. 1996. 'Determination of the Number of Zones in a Biostratigraphical Sequence'. *New Phytologist* 132 (1): 155–70. https://doi.org/10.1111/j.1469-8137.1996.tb04521.x.

Berglund, B. E., H. J. B. Birks, M. Ralska-Jasiewiczowa, and H. E. Wright. 1996. *Palaeoecological Events During the Last 15,000 Years: Regional Synthesis of Palaeoecological Studies of Lakes and Mires in Europe.* Chichester: John Wiley & Sons. http://discovery.ucl.ac.uk/165845/.

Bianchi, T. S., C. Rolff, B. Widbom, and R. Elmgren. 2002. 'Phytoplankton Pigments in Baltic Sea Seston and Sediments: Seasonal Variability, Fluxes, and Transformations'. *Estuarine, Coastal and Shelf Science* 55 (3): 369–83. https://doi.org/10.1006/ecss.2001.0911.

Bianchi, T. S., R. Dawson, and P. Sawangwong. 1988. 'The Effects of Macrobenthic Deposit-Feeding on the Degradation of Chloropigments in Sandy Sediments'. *Journal of Experimental Marine Biology and Ecology* 122 (3): 243–55. https://doi.org/10.1016/0022-0981(88)90126-8.

Bjerring, R., J. Olsen, E. Jeppesen, B. Buchardt, J. Heinemeier, S. McGowan, P. R. Leavitt, R. Enevold, and B. V. Odgaard. 2013. 'Climate-Driven Changes in Water Level: A Decadal Scale Multi-Proxy Study Recording the 8.2-Ka Event and Ecosystem Responses in Lake Sarup (Denmark)'. *Journal of Paleolimnology* 49 (2): 267–85. https://doi.org/10.1007/s10933-012-9673-7.

Blaauw, M., and J. A. Christen. 2005. 'Radiocarbon Peat Chronologies and Environmental Change'. *Journal of the Royal Statistical Society: Series C (Applied Statistics)* 54 (4): 805–16. https://doi.org/10.1111/j.1467-9876.2005.00516.x.

Blaauw, M., and J. A. Christen. 2011. 'Flexible Paleoclimate Age-Depth Models Using an Autoregressive Gamma Process'. *Bayesian Analysis* 6 (3): 457–74. https://doi.org/10.1214/11-BA618.

Blaauw, M., J. A. Christen, K. D. Bennett, and P. J. Reimer. 2018. 'Double the Dates and Go for Bayes — Impacts of Model Choice, Dating Density and Quality on Chronologies'. *Quaternary Science Reviews* 188 (May): 58–66. https://doi.org/10.1016/j.quascirev.2018.03.032.

Boehrer, B., and M. Schultze. 2008. 'Stratification of Lakes'. *Reviews of Geophysics* 46 (2). https://doi.org/10.1029/2006RG000210.

Braconnot, P., S. P. Harrison, M. Kageyama, P. J. Bartlein, V. Masson-Delmotte, A. Abe-Ouchi, B. Otto-Bliesner, and Y. Zhao. 2012. 'Evaluation of Climate Models Using Palaeoclimatic Data'. *Nature Climate Change* 2 (6): 417–24. https://doi.org/10.1038/nclimate1456.

Brown, E. T., T. C. Johnson, C. A. Scholz, A. S. Cohen, and J. W. King. 2007. 'Abrupt Change in Tropical African Climate Linked to the Bipolar Seesaw over the Past 55,000 Years'. *Geophysical Research Letters* 34 (20). https://doi.org/10.1029/2007GL031240.

Brown, S. R., H. J. McIntosh, and J. P. Smol. 1984. 'Recent Paleolimnology of a Meromictic Lake: Fossil Pigments of Photosynthetic Bacteria'. *SIL Proceedings, 1922-2010* 22 (3): 1357–60. https://doi.org/10.1080/03680770.1983.11897499.

Buchaca, T., and J. Catalan. 2008. 'On the Contribution of Phytoplankton and Benthic Biofilms to the Sediment Record of Marker Pigments in High Mountain Lakes'. *Journal of Paleolimnology* 40 (1): 369–83. https://doi.org/10.1007/s10933-007-9167-1.

Butz, C., M. Grosjean, D. Fischer, S. Wunderle, W. Tylmann, and B. Rein. 2015. 'Hyperspectral Imaging Spectroscopy: A Promising Method for the Biogeochemical Analysis of Lake Sediments'. *Journal of Applied Remote Sensing* 9 (1): 096031. https://doi.org/10.1117/1.JRS.9.096031.

Butz, C., M. Grosjean, T. Goslar, and W. Tylmann. 2017. 'Hyperspectral Imaging of Sedimentary Bacterial Pigments: A 1700-Year History of Meromixis from Varved Lake Jaczno, Northeast Poland'. *Journal of Paleolimnology* 58 (1): 57–72. https://doi.org/10.1007/s10933-017-9955-1.

Butz, C., M. Grosjean, A. Poraj-Górska, D. Enters, and W. Tylmann. 2016. 'Sedimentary Bacteriopheophytin a as an Indicator of Meromixis in Varved Lake Sediments of Lake Jaczno, North-East Poland, CE 1891–2010'. *Global and Planetary Change* 144 (September): 109–18. https://doi.org/10.1016/j.gloplacha.2016.07.012.

Carpenter, S. R., M. M. Elser, and J. J. Elser. 1986. 'Chlorophyll Production, Degradation, and Sedimentation: Implications for Paleolimnology: Pigment Sedimentation'. *Limnology and Oceanography* 31 (1): 112–24. https://doi.org/10.4319/lo.1986.31.1.0112.

Cartaxana, P, B Jesus, and V Brotas. 2003. 'Pheophorbide and Pheophytin A-like Pigments as Useful Markers for Intertidal Microphytobenthos Grazing by Hydrobia Ulvae'. *Estuarine, Coastal and Shelf Science* 58 (2): 293–97. https://doi.org/10.1016/S0272-7714(03)00081-7.

Chapligin, B., H. Meyer, A. Bryan, J. Snyder, and H. Kemnitz. 2012. 'Assessment of Purification and Contamination Correction Methods for Analysing the Oxygen Isotope Composition from Biogenic Silica'. *Chemical Geology* 300–301 (March): 185–99. https://doi.org/10.1016/j.chemgeo.2012.01.004.

Cohen, A. S. 2003. *Palaeolimnology: The History and Evolution of Lake Systems*. Oxford University Press, New York.

Conley, D.l J., and C. L. Schelske. 2001. 'Biogenic Silica'. In *Tracking Environmental Change Using Lake Sediments: Terrestrial, Algal, and Siliceous Indicators*, edited by John P. Smol, H. John B. Birks, William M. Last, Raymond S. Bradley, and Keith Alverson, 281–93. Developments in Paleoenvironmental Research. Dordrecht: Springer Netherlands. https://doi.org/10.1007/0-306-47668-1_14.

Croudace, Ian W., and R. G. Rothwell, eds. 2015. *Micro-XRF Studies of Sediment Cores*. Vol. 17. Developments in Paleoenvironmental Research. Dordrecht: Springer Netherlands. https://doi.org/10.1007/978-94-017-9849-5.

Davies, S. J., H. F. Lamb, and S. J. Roberts. 2015. 'Micro-XRF Core Scanning in Palaeolimnology: Recent Developments'. In *Micro-XRF Studies of Sediment Cores: Applications of a Non-Destructive Tool for the Environmental Sciences*, edited by Ian W. Croudace and R. Guy Rothwell, 189–226. Developments in Paleoenvironmental Research. Dordrecht: Springer Netherlands. https://doi.org/10.1007/978-94-017-9849-5_7.

Dean, W.r E. 1974. 'Determination of Carbonate and Organic Matter in Calcareous Sediments and Sedimentary Rocks by Loss on Ignition; Comparison with Other Methods'. *Journal of Sedimentary Research* 44 (1): 242–48. https://doi.org/10.1306/74D729D2-2B21-11D7-8648000102C1865D.

Deshpande, B. N., R. Tremblay, R. Pienitz, and W. F. Vincent. 2014. 'Sedimentary Pigments as Indicators of Cyanobacterial Dynamics in a Hypereutrophic Lake'. *Journal of Paleolimnology* 52 (3): 171–84. https://doi.org/10.1007/s10933-014-9785-3.

Diaz, R. J., and R. Rosenberg. 2008. 'Spreading Dead Zones and Consequences for Marine Ecosystems'. *Science* 321 (5891): 926–29. https://doi.org/10.1126/science.1156401.

Dreßler, M., T. Hübener, S. Görs, P. Werner, and U. Selig. 2007. 'Multi-Proxy Reconstruction of Trophic State, Hypolimnetic Anoxia and Phototrophic Sulphur Bacteria Abundance in a Dimictic Lake in Northern Germany over the Past 80 Years'. *Journal of Paleolimnology* 37 (2): 205–19. https://doi.org/10.1007/s10933-006-9013-x.

Fast, A.rlo W., and P. A. Tyler. 1981. 'The Re-Establishment of Meromixis in Hemlock Lake, Michigan, After Artificial Destratification'. *Internationale Revue der gesamten Hydrobiologie und Hydrographie* 66 (5): 665–74. https://doi.org/10.1002/iroh.19810660503.

Fearn, M. Lee. 1998. 'Phytoliths in Sediment as Indicators of Grass Pollen Source'. *Review of Palaeobotany and Palynology* 103 (1): 75–81. https://doi.org/10.1016/S0034-6667(98)00028-1.

Fedotov, A. P., V. A. Trunova, I. V. Enushchenko, S. S. Vorobyeva, O. G. Stepanova, S. K. Petrovskii, M. S. Melgunov, V. V. Zvereva, S. M. Krapivina, and T. O. Zheleznyakova. 2015. 'A 850-Year Record Climate and Vegetation Changes in East Siberia (Russia), Inferred from Geochemical and Biological Proxies of Lake Sediments'. *Environmental Earth Sciences* 73 (11): 7297–7314. https://doi.org/10.1007/s12665-014-3906-1.

Fiłoc, M., Mi. Kupryjanowicz, K. Szeroczyńska, M. Suchora, and M. Rzodkiewicz. 2017. 'Environmental Changes Related to the 8.2-Ka Event and Other Climate Fluctuations during the Middle Holocene: Evidence from Two Dystrophic Lakes in NE Poland'. *The Holocene* 27 (10): 1550–66. https://doi.org/10.1177/0959683617702233.

Filzmoser, P., K. Hron, and C. Reimann. 2009. 'Principal Component Analysis for Compositional Data with Outliers'. *Environmetrics* 20 (6): 621–32. https://doi.org/10.1002/env.966.

Friedrich, J., F. Janssen, D. Aleynik, H. W. Bange, N. Boltacheva, M. N. Çagatay, Andrew W. Dale, et al. 2014. 'Investigating Hypoxia in Aquatic Environments: Diverse Approaches to Addressing a Complex Phenomenon'. *Biogeosciences (BG)* 11 (doi:10.5194/bg-11-1215-2014): 1215–59.

Gałka, M., and M. Sznel. 2013. 'Late Glacial and Early Holocene Development of Lakes in Northeastern Poland in View of Plant Macrofossil Analyses'. *Quaternary International*, Pan-European Correlations in Quaternary Stratigraphy: SEQS 2011, INQUA Congress, Bern, 292 (March): 124–35. https://doi.org/10.1016/j.quaint.2012.11.014.

Goslar, T., K. Bałaga, M. Arnold, N. Tisnerat, E. Starnawska, M. Kuźniarski, L. Chróst, A. Walanus, and K. Więckowski. 1999. 'Climate-Related Variations in the Composition of the Late Glacial and Early Holocene Sediments of Lake Perespilno (Eastern Poland)'. *Quaternary Science Reviews* 18 (7): 899–911. https://doi.org/10.1016/S0277-3791(99)00004-9.

Grafenstein, U. von, H. Erlenkeuser, J. Müller, J. Jouzel, and S. Johnsen. 1998. 'The Cold Event 8200 Years Ago Documented in Oxygen Isotope Records of Precipitation in Europe and Greenland'. *Climate Dynamics* 14 (2): 73–81. https://doi.org/10.1007/s003820050210.

Grimm, E. C. 1987. 'CONISS: A Fortran 77 Program for Stratigraphically Constrained Cluster Analysis by the Method of Incremental Sum of Squares'. *Computers & Geosciences* 13 (1): 13–35. https://doi.org/10.1016/0098-3004(87)90022-7.

Grosjean, M., Amann, B., Butz, C., Rein, B. and Tylmann, W. 2014. 'Hyperspectral Imaging: A Novel, Non-Destructive Method for Investigating Sub-Annual Sediment Structures and Composition'. *Past Global Changes Magazine* 22 (1): 10–11. https://doi.org/10.22498/pages.22.1.10.

Guilizzoni, P., A. Lami, A. Marchetto, V. Jones, M. Manca, and R. Bettinetti. 2002. 'Palaeoproductivity and Environmental Changes during the Holocene in Central Italy as Recorded in Two Crater Lakes (Albano and Nemi)'. *Quaternary International*, The Value of Annually Laminated Sediments in Palaeoenvironment Re constructions: Dedicated to Bjorn E. Berglund, 88 (1): 57–68. https://doi.org/10.1016/S1040-6182(01)00073-8.

Guilizzoni, P., G. Bonomi, G. Galanti, and D. Ruggiu. 1983. 'Relationship between Sedimentary Pigments and Primary Production: Evidence from Core Analyses of Twelve Italian Lakes'. In *Paleolimnology*, edited by J. Meriläinen, P. Huttunen, and R. W. Battarbee, 103–6. Developments in Hydrobiology. Springer Netherlands.

Guilizzoni, P., and A. Lami. 2003. 'Paleolimnology: Use of Algal Pigments as Indicators'. In *Encyclopedia of Environmental Microbiology*. American Cancer Society. https://doi.org/10.1002/0471263397.env313.

Guilizzoni, P., A. Marchetto, A. Lami, S. Gerli, and S. Musazzi. 2011. 'Use of Sedimentary Pigments to Infer Past Phosphorus Concentration in Lakes'. *Journal of Paleolimnology* 45 (4): 433–45. https://doi.org/10.1007/s10933-010-9421-9.

Gulati, R. D. 2017. *Ecology of Meromictic Lakes*. New York, NY: Springer Berlin Heidelberg.

Håkanson, L., and M. Jansson. 2002. *Principles of Lake Sedimentology, 2nd Ed.* The Blackburn Press, New Jersey. http://www.diva-portal.org/smash/record.jsf?pid=diva2:73855.

Hamilton-Taylor, J., and W. Davison. 1995. 'Redox-Driven Cycling of Trace Elements in Lakes'. In *Physics and Chemistry of Lakes*, edited by Abraham Lerman, Dieter M. Imboden, and Joel R. Gat, 217–63. Berlin, Heidelberg: Springer Berlin Heidelberg. https://doi.org/10.1007/978-3-642-85132-2_8.

Heiri, O.r, A. F. Lotter, and G. Lemcke. 2001. 'Loss on Ignition as a Method for Estimating Organic and Carbonate Content in Sediments: Reproducibility and Comparability of Results'. *Journal of Paleolimnology* 25 (1): 101–10. https://doi.org/10.1023/A:1008119611481.

Hilton, J., J. P. Lishman, and P. V. Allen. 1986. 'The Dominant Processes of Sediment Distribution and Focusing in a Small, Eutrophic, Monomictic Lake'. *Limnology and Oceanography* 31 (1): 125–33. https://doi.org/10.4319/lo.1986.31.1.0125.

Hodgson, D. A., Simon W. Wright, P. A. Tyler, and N. Davies. 1998. 'Analysis of Fossil Pigments from Algae and Bacteria in Meromictic Lake Fidler, Tasmania, and its Application to Lake Management'. *Journal of Paleolimnology* 19 (1): 1–22. https://doi.org/10.1023/A:1007909018527.

Hongve, D.. 2002. 'Seasonal Mixing and Genesis of Endogenic Meromixis in Small Lakes in Southeast Norway'. *Hydrology Research* 33 (2–3): 189–206. https://doi.org/10.2166/nh.2002.0022.

Hurley, J. P., and D. E. Armstrong. 1990. 'Fluxes and Transformations of Aquatic Pigments in Lake Mendota, Wisconsin'. *Limnology and Oceanography* 35 (2): 384–98. https://doi.org/10.4319/lo.1990.35.2.0384.

Hutchinson, G. E., and H. Löffler. 1956. 'The thermal classification of lakes'. *Proceedings of the National Academy of Sciences of the United States of America* 42 (2): 84–86.

Ilvonen, L., L. Holmström, H. Seppä, and S. Veski. 2016. 'A Bayesian Multinomial Regression Model for Palaeoclimate Reconstruction with Time Uncertainty: paleoclimate reconstruction. *Environmetrics* 27 (7): 409–22. https://doi.org/10.1002/env.2393.

Imboden, D. M., A. Lerman, J. R. Gat, and L. Chou. 1995. *Physics and Chemistry of Lakes*. 2nd ed. Berlin, Heidelberg, New York [etc.]: Springer.

IPCC, Intergovernmental Panel on Climate. 2013. *IPCC 2013: Climate Change 2013: The Physical Science Basis: Working Group I Contribution to the Fifth Assessment Report of the Intergovernmental Panel on Climate Change*. Cambridge University Press.

Jacquet, S., J. Briand, C. Leboulanger, C. Avois-Jacquet, L. Oberhaus, B. Tassin, B. Vinçon-Leite, et al. 2005. 'The Proliferation of the Toxic Cyanobacterium Planktothrix Rubescens Following Restoration of the Largest Natural French Lake (Lac Du Bourget)'. *Harmful Algae* 4 (4): 651–72. https://doi.org/10.1016/j.hal.2003.12.006.

Jeffrey, S. W., R.F.C Mantoura, and S. W. Wright. 1997. 'Phytoplankton Pigments in Oceanography: Guidelined to Modern Methods'. UNESCO Publishing.

Jenny, J., F. Arnaud, B. Alric, J. Dorioz, P. Sabatier, M. Meybeck, and M. Perga. 2014. 'Inherited Hypoxia: A New Challenge for Reoligotrophicated Lakes under Global Warming'. *Global Biogeochemical Cycles* 28 (12): 1413–23. https://doi.org/10.1002/2014GB004932.

Jenny, J., P. Francus, A. Normandeau, F. Lapointe, M. Perga, A. Ojala, A. Schimmelmann, and B. Zolitschka. 2016. 'Global Spread of Hypoxia in Freshwater Ecosystems during the Last Three Centuries Is Caused by Rising Local Human Pressure'. *Global Change Biology* 22 (4): 1481–89. https://doi.org/10.1111/gcb.13193.

Klitgaard-Kristensen, D., H. Sejrup, H. Haflidason, S. Johnsen, and M. Spurk. 1998. 'A Regional 8200 Cal. Yr BP Cooling Event in Northwest Europe, Induced by Final Stages of the Laurentide Ice-

Sheet Deglaciation?' *Journal of Quaternary Science* 13 (2): 165–69. https://doi.org/10.1002/(SICI)1099-1417(199803/04)13:2<165::AID-JQS365>3.0.CO;2-#.
Koning, E., M. Gehlen, A. -M. Flank, G. Calas, and E. Epping. 2007. 'Rapid Post-Mortem Incorporation of Aluminum in Diatom Frustules: Evidence from Chemical and Structural Analyses'. *Marine Chemistry*, Special issue: Dedicated to the memory of Professor Roland Wollast, 106 (1): 208–22. https://doi.org/10.1016/j.marchem.2006.06.009.
Larsen, C. P. S., and G. M. MacDonald. 1993. 'Lake Morphometry, Sediment Mixing and the Selection of Sites for Fine Resolution Palaeoecological Studies'. *Quaternary Science Reviews* 12 (9): 781–92. https://doi.org/10.1016/0277-3791(93)90017-G.
Last, William M., and John P. Smol, eds. 2001. *Tracking Environmental Change Using Lake Sediments: Volume 2: Physical and Geochemical Methods*. Developments in Paleoenvironmental Research, Tracking Environmental Change Using Lake Sediments. Springer Netherlands. //www.springer.com/de/book/9781402006289.
Lauterbach, S., A. Brauer, N. Andersen, D. L. Danielopol, P. Dulski, M. Hüls, K. Milecka, et al. 2011. 'Multi-Proxy Evidence for Early to Mid-Holocene Environmental and Climatic Changes in Northeastern Poland'. *Boreas* 40 (1): 57–72. https://doi.org/10.1111/j.1502-3885.2010.00159.x.
Leavitt, P. R. 1993. 'A Review of Factors That Regulate Carotenoid and Chlorophyll Deposition and Fossil Pigment Abundance'. *Journal of Paleolimnology* 9 (2): 109–27. https://doi.org/10.1007/BF00677513.
Leavitt, P. R., and D. A. Hodgson. 2001. 'Sedimentary Pigments'. In *Tracking Environmental Change Using Lake Sediments: Terrestrial, Algal, and Siliceous Indicators*, edited by John P. Smol, H. John B. Birks, William M. Last, Raymond S. Bradley, and Keith Alverson, 295–325. Developments in Paleoenvironmental Research. Dordrecht: Springer Netherlands. https://doi.org/10.1007/0-306-47668-1_15.
Levin, L. A., W. Ekau, A. J. Gooday, F. Jorissen, J. J. Middelburg, S. W. A. Naqvi, C. Neira, N. N. Rabalais, and J. Zhang. 2009. 'Effects of Natural and Human-Induced Hypoxia on Coastal Benthos'. http://drs.nio.org/drs/handle/2264/3413.
Liu, Xiuju, S. M. Colman, E. T. Brown, E. C. Minor, and H. Li. 2013. 'Estimation of Carbonate, Total Organic Carbon, and Biogenic Silica Content by FTIR and XRF Techniques in Lacustrine Sediments'. *Journal of Paleolimnology* 50 (3): 387–98. https://doi.org/10.1007/s10933-013-9733-7.
Löwemark, L., H. -F. Chen, T. -N. Yang, M. Kylander, E. -F. Yu, Y. -W. Hsu, T. -Q. Lee, S. -R. Song, and S. Jarvis. 2011. 'Normalizing XRF-Scanner Data: A Cautionary Note on the Interpretation of High-Resolution Records from Organic-Rich Lakes'. *Journal of Asian Earth Sciences*, Quaternary Paleoclimate of the Western Pacific and East Asia: State of the Art and New Discovery, 40 (6): 1250–56. https://doi.org/10.1016/j.jseaes.2010.06.002.
Lundqvist, J., and V. Mejdahl. 1995. 'Luminescence Dating of the Deglaciation in Northern Sweden'. *Quaternary International* 28 (January): 193–97. https://doi.org/10.1016/1040-6182(95)00031-D.
Markfort, C. D., A. L. S. Perez, J. W. Thill, D. A. Jaster, F. Porté-Agel, and H. G. Stefan. 2010. 'Wind Sheltering of a Lake by a Tree Canopy or Bluff Topography'. *Water Resources Research* 46 (3). https://doi.org/10.1029/2009WR007759.
Meyer-Jacob, C., H. Vogel, F. Boxberg, P. Rosén, M. E. Weber, and R. Bindler. 2014. 'Independent Measurement of Biogenic Silica in Sediments by FTIR Spectroscopy and PLS Regression'. *Journal of Paleolimnology* 52 (3): 245–55. https://doi.org/10.1007/s10933-014-9791-5.
Meyers, P. A. 1994. 'Preservation of Elemental and Isotopic Source Identification of Sedimentary Organic Matter'. *Chemical Geology* 114 (3): 289–302. https://doi.org/10.1016/0009-2541(94)90059-0.

———. 1997. ‘Organic Geochemical Proxies of Paleoceanographic, Paleolimnologic, and Paleoclimatic Processes’. *Organic Geochemistry* 27 (5–6): 213–50. https://doi.org/10.1016/S0146-6380(97)00049-1.

Meyers, P. A., and J. L. Teranes. 2001. ‘Tracking Environmental Change Using Lake Sediments: Volume 2: Physical and Geochemical Methods’. In *Sediment Organic Matter*, edited by William M. Last and John P. Smol. Developments in Paleoenvironmental Research. Netherlands: Springer.

Miesch, A. T. 1969. ‘The Constant Sum Problem in Geochemistry’. In *Computer Applications in the Earth Sciences*, edited by Daniel F. Merriam, 161–76. Springer US.

Milecka, K., G. Kowalewski, and K. Szeroczyńska. 2011. ‘Climate-Related Changes during the Late Glacial and Early Holocene in Northern Poland, as Derived from the Sediments of Lake Sierzywk’. *Hydrobiologia* 676 (1): 187. https://doi.org/10.1007/s10750-011-0874-2.

Moberg, A., D. M. Sonechkin, K. Holmgren, N. M. Datsenko, and W. Karlén. 2005. ‘Highly Variable Northern Hemisphere Temperatures Reconstructed from Low- and High-Resolution Proxy Data’. *Nature* 433 (7026): 613–17. https://doi.org/10.1038/nature03265.

Moros, M., K. Emeis, B. Risebrobakken, I. Snowball, A. Kuijpers, J. McManus, and E. Jansen. 2004. ‘Sea Surface Temperatures and Ice Rafting in the Holocene North Atlantic: Climate Influences on Northern Europe and Greenland’. *Quaternary Science Reviews*, 23 (20): 2113–26. https://doi.org/10.1016/j.quascirev.2004.08.003.

Naeher, S., A. Gilli, R. P. North, Y. Hamann, and C. J. Schubert. 2013. ‘Tracing Bottom Water Oxygenation with Sedimentary Mn/Fe Ratios in Lake Zurich, Switzerland’. *Chemical Geology* 352 (August): 125–33. https://doi.org/10.1016/j.chemgeo.2013.06.006.

Ohlendorf, C., and M. Sturm. 2008. ‘A Modified Method for Biogenic Silica Determination’. *Journal of Paleolimnology* 39 (1): 137–42. https://doi.org/10.1007/s10933-007-9100-7.

Overmann, J., and A. K. Manske. 2006. ‘Anoxigenic phototrophic bacteria in the black sea chemocline’. In *Past and Present Water Column Anoxia*, edited by Lev N. Neretin, 523–41. Nato Science Series: IV: Earth and Environmental Sciences. Springer Netherlands.

Parkin, T. B., and T. D. Brock. 1980. ‘The Effects of Light Quality on the Growth of Phototrophic Bacteria in Lakes’. *Archives of Microbiology* 125 (1): 19–27. https://doi.org/10.1007/BF00403193.

Piperno, D. R. 2001. ‘Phytoliths’. In *Tracking Environmental Change Using Lake Sediments: Terrestrial, Algal, and Siliceous Indicators*, edited by John P. Smol, H. John B. Birks, William M. Last, Raymond S. Bradley, and Keith Alverson, 235–51. Developments in Paleoenvironmental Research. Dordrecht: Springer Netherlands. https://doi.org/10.1007/0-306-47668-1_11.

Posch, T., O. Köster, M. M. Salcher, and J. Pernthaler. 2012. ‘Harmful Filamentous Cyanobacteria Favoured by Reduced Water Turnover with Lake Warming’. *Nature Climate Change* 2 (11): 809–13. https://doi.org/10.1038/nclimate1581.

Reuss, N., D. J. Conley, and T. S. Bianchi. 2005. ‘Preservation Conditions and the Use of Sediment Pigments as a Tool for Recent Ecological Reconstruction in Four Northern European Estuaries’. *Marine Chemistry* 95 (3): 283–302. https://doi.org/10.1016/j.marchem.2004.10.002.

Rodrigo, M. A., M. R. Miracle, and E. Vicente. 2001. ‘The Meromictic Lake La Cruz (Central Spain). Patterns of Stratification’. *Aquatic Sciences* 63 (4): 406–16. https://doi.org/10.1007/s00027-001-8041-x.

Rogozin, D. Y., M. O. Tarnovsky, V. M. Belolipetskii, V. V. Zykov, E. S. Zadereev, A. P. Tolomeev, A. V. Drobotov, et al. 2017. ‘Disturbance of Meromixis in Saline Lake Shira (Siberia, Russia): Possible Reasons and Ecosystem Response’. *Limnologica* 66 (September): 12–23. https://doi.org/10.1016/j.limno.2017.06.004.

Rogozin, D. Yu., V. V. Zykov, and A. G. Degermendzhi. 2012. 'Ecology of Purple Sulfur Bacteria in the Highly Stratified Meromictic Lake Shunet (Siberia, Khakassia) in 2002–2009'. *Microbiology* 81 (6): 727–35. https://doi.org/10.1134/S0026261712060148.

Roy, S., C. A. Llewellyn, E. Skarstad Egeland, and G. Johnsen. 2011. *Phytoplankton Pigments: Characterization, Chemotaxonomy and Applications in Oceanography*. Cambridge University Press.

Rundgren, M.. 2008. 'Stratigraphy of Peatlands in Central and Northern Sweden: Evidence of Holocene Climatic Change and Peat Accumulation'. *GFF* 130 (2): 95–107. https://doi.org/10.1080/11035890801302095.

Rybak, M., and M. Dickman. 1988. 'Paleoecological Reconstruction of Changes in the Productivity of a Small, Meromictic Lake in Southern Ontario, Canada'. *Hydrobiologia* 169 (3): 293–306. https://doi.org/10.1007/BF00007552.

Sahoo, G. B., S. G. Schladow, J. E. Reuter, and R. Coats. 2011. 'Effects of Climate Change on Thermal Properties of Lakes and Reservoirs, and Possible Implications'. *Stochastic Environmental Research and Risk Assessment* 25 (4): 445–56. https://doi.org/10.1007/s00477-010-0414-z.

Scharf, Burkhard W., and S. Björk. 1992. 'Limnology of Eifel Maar Lakes'. 1992.

Schelske, C. L., D. J. Conley, E. F. Stoermer, T. L. Newberry, and C. D. Campbell. 1987. 'Biogenic Silica and Phosphorus Accumulation in Sediments as Indices of Eutrophication in the Laurentian Great Lakes'. In *Paleolimnology IV*, edited by Heinz Löffler, 79–86. Developments in Hydrobiology. Springer Netherlands.

Schneider, T., D. Rimer, C.h Butz, and M. Grosjean. 2018. 'A High-Resolution Pigment and Productivity Record from the Varved Ponte Tresa Basin (Lake Lugano, Switzerland) since 1919: Insight from an Approach That Combines Hyperspectral Imaging and High-Performance Liquid Chromatography'. *Journal of Paleolimnology* 60 (3): 381–98. https://doi.org/10.1007/s10933-018-0028-x.

Schnurrenberger, D., J. Russell, and K. Kelts. 2003. 'Classification of Lacustrine Sediments Based on Sedimentary Components'. *Journal of Paleolimnology* 29 (2): 141–54. https://doi.org/10.1023/A:1023270324800.

Seppä, H., A. E. Bjune, R. J. Telford, H. J. B. Birks, and S. Veski. 2009. 'Last Nine-Thousand Years of Temperature Variability in Northern Europe'. *Climate of the Past* 5 (3): 523–35. https://doi.org/10.5194/cp-5-523-2009.

Snyder, C. W. 2010. 'The Value of Paleoclimate Research in Our Changing Climate: An Editorial Comment'. *Climatic Change* 100 (3–4): 407–18. https://doi.org/10.1007/s10584-010-9842-5.

Squier, A. H, D. A Hodgson, and B. J Keely. 2002. 'Sedimentary Pigments as Markers for Environmental Change in an Antarctic Lake'. *Organic Geochemistry* 33 (12): 1655–65. https://doi.org/10.1016/S0146-6380(02)00177-8.

Stančikaitė, M., D. Kisielienė, D. Moe, and G. Vaikutienė. 2009. 'Lateglacial and Early Holocene Environmental Changes in Northeastern Lithuania'. *Quaternary International*, Pleistocene and Holocene Palaeoenvironments and Recent Processes across NE Europe, 207 (1): 80–92. https://doi.org/10.1016/j.quaint.2008.10.009.

Steffen, W., K. Richardson, J. Rockstrom, S. E. Cornell, I. Fetzer, E. M. Bennett, R. Biggs, et al. 2015. 'Planetary Boundaries: Guiding Human Development on a Changing Planet'. *Science* 347 (6223): 1259855–1259855. https://doi.org/10.1126/science.1259855.

Stevens, L., E. Ito, and D. Olson. 2000. 'Relationship of Mn-Carbonates in Varved Lake-Sediments to Catchment Vegetation in Big Watab Lake, MN, USA'. *Journal of Paleolimnology* 24 (2): 199–211. https://doi.org/10.1023/A:1008169526577.

Subetto, D. A., B. Wohlfarth, N. N. Davydova, T. V. Sapelko, L. Björkman, N. Solovieva, S. Wastegård, G. Possnert, and V. I. Khomutova. 2002. 'Climate and Environment on the Karelian Isthmus, Northwestern Russia, 13000-9000 Cal. Yrs BP'. *Boreas* 31 (1): 1–19. https://doi.org/10.1111/j.1502-3885.2002.tb01051.x.

Swann, G. E. A., and S. V. Patwardhan. 2011. 'Application of Fourier Transform Infrared Spectroscopy (FTIR) for Assessing Biogenic Silica Sample Purity in Geochemical Analyses and Palaeoenvironmental Research'. *Climate of the Past* 7 (February): 65–74.

Synal, H., M. Stocker, and M. Suter. 2007. 'MICADAS: A New Compact Radiocarbon AMS System'. *Nuclear Instruments and Methods in Physics Research Section B: Beam Interactions with Materials and Atoms*, Accelerator Mass Spectrometry, 259 (1): 7–13. https://doi.org/10.1016/j.nimb.2007.01.138.

Tallberg, P., S. Opfergelt, J. Cornelis, A. Liljendahl, and J. Weckström. 2015. 'High Concentrations of Amorphous, Biogenic Si (BSi) in the Sediment of a Small High-Latitude Lake: Implications for Biogeochemical Si Cycling and for the Use of BSi as a Paleoproxy'. *Aquatic Sciences* 77 (2): 293–305. https://doi.org/10.1007/s00027-014-0387-y.

Tarand, A., and P. Ø. Nordli. 2001. 'The Tallinn Temperature Series Reconstructed Back Half a Millennium by Use of Proxy Data'. In *The Iceberg in the Mist: Northern Research in Pursuit of a "Little Ice Age"*, edited by Astrid E. J. Ogilvie and Trausti Jónsson, 189–99. Dordrecht: Springer Netherlands. https://doi.org/10.1007/978-94-017-3352-6_9.

Thorndike, R. L. 1953. 'Who Belongs in the Family?' *Psychometrika* 18 (4): 267–76. https://doi.org/10.1007/BF02289263.

Tylmann, W., P. Głowacka, and A. Szczerba. 2017. 'Tracking Climate Signals in Varved Lake Sediments: Research Strategy and Key Sites for Comprehensive Process Studies in the Masurian Lakeland'. *Limnological Review* 17 (3): 159–66. https://doi.org/10.1515/limre-2017-0015.

Tylmann, W., K. Łysek, M.a Kinder, and J. Pempkowiak. 2011. 'Regional Pattern of Heavy Metal Content in Lake Sediments in Northeastern Poland'. *Water, Air, & Soil Pollution* 216 (1): 217–28. https://doi.org/10.1007/s11270-010-0529-3.

Tylmann, W., B. Zolitschka, D. Enters, and C. Ohlendorf. 2013. 'Laminated Lake Sediments in Northeast Poland: Distribution, Preconditions for Formation and Potential for Paleoenvironmental Investigation'. *Journal of Paleolimnology* 50 (4): 487–503. https://doi.org/10.1007/s10933-013-9741-7.

Väliranta, M., A. Korhola, H. Seppä, E. Tuittila, K. Sarmaja-Korjonen, J. Laine, and J. Alm. 2007. 'High-Resolution Reconstruction of Wetness Dynamics in a Southern Boreal Raised Bog, Finland, during the Late Holocene: A Quantitative Approach'. *The Holocene* 17 (8): 1093–1107. https://doi.org/10.1177/0959683607082550.

Van Gemerden, H., and J. Mas. 2004. 'Ecology of Phototrophic Sulfur Bacteria'. In *Adv Photosynth Respiration*, 2:49–85. https://doi.org/10.1007/0-306-47954-0_4.

Veski, S., H.i Seppä, and Antti E. K. Ojala. 2004. 'Cold Event at 8200 Yr B.P. Recorded in Annually Laminated Lake Sediments in Eastern Europe'. *Geology* 32 (8): 681–84. https://doi.org/10.1130/G20683.1.

Vogel, H., C. Meyer-Jacob, L. Thöle, Jörg A. Lippold, and S. L. Jaccard. 2016. 'Quantification of Biogenic Silica by Means of Fourier Transform Infrared Spectroscopy (FTIRS) in Marine Sediments'. *Limnology and Oceanography: Methods* 14 (12): 828–38. https://doi.org/10.1002/lom3.10129.

Vogel, H., P. Rosén, B. Wagner, M. Melles, and P. Persson. 2008. 'Fourier Transform Infrared Spectroscopy, a New Cost-Effective Tool for Quantitative Analysis of Biogeochemical Properties in Long Sediment Records'. *Journal of Paleolimnology* 40 (2): 689–702. https://doi.org/10.1007/s10933-008-9193-7.

Wacnik, A., T. Goslar, and J. Czernik. 2012. 'Vegetation Changes Caused by Agricultural Societies in the Great Mazurian Lake District', 50.Vegetation history and archeobotany 25 (5):479-498. https://doi.org/10.1007/s00334-016-0565-z.

Walker, Keith F., and Gene E. Likens. 1975. 'Meromixis and a Reconsidered Typology of Lake Circulation Patterns'. *SIL Proceedings, 1922-2010* 19 (1): 442–58. https://doi.org/10.1080/03680770.1974.11896084.

Waters, M.N., J. M. Smoak, and C. J. Saunders. 2013. 'Historic Primary Producer Communities Linked to Water Quality and Hydrologic Changes in the Northern Everglades'. *Journal of Paleolimnology* 49 (1): 67–81. https://doi.org/10.1007/s10933-011-9569-y.

Weltje, G., and R. Tjallingii. 2008. 'Calibration of XRF Core Scanners for Quantitative Geochemical Logging of Sediment Cores: Theory and Application'. *Earth and Planetary Science Letters* 274 (3): 423–38. https://doi.org/10.1016/j.epsl.2008.07.054.

Wetzel, R.. 2001. *Limnology : Lake and River Ecosystems*. 3rd ed. San Diego: Academic Press.

Wick, L., G. Lemcke, and M. Sturm. 2003. 'Evidence of Lateglacial and Holocene Climatic Change and Human Impact in Eastern Anatolia: High-Resolution Pollen, Charcoal, Isotopic and Geochemical Records from the Laminated Sediments of Lake Van, Turkey'. *The Holocene* 13 (5): 665–75. https://doi.org/10.1191/0959683603hl653rp.

Wohlfarth, B., T. Lacourse, O. Bennike, D. Subetto, P. Tarasov, I. Demidov, L. Filimonova, and T. Sapelko. 2007. 'Climatic and Environmental Changes in North-Western Russia between 15,000 and 8000calyrBP: A Review'. *Quaternary Science Reviews* 26 (13): 1871–83. https://doi.org/10.1016/j.quascirev.2007.04.005.

Woolway, R. I., and C. J. Merchant. 2019. 'Worldwide Alteration of Lake Mixing Regimes in Response to Climate Change'. *Nature Geoscience* 12 (4): 271–76. https://doi.org/10.1038/s41561-019-0322-x.

Yu, G., and S. P. Harrison. 1995. 'Holocene Changes in Atmospheric Circulation Patterns as Shown by Lake Status Changes in Northern Europe'. *Boreas* 24 (3): 260–68. https://doi.org/10.1111/j.1502-3885.1995.tb00778.x.

Zolitschka, B., P. Francus, A. E. K. Ojala, and A. Schimmelmann. 2015. 'Varves in Lake Sediments – a Review'. *Quaternary Science Reviews* 117 (June): 1–41. https://doi.org/10.1016/j.quascirev.2015.03.019.

Appendix

ANNEX 1: Sediments

Table A.1.1: Detailed sediment description of the master core sequence from Lake Rzęśniki

Macroscopic description			
Segment nr.	**master core segment (RZE)**	**Core length (cm)**	**Sediment description**
1	RZE17/A	0 - 8.5 8.5 - 23.5	green foam alternating black-yellowish brown, sharp, fine laminated calcareous gyttja
2	RZE17/10_0.75-1.75	25.5 – 101.25	homogenous dark-greyish brown calcareous gyttja with some diffuse greyish brown layer
3	RZE17/9_1-2	2 - 73.5 73.5 – 82.75	diffuse laminated calcareous gyttja with light olive-brown laminations alternating olive black-light olive brown, sharp laminated calcareous gyttja
4	RZE17/10_1.75-2.75	69.5 - 81.5 81.5 - 88 88 - 96	alternating olive brown-light olive brown, fine laminated gyttja alternating grey-clay, sharp, fine laminated gyttja alternating black-light yellowish brown, sharp, fine laminated calcareous gyttja
5	RZE17/9_2-3	2.75 - 64.5	alternating black-light yellowish brown, laminated calcareous gyttja with some coring artefacts
6	RZE17/10_2.75-3.75	37.5 – 102.8	alternating black-light yellowish brown, fine laminated calcareous gyttja with some coring artefacts
7	RZE17/10_3.75-4.75	2 - 96.2	alternating black-light yellowish brown, fine laminated calcareous gyttja with some coring artefacts
8	RZE17/9_4.75-5.75	10.2 - 60 60 - 80	barely visible, but sharp laminated dark to black, fine detritus gyttja alternating black-light olive brown, sharp and fine laminated calcareous fine detritus gyttja (tilted laminations)
9	RZE17/10_4.75-5.75	66.3 - 85.6	alternating black-light olive brown, sharp and fine laminated calcareous fine detritus gyttja (tilted laminations)
10	RZE17/6_4.75-5.75	16.5-38.5	alternating black-light olive brown, sharp and fine laminated calcareous fine detritus gyttja (tilted laminations)
11	RZE17/10_5.75-6.75	34 - 96.5	alternating black-light olive brown sharp and fine detritus gyttja
12	RZE17/10_6.75-7.75	0.25 - 42 42 - 81	alternating black-light olive brown sharp and fine detritus gyttja alternating black-yellowish brown sharp and fine laminated gyttja
13	RZE17/10_7.75-8.75	0 - 17 17 - 27.5 27.5 - 33.5 33.5 - 51.1 51.1 - 101	floral foam blackish clay gyttja greyish-brown clay coarse detritus (classified as fragmented woods peat) sand

Table A.1.2: Core-to core correlation with sequence and master depth in cm, Lake Rzęśniki

Segment nr.	Core	Depth for composite [cm]	Correlation Top [cm]	Correlation Bottom [cm]	Master Core Top [cm]	Master Core Bottom [cm]	Core section length [cm]
1	17/A	8.5-23.5	8.5	23.25	0	14.75	14.75
2	17/10_0.75 -1.75	25.5 - 102	25.5	101.25	14.75	90.75	76
	gap	0-2	0	2	91.5	93.5	2
3	17/9_1-2	2-77.25	2	92.75	168	169	1
4	17/10 1.75 - 2.75	69.5 - 96	69.5	96	168	194.5	26.5
5	17/9_2-3	2.5 - 64.5	2.75	64.5	194.25	256	61.75
6	17/10_2.75 - 3.75	37.5 - 103.2	37.5	102.8	256	313.3	57.3
	gap	0-2	0	2	323.2	325.2	2
7	17/10_3.75-4.75	0 - 96.2	2	96.2	323.3	417.5	94.2
8	17/9_4 - 5	10.2 - 80.0	10.2	80	417.5	487.3	69.8
9	17/10_4.75 - 5.75	66.3 - 85.7	66.3	85.6	487.3	506.6	19.3
10	17/6_6 - 6.7	16.5 - 38.3	16.5	38.5	506.6	528.6	22
11	17/10_5.75 - 6.75	34.2 - 97.5	34	96.5	528.6	591.1	62.5
	gap	0-2	0	2	593.9	595.9	2
12	17/10_6.75 - 7.75	0 - 81	0.25	81	593.1	673.85	80.75
	gap	0-21.6	0	21.6	673.85	695.45	21.6
13	17/10_7.75 - 8.75	16.5 - 102	17	101	695.45	771.25	75.8

ANNEX 2: Chronology

Table A.2 1: Macrofossil sampling for ^{14}C chronology, Lake Rzęśniki

Nr	Core	Segement depth (cm)		master core depth [cm]		average (cm)	measurement (gas/graphite)	Macrofossils
7	RZE17/9 1-2	72.5	73.5	**163.25**	**164.25**	**163.75**	graphite	*Pinus* s.t. P, 1 fragment (total area ca 36mm2)
8	RZE17/10 1.75-2.75	79.5	80.5	**178**	**179**	**178.5**	gas	Conif. scale, small dicot. leaf fragments
9	RZE17/9 2-3	16	17	**207.5**	**208.5**	**208**	gas	*Pinus s.* t. P, 8 fragments (total area ca 12mm^2), *Betula alba* fruit fragments, Conif. Scale, c.f. Pinus s.t. needle fragment
11	RZE17/9 2-3	61	62	**252.5**	**253.5**	**253**	graphite	*Pinus s* .t. P, 11 fragments (total area ca 85 mm2), *betula alba* fruit - wing fragment, Conif. scale
13	RZE17/10 2-75-3.75	79	80	**297.5**	**298.5**	**298**	gas	*Pinus s.* t. P, 2 fragments (total area ca 9mm^2), 2 conif. scales
14	RZE17/10 2-75-3.75	65.8				**284.3**	graphite	*Pinus s.* t. P, 1 fragment (area ca 70mm^2)
15	RZE17/10 3.75-4.74	5.8	6.8	**327.1**	**328.1**	**327.6**	graphite	*Pinus s.* t. P, 10 fragments (total area ca 130mm^2), conif. scale
16	RZE17/10 3.75-4.74	35.8	36.8	**357.1**	**358.1**	**357.6**	graphite	*Pinus s.* t. P, 7 fragments (total area ca 58mm^2)
17	RZE17/10 3.75-4.74	65.8	66.8	**387.1**	**388.1**	**387.6**	graphite	Pinus s.t. P, 9 fragments (total area ca 33mm2), dicot. Leaf, 5 fragments
18	RZE17/19 4-5	10.2	11.2	**417.5**	**418.1**	**417.8**	graphite	*Pinus s.* t. P, 2 fragments (total area ca 42mm^2)
19	RZE17/19 4-5	39.8	40.8	**447.1**	**448.1**	**447.6**	graphite	*Pinus s.* t. P, 4 fragments (total area ca 17mm^2), 2 Betula alba fruits, 10 conif. scales
20	RZE17/19 4-5	60.5	61.5	**467.8**	**468.8**	**468.3**	graphite	Pinus s.t. P, 7 fragments (total area ca 47mm2), 2 conif. scales
21	RZE17/19 4-5	69.8	70.8	**477.1**	**478.1**	**477.6**	graphite	Pinus s.t. P, 10 fragments (total area ca 76mm2), 4 Pinus s.t. needle fragments
22	RZE17/10 4.75-5.75	76.1	77.1	**497.1**	**498.1**	**497.6**	graphite	*Pinus s.* t. P, 7 fragments (total area ca 36mm^2), Betula alba fruit, 5 *Pinus s* .t. needle fragments
24	RZE17/10 5.75-6.75	42.6	43.6	**537.2**	**538.2**	**537.7**	gas	conif. scale
25	RZE17/10 5.75-6.75	72.6	73.6	**567.2**	**568.2**	**567.7**	gas	*Pinus s.* t. P, 4 fragments (total area ca 19mm^2)
26	RZE17/10 6.75-7.75	3.1	4.1	**595.95**	**596.95**	**596.45**	gas	*Pinus s.* t. P, 2 fragments (total area ca 11mm^2), conif. Scale
28	RZE17/10 6.75-7.75	78.1	79.1	**670.95**	**671.95**	**671.45**	gas	*Pinus s.* t. P, 4 fragments (total area ca 7mm^2), conif. scale
29	RZE17/ 10 7.75-8.75	36				**712.75**	graphite	2 *Pinus s.* t. short shoots with 2 needles each
30	RZE17/ 10 7.75-8.75	27.5	28.5	**705.05**	**705.95**	**705.5**	graphite	*Pinus s.* t. P, 2 fragments (total area ca 32mm^2), Pinus s.t. short shoot with 2 needles, 3 Pinus s.t. needle fragments
31	RZE17/ 10 7.75-8.75	76.5	77.5	**749.15**	**750.05**	**749.6**	graphite	*Pinus s.* t. P, 5 fragments (total area ca 20mm^2), Pinus s.t. needle tip
32	RZE17/ 10 7.75-8.75	100	101.3	**770.35**	**771.25**	**770.8**	graphite	*Pinus s.* t. P, 7 fragments (total area ca 53mm^2), 2 Pinus s.t. needle fragments
33	RZE17/9 4-5	47	48	**447.1**	**448.1**	**447.6**	gas	2 conif. Scales, 1 Betula alba bract (fruit scale)
35	RZE17/9 4-5	57	58	**465.1**	**466.1**	**465.6**	gas	Pinus s.t. P, 2 fragments (total area ca 9mm^2)
36	RZE17/6 6-6.7	21	22	**512**	**513**	**512.5**	graphite	Betula alba fruit, Pinus s.t. P, 8 fragments (total area ca 30mm2)

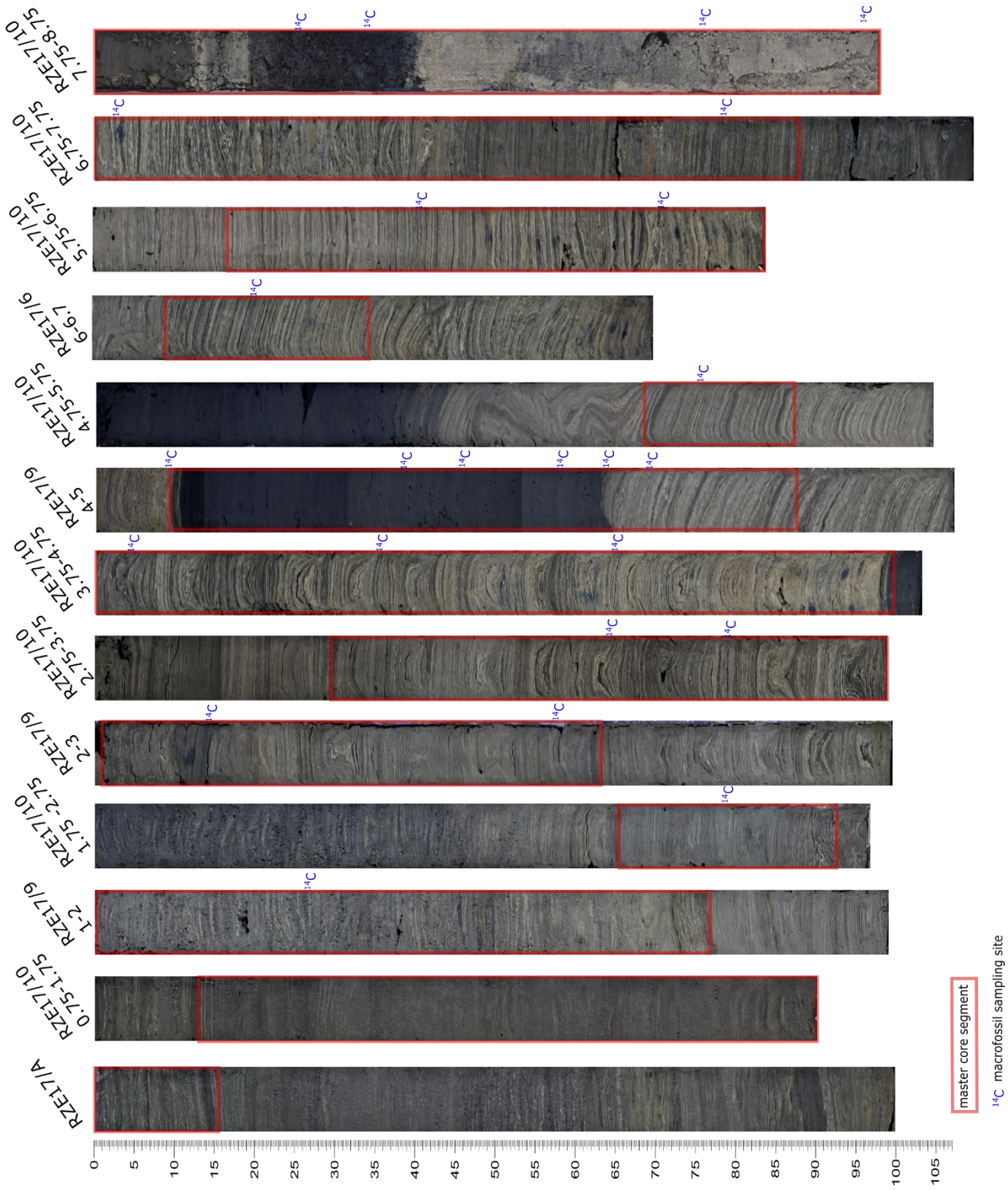

Fig. A.2 1: Master core segments in red and ^{14}C sampling location in blue, Lake Rzęśniki

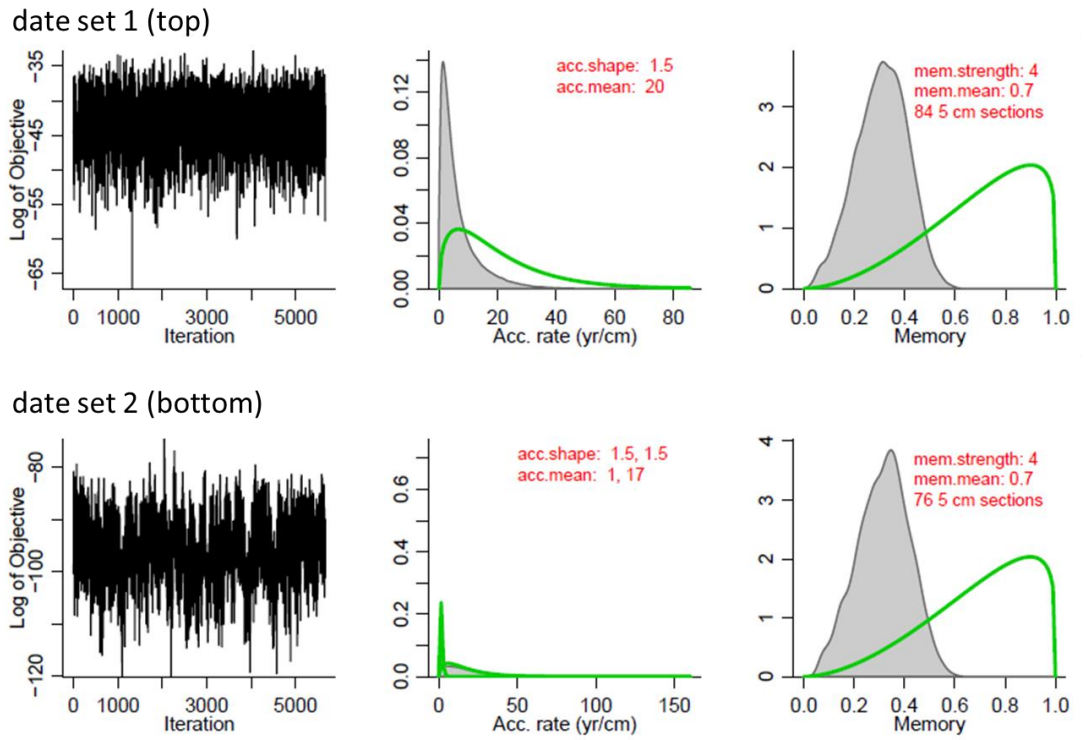

Fig. A.2 2: Performance plot of the two BACON model runs, used for the age-depth model

ANNEX 3: Results

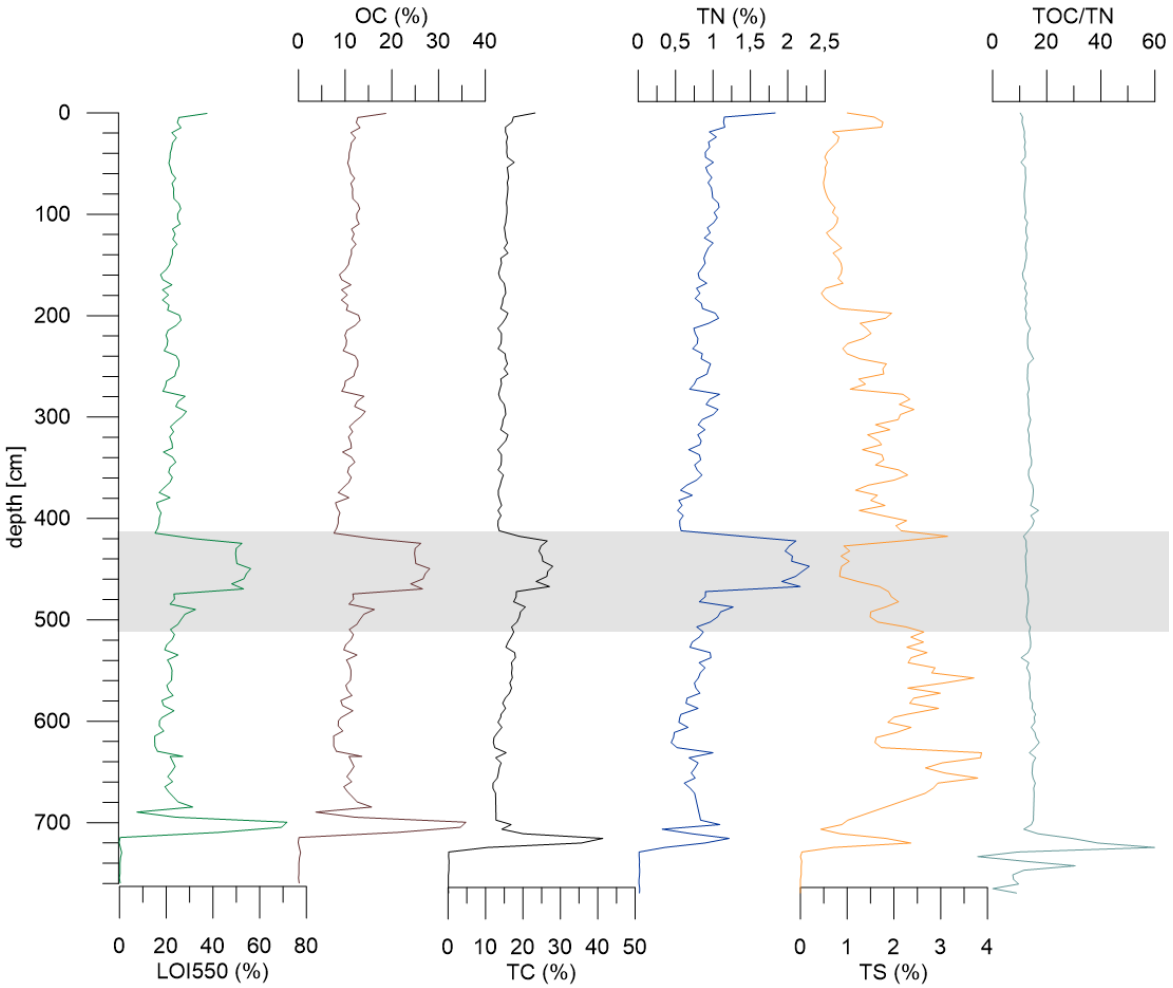

Fig. A.3. 1: Results of the LOI and CNS analyses plotted in depth. The TS is qualitatively usable (tailing in the measurement and carryover effect), but is still in good agreement with the S data retrieved by XRF scanning. The slump sequence is highlighted in grey

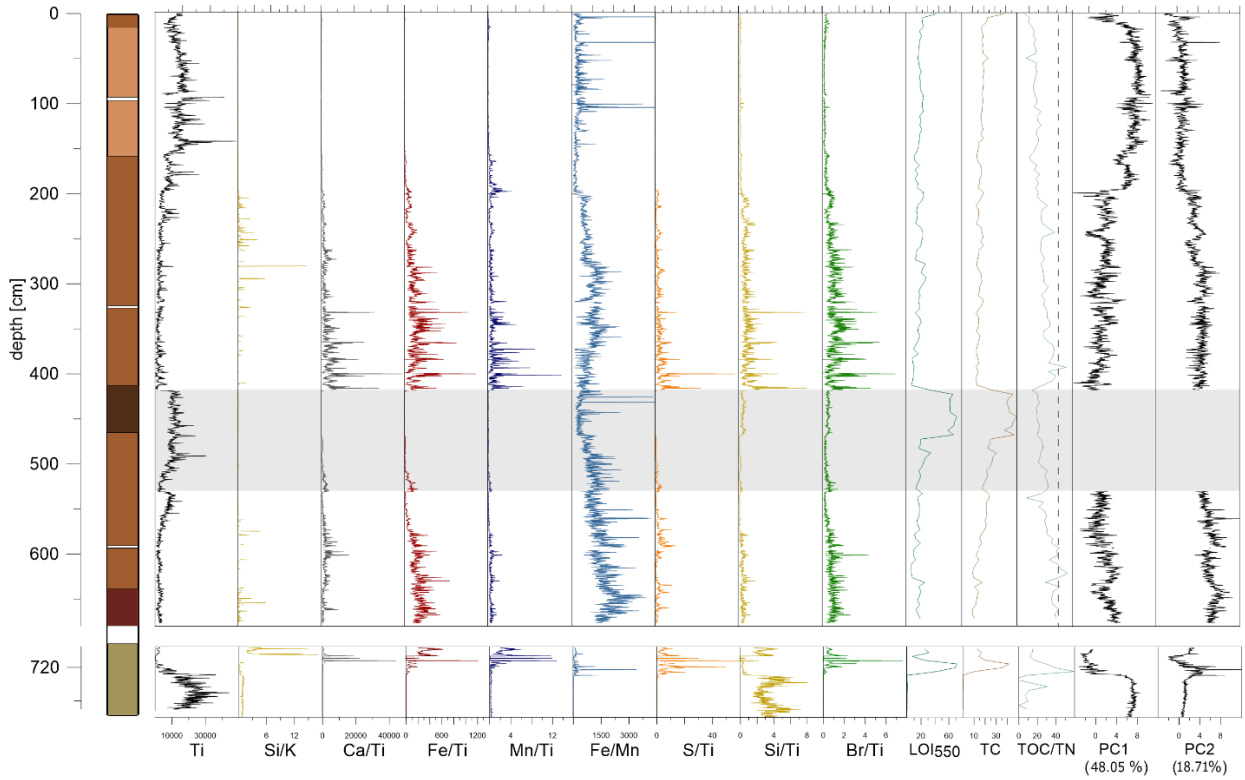

Fig. A.3. 2: XRF data profiles shown as ratios with Ti.

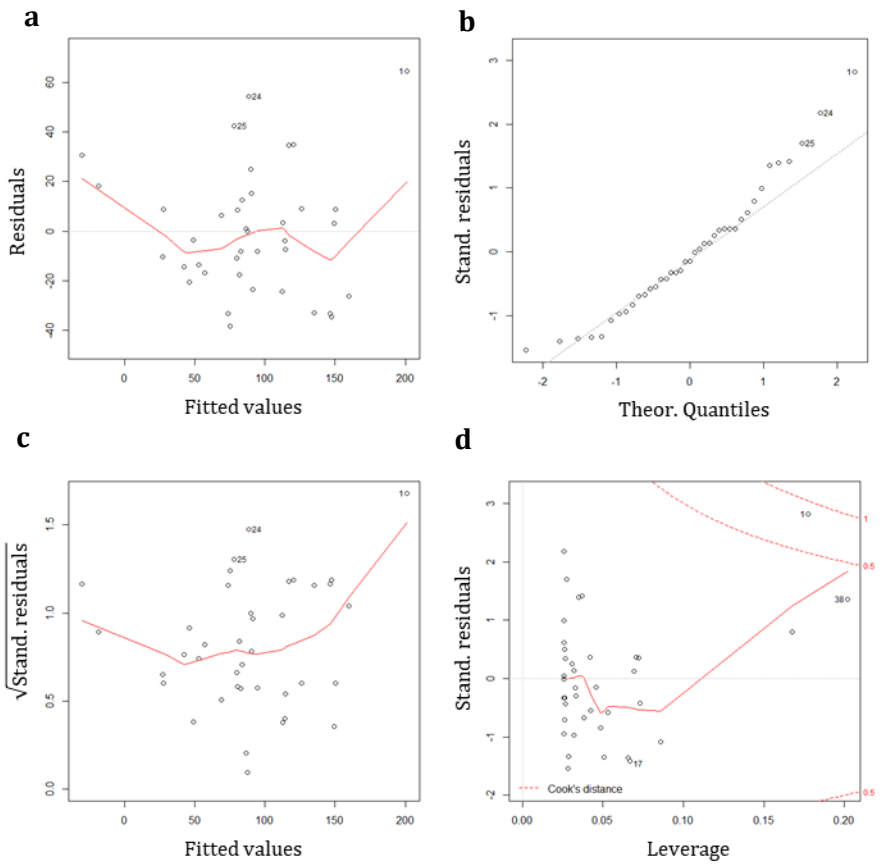

Fig. A.3.3: Different residual plots of the linear calibration model of $RABD_{673}$ with absolute TChl concentrations are shown in a) residuals versus fitted values, b) standardized residuals versus theoretical quantiles, c) scale-location plot and d) standardized residuals versus leverage plot

9. Acknowledgements

First, I would like to thank my paleolim colleagues (past and present) for a great time in the group: Tobi, Christoph B., Christoph D., Ivan, Aurea, Andrea, Luyao, Paul, Raphi, Linus, Louis and my advisor Stamatina. Many thanks also to everyone who contributed to my thesis: Dr. Sönke Szidat from the Department of Chemistry and Biochemistry for the ^{14}C-measurements; Dr. Martin Imseng for his essential help in the lab; Andrea Sanchini for the HPLC measurement; Dr. Hendrik Vogel for the FTIRS measurement and calibration, and general help regarding XRF data; and the paleolimnology group from the University of Gdansk for providing and sharing their insider knowledge about Polish lakes. A special thanks to Paul Zander and Andrea Sanchini, who were always open for any kind of questions in the last stage of my Master's thesis. A special thanks also to Dr. Daniela Fischer and Dr. Tobias Schneider for sharing their knowledge and having always an open ear (even from far away) over the past years. Thanks to my sister Anna, Ralph and Paul for reviewing my thesis and their helpful comments and in particular to my parents always being there for me, being my moral support and for believing I could do this. Most of all, I would like to thank Prof. Dr. Martin Grosjean and Dr. Hendrik Vogel for supervising my thesis. I would also like to thank Martin for all the support and possibilities to learn many thinks about science and research in the last three years as a bachelor student, research assistant or Master's student.

Declaration of consent

on the basis of Article 30 of the RSL Phil.-nat. 18

Name/First Name: Wienhues, Giulia

Registration Number: 13-125-216

Study program: Masters of Climate Sciences

Bachelor ☐ Master ☑ Dissertation ☐

Title of the thesis: Multi-proxy reconstruction of Holocene environmental change from sediments of Lake Rzęśniki, Northeast Poland

Supervisor: Prof. Dr. Martin Grosjean
PD. Dr. Hendrik Vogel

I declare herewith that this thesis is my own work and that I have not used any sources other than those stated. I have indicated the adoption of quotations as well as thoughts taken from other authors as such in the thesis. I am aware that the Senate pursuant to Article 36 paragraph 1 litera r of the University Act of 5 September, 1996 is authorized to revoke the title awarded on the basis of this thesis.

For the purposes of evaluation and verification of compliance with the declaration of originality and the regulations governing plagiarism, I hereby grant the University of Bern the right to process my personal data and to perform the acts of use this requires, in particular, to reproduce the written thesis and to store it permanently in a database, and to use said database, or to make said database available, to enable comparison with future theses submitted by others.

Bern, 02.09.2019
Place/Date

Giulia Wienhues
Signature